Department of Precision and Microsystems Engineering

Precision mechanism design for 3-DOF in-plane alignment in µm and sub-mrad level

A. Rathi

Report no : 2021.061
Coach : Dr. ir. L. A. Cacace
Professor : ir. J. W. Spronck
Specialisation : Opto-Mechatronics
Type of report : Master Thesis
Date : August 30, 2021

Precision mechanism design for 3-DOF in-plane alignment in µm and sub-mrad level

by

A. Rathi

to obtain the degree of Master of Science

at the Delft University of Technology,

to be defended publicly on August 30, 2021 at 02:00 PM.

Student number:	5002311	
Project duration:	September 1, 2020 – August 30, 2021	
Thesis committee:	ir. J. W. Spronck,	chair, TU Delft
	Dr. ir. L. A. Cacace,	supervisor, TU Delft
	ir. J. P. Kappelhof,	member, TU Delft
	Dr. ir. R. Hendrix,	supervisor, Prodrive Technologies

This thesis is confidential and cannot be made public until August 30, 2023.

TU Delft PRODRIVE TECHNOLOGIES

Abstract

To assist in the fast alignment of tiny components, Prodrive Technologies has developed a type of camera system called the Component Alignment Sensor (CAS) that is used on a pick-and-place machine. The system uses an optical target as the reference during its assembly and final testing steps. Two main components of the target are a glass reticle and a stainless steel carrier that are bonded together. These two components need to be precisely aligned w.r.t. each other. Till now, the alignment between the reticle and carrier has been performed manually by relative movement between them created by hand. However, this method has some limitations, including, but not limited to, an increase in the alignment time and sensitivity to external jerks or disturbances. Accordingly, the thesis objective is to create a (detailed) design of an alignment mechanism to perform the 3-DOF in-plane alignment in μm and sub-mrad level. The research starts with the formulation of design requirements, followed by concept design, evaluation and selection, and finally a detailed design of the mechanism. A flexure-based alignment mechanism was proposed and designed that uses fine screws for actuation. Various design principles were applied to construct a stiff and compact mechanism that uses a limited number of adjustment steps for the alignment. The process was supported by calculations and analyses that contributed to decision making. Besides, the assembly and alignment procedures of the alignment mechanism were described. The thesis is concluded with a plan to verify if the matured design meets the set requirements.

Acknowledgements

I would like to extend my heartfelt gratitude to a number of people who have made a valuable impact on my professional journey, together with my personal development.

Firstly, Ron for being an amazing mentor and an approachable guide. I really enjoyed our weekly discussions where I always ended up learning something. With this, I would also like to thank Prodrive for offering me this challenging practical assignment and continuously supporting me over the past year in such difficult times.

Secondly, Lennino for patiently coaching me to tackle similar design problems and have a smooth transition to the industry. Thirdly, Pieter for introducing me to this exciting project opportunity and bringing his vast experience of Opto-Mechanics on the table. I am forever grateful for that. Not to forget the bi-weekly discussions with my fellow OM students, along with Lennino and Pieter. These helped me immensely to gain diverse perspectives, get familiar with a varied range of problems, and ultimately shape my thesis.

Lastly, to my family in India and Canada, and the friends I have made during the course of my time at TU Delft. Their persistent support and motivation have been a major contributor to my happiness and good health.

Nomenclature

Abbreviations

A1–A6	Adapter
AC1–AC3	Actuator screw with knob
AD1–AD3	Adjustment screw with locknut
AISI	American iron and steel institute
Al	Aluminium
C	Assembly of carrier
C1	Compression spring
CAS	Component alignment sensor
CMM	Coordinate measuring machine
DFA	Design for assembly
DFM	Design for manufacturing
DOF	Degree of freedom
E	Sideways alignment
E1–E6	Extensions spring
EDM	Electric discharge machining
etc.	et cetera
FEMM Magnetics	An open source finite element analysis tool for electro-magnetics
FOV	Field of view
H	Reticle holder (without knob)
HertzWin	A free Hertzian contact stress calculator
i.e.	that is
I1–I3	Interface strip
IPA	Isopropyl alcohol solution
ISO	International organization for standardization
K	Holder knob
LED	Light emitting diode
LITF pivot	Leaf-type isosceles-trapezoidal flexural pivot
Max.	Maximum
MIM	Minimum incremental motion
Min.	Minimum
MSD	Magnetic switchable device
NBR	Nitrile butadiene rubber
NdFeB	Neodymium magnet
P	Preload assembly
PC1, PC2	Protective cover
PCB	Printed circuit board
PM	Permanent magnet
PMI	Product and manufacturing information
PU	Polyurethane
R	Assembly of reticle
R1–R4	Rubber foot

ReCa assembly	Assembly of reticle and carrier
resp.	respectively
Rx	Rotation about X-axis
Ry	Rotation about Y-axis
Rz	Rotation about Z-axis
S1–S2	Support feature
Siemens NX	A CAD tool by Siemens PLM Software
Simcenter Nastran	A FEM solver by Siemens Digital Industry Software
SS	Stainless steel
TL	Transport lock
TPI	Threads per inch
Tx	Translation along X-axis
Ty	Translation along Y-axis
Tz	Translation along Z-axis
UV	Ultraviolet
VC	Vibration criterion
vs.	versus
w.r.t.	with respect to

Symbols

$\|B\|$	Magnetic flux density	[T]
β	Circular hinge parameter	[-]
μ	Coefficient of friction	[-]
a	Acceleration of the system	[m/s^2]
C_x	Stiffness of leaf spring	[N/m]
C_{Az}, C_{Bz}	Stiffness along Z-axis in circular hinge	[N/m]
C_{spring}	Stiffness of extension spring	[N/m]
D_{hin}	Diameter of circular hinge	[m]
E	Modulus of elasticity of Al 7075	[GPa]
F_1	Reaction force on left adjustment screw of carrier	[N]
F_2	Reaction force on right adjustment screw of carrier	[N]
F_o	Initial force of extension spring	[N]
F_x	Force applied to leaf spring along X-axis	[N]
F_z	Force applied along Z-axis in circular hinge	[N]
$F_{actuator}$	Preload force for extension spring in line with actuator	[N]
$F_{adjustment\ screw}$	Preload force for compression spring in line with adjustment screw	[N]
F_{buck}	Buckling force of leaf spring	[N]
F_{hor}	Force experienced by metal plate in horizontal direction	[N]
$F_{pretension}$	Pretension force of spring	[N]
F_{th}	Theoretical holding force	[N]
F_{ver}	Force experienced by metal plate in vertical direction	[N]
g	Acceleration due to gravity	[m/s^2]
h_{hin}	Thickness of thin section in circular hinge	[m]
I	Area moment of inertia of leaf spring	[m^4]
K_{Ay}	Rotational stiffness of point A along Y-axis in circular hinge	[Nm/rad]
L_o	Initial length of extension spring	[m]
L_{hin}	Length of circular hinge	[m]
L_{leaf}	Length of leaf spring	[m]
L_{RF}	Length of reinforced part of leaf spring	[m]

m	Mass of held component	[kg]
$m_{adhesive\ hook}$	Mass of adhesive hook	[kg]
$m_{glass\ piece}$	Mass of glass piece	[kg]
$m_{hook\ weight(s)}$	Mass of hook weight(s)	[kg]
R_{hin}	Rotation angle formed in circular hinge	[rad]
S	Safety factor	[-]
s	Extension of spring	[m]
Sh	Shore-A hardness	[-]
t_{hin}	Width of circular hinge	[m]
t_{leaf}	Thickness of leaf spring	[m]
t_{RF}	Thickness of reinforced part of leaf spring	[m]
u_{xleaf}	Stroke of leaf spring along X-axis	[m]
u_{zhin}	Stroke of circular hinge along Z-axis	[m]
u_{zleaf}	Parasitic displacement of leaf spring along Z-axis	[m]
w_{leaf}	Width of leaf spring	[m]
Y	Young's modulus	[MPa]

Contents

1

Introduction

This chapter covers the background of the CAS product and introduces the main components (reticle and carrier). Current method of forming the ReCa assembly is described. Its limitations are stated, along with the need for an alignment mechanism. The proposed alignment mechanism is shown in the form of a schematic and explained, together with the alignment approach.

1.1. Relevance & Background

Component Alignment Sensor (CAS) is one of the products being designed and manufactured by Prodrive Technologies. It is a type of camera system that falls under the Vision and Sensing division of the company. As the name suggests, CAS assists in the fast alignment of components (with areas as small as 0.1 mm × 0.05 mm). This camera system is part of a bigger pick-and-place machine (see figure 1.1). The machine picks up a component using its vacuum nozzle and brings it into the FOV of CAS. The component's shape is then reconstructed by rotating it 360° and measuring its width from all angles. The values of offset and rotation are computed and used to determine the correct rotation of the component. Finally, the component is aligned and placed at the desired location with the help of the nozzle.

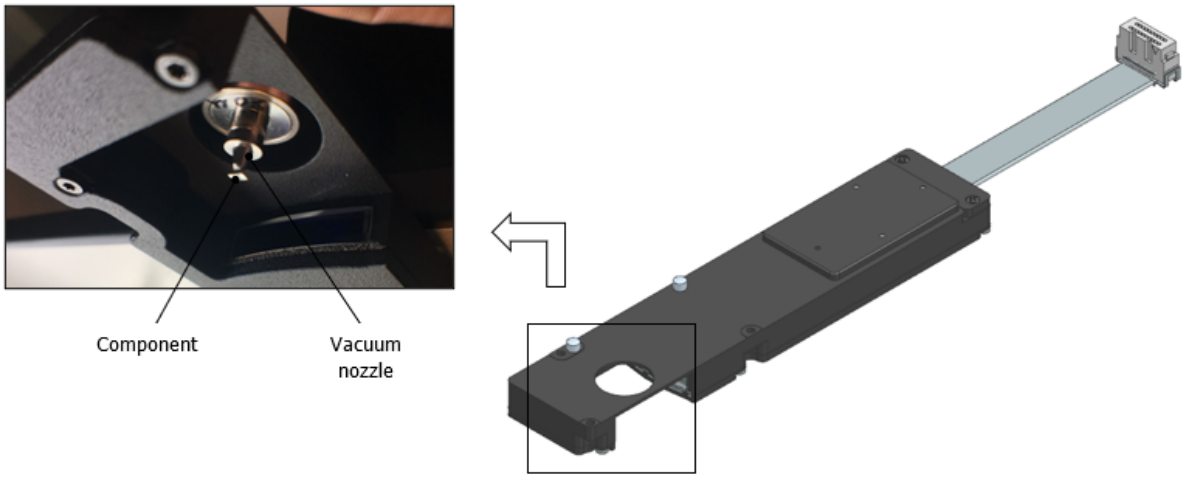

Figure 1.1: CAS (right) and its use with a pick-and-place machine (left)

Figure 1.2 shows the CAS without its lid. It consists of several parts that are mounted or bonded inside a housing. The light ray initiates from an LED lamp and gets partially blocked by an object placed in the FOV. The ray then continues to travel to a singlet lens, an aperture stop, a doublet lens, a prism, a glass window (on top of the image sensor) and lastly an image sensor that forms the image. To ensure the image is formed correctly, the prism and image sensor (soldered to its PCB) need to be actively aligned w.r.t. each other and the housing. This is one of the crucial steps in the product's assembly. For this, an optical target is used in the

FOV. The target mainly comprises a glass reticle and a metal carrier. The reticle consists of optical patterns that are used as an optical reference. However, the absence of any mounting features on the reticle makes it difficult to use it as a standalone component. Hence, a metal carrier is used along with the reticle to mount it. These two components - the reticle and carrier, are precisely aligned w.r.t. each other and their assembly (hereinafter referred to as the **"ReCa assembly"**) is used to build the CAS.

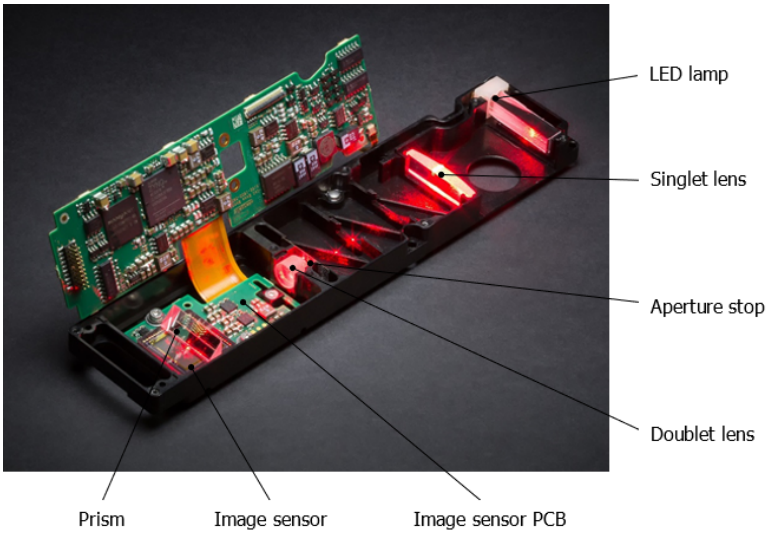

Figure 1.2: CAS with its parts

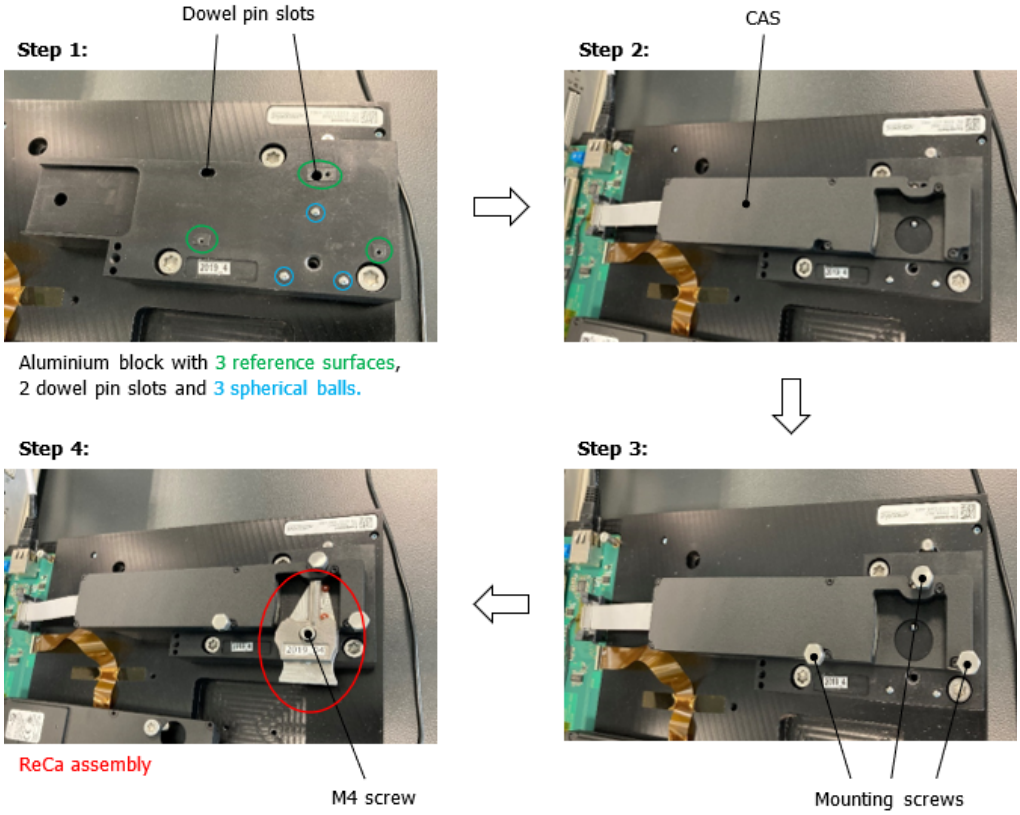

Figure 1.3: Calibration process steps for CAS

The same ReCa assembly is also used to perform calibration for the CAS once it is closed for final testing (see figure 1.3). This is carried out to examine any possible deviations that may have been introduced during the

final assembly steps of the product. An aluminium block is used as the base structure to mount the CAS and ReCa assembly. The CAS is mounted on three reference surfaces, aligned using two dowel pins and fixed using three mounting screws. Next, the ReCa assembly is placed on top of three bearing balls (that are press fit to the aluminium block) via the V-grooves located at the bottom of the carrier. This forms a kinematic coupling in combination with a pretension spring and a mounting screw.

1.2. Main Components

As seen in the previous section, the active alignment and calibration processes for CAS are some important steps to develop the product. The ReCa assembly is used in both the processes. **The two main components of the ReCa assembly: reticle and carrier**, are discussed in the coming subsections. Note that the assembly comprises other components as well, each having a specific purpose (refer section 1.3 for details).

1.2.1. Reticle

The reticle is a single-body component made of B270 glass material. It comprises two optical patterns represented by black regions on its front and back surfaces (see figure 1.4). The remaining surfaces do not have any patterns on them. Each black region in the reticle has a specific purpose (see figure 1.5). The slant patterns are used for the Ry alignment, the square regions (shown in green) on both sides are for the Rx and Rz alignments, and the 0.25 mm squares (shown in blue) on either bottom side are used to align the reticle to the carrier. This alignment happens via the two desired points of the reticle that are located in the corner of the 0.25 mm squares (highlighted in red).

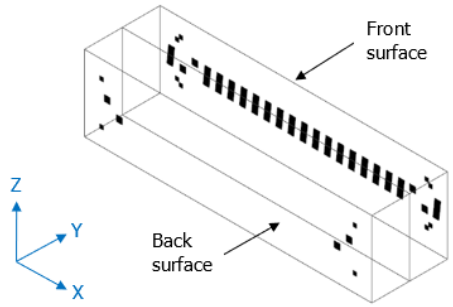

Figure 1.4: Reticle with optical patterns (isometric view)

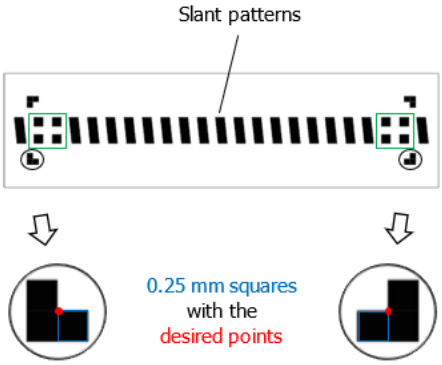

Figure 1.5: Desired points of reticle (front view)

Table 1.1: Specifications of reticle

Characteristic	Description
Length (X)	19 mm ± 0.2 mm
Width (Y)	5 mm ± 0.1 mm
Height (Z)	5 mm ± 0.2 mm
Nominal dimensions (X × Y × Z)	19 mm × 5 mm × 5 mm
Material	B270 glass
Density	2560 kg m^{-3}
Mass	1.2 g
Surface quality	Standard scratch/dig 60/40
Distance between the two desired points	16.5 mm
Position tolerance of optical pattern w.r.t. substrate edges	± 0.1 mm
Centering tolerance between optical patterns	< 10 µm
Edge tolerance of optical patterns	± 1 µm

The specifications of the reticle are shown in table 1.1. Note that the reticle is an expensive component with a long lead time. It is also delicate around the edges. Hence, care should be taken to prevent it from getting damaged - especially at the front and back surfaces with optical patterns on them.

1.2.2. Carrier

Carrier is a component made of AISI 304 stainless steel material. It comprises knife edges (see figure 1.6) that are designed to be sharp and without burrs. Therefore, wire EDM is chosen as the way to create them. The intersection of the horizontal and vertical knife edges on either side form two desired points of the carrier (highlighted in red). These two points, along with the two points of the reticle are used to align the two components together. The carrier also comprises cylindrical supports to mount two O-rings. The purpose of the O-rings will be explained in section 1.3.

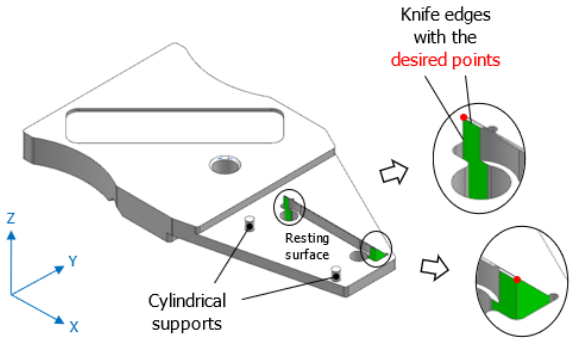

Figure 1.6: Carrier with knife edges (isometric view)

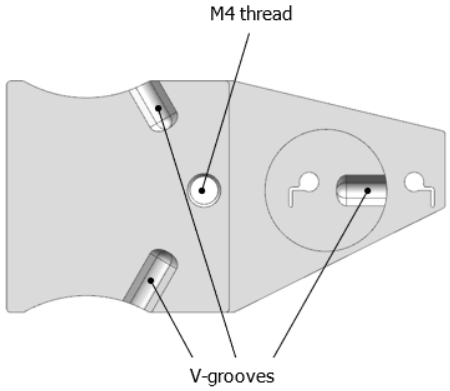

Figure 1.7: V-grooves of carrier (bottom view)

Table 1.2: Specifications of carrier

Characteristic	Description
Nominal dimensions (X × Y × Z)	52.2 mm × 27.5 mm × 4.6 mm
Material	AISI 304 stainless steel
Density	8000 kg m^{-3}
Mass	29.9 g
Distance between the two desired points	16.5 mm
Distance between horizontal knife edge & resting surface	1.6 mm

The specifications of the carrier are shown in table 1.2. As seen in figure 1.7, the carrier has three V-grooves on its bottom surface. The axes of these V-grooves intersect at a point called the thermal center. This point coincides with the axis of the M4 screw thread. The V-grooves when brought in contact with three spherical balls (on the mating body) create six local contact areas. This forms an exact constraint design that provides a rigid, precise and repeatable connection between the carrier and mating body. This type of coupling is known as Maxwell kinematic coupling [8].

1.3. Current Alignment Method

Till now, the alignment between the reticle and carrier has been performed manually by relative movement between them created by hand. This process is observed and carried out under the microscope as shown in figure 2.2. The steps to perform the alignment are described below:

1. The carrier is taken and two O-rings are placed on the cylindrical supports using a tweezer. The O-rings, which provide the necessary pretension force, ensure in-plane contact between the front surface of the reticle and the green faces of the carrier (that includes knife edges).
2. The reticle is placed in the gap between the O-rings and green faces of the carrier.
3. The 3-DOF alignment is performed manually (in Tx, Tz and Ry) to align the desired points of the components w.r.t. each other. This is done as closely and skillfully as possible depending on the operator.
4. Once aligned, the assembly is gently put on the table for the adhesive bonding. This is done very carefully to avoid any accidental jerks or disturbance forces that could ruin the alignment.

5. UV adhesive is applied to the four regions (encircled in figure 1.9) and cured using a handheld UV light for approximately 30 s at room temperature.

6. A pin of rectangular cross-section is bonded for reinforcement, along with a protective cover for the reticle. The purpose of the cover is to protect the reticle from accidentally getting damaged.

7. Once cured, an M4 screw with spring is inserted for mounting the assembly on the aluminium block. Figure 1.8 shows the current ReCa assembly with its supporting components.

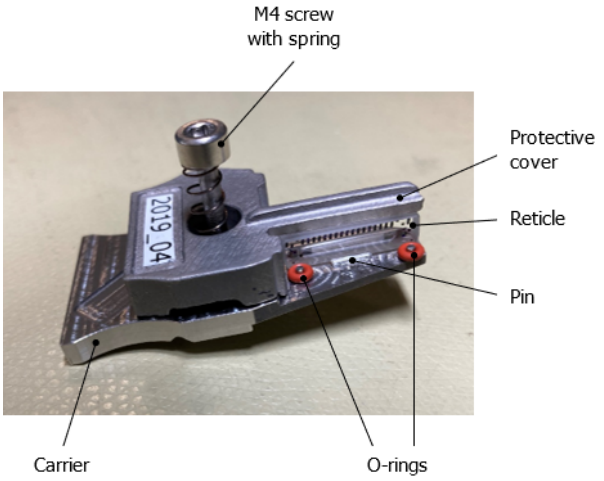

Figure 1.8: Current ReCa assembly

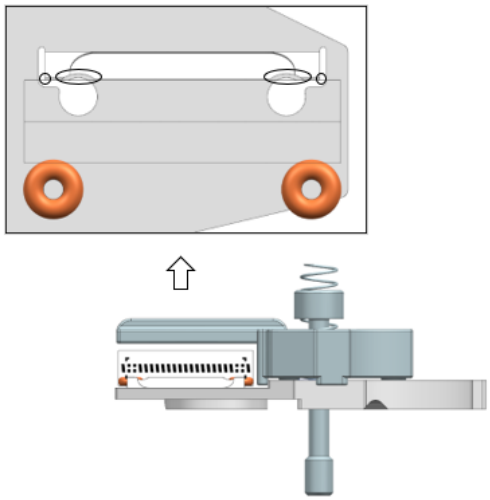

Figure 1.9: UV adhesive application regions

1.4. Limitations and Thesis Objective

From the earlier section, it appears that the current method of forming the ReCa assembly is not robust. Although the alignment is performed, the relative movement of the reticle and carrier in the absence of structural support increases the alignment time. The current process is also sensitive to external jerks or disturbances that can be introduced before the adhesive bond is applied. Moreover, there is a probability of the reticle getting damaged, if proper care is not taken by the operator. This cannot be risked as the reticle is a costly component that has a long lead time. Additionally, the O-rings are limited in their practicality despite providing the pretension force. The rubber tends to move or rotate during adjustments that gives hysteresis. This affects the in-plane contact between the front surface of the reticle and the green faces of the carrier, as the O-rings use a limited height (= 1.6 mm, refer table 1.2) to constrain the Rx DOF.

Due to the above-mentioned issues and limitations, there is a need to improve the alignment process between the reticle and carrier. Accordingly, **the objective of the thesis is to create a (detailed) design of an alignment mechanism that can be used to perform the 3-DOF alignment (in Tx, Tz and Ry) between the main components.** The alignment must be performed in µm and sub-mrad precision level. Parallelly, the process flow of performing the alignment should be defined to make it easy and structured for the operator. An alternative approach (other than designing the alignment mechanism) can be explored to solve the alignment problem in a relatively simple fashion.

Another thesis objective is building a working prototype of the mechanism that can create an opportunity to verify its functionality and performance. The verification, for instance, can be done by examining if the provided input stroke to the mechanism results in the expected adjustment. The time available during the thesis period will determine the extent to which the prototype can be finalized and used for verification.

Note that the position tolerance of the optical pattern w.r.t. substrate edges is large (= ± 0.1 mm, refer table 1.1). Therefore, the carrier is provided with two knife edges that are measured w.r.t. the CAS mounting and alignment surfaces as seen in figure 1.3 (using CMM). Finally, the optical domain of the reticle (with 0.25 mm squares) is aligned to the mechanical domain of the carrier (with knife edges), and the assembly is bonded in place. In this way, the use of the ReCa assembly is justified.

1.5. Proposed Alignment Mechanism

1.5.1. Schematic Overview

Figure 1.10 shows a simple schematic of the proposed alignment mechanism in its upright orientation. A manipulator body forms the core of the mechanism. It is composed of a fixed structure, a moving structure that can be adjusted in 3 DOFs (Tx, Tz and Ry) and a guide that connects the two structures in the remaining 3 DOFs (Rx, Rz and Ty). The point of rotation for the Ry adjustment is highlighted in red. Moreover, the actuators that carry out the adjustments are attached to the fixed structure - one on the top (actuator '2') and two on the left (actuators '3' and '1'). Any adjustment from the actuators is transmitted to the moving structure via the guide.

A holder is considered for the reticle to grip it in the mechanism for the adjustments. It is attached to the moving structure with its holding surface pointing downwards. Similarly, a mount is considered for the carrier to attach it to the fixed structure. The rectangle displays an approximate area for the carrier mount. Note that enough space is reserved between the holder and the carrier to incorporate the reticle, along with some additional components. These components are necessary for the functioning of the holder and will be covered in the later chapters. Besides, an overload protection mechanism is integrated in the manipulator body to prevent the reticle from getting damaged during adjustments. Finally, a preload assembly is attached to the fixed structure of the manipulator body (see side view of the figure) to constrain the remaining three DOFs by forming an in-plane contact between the main components.

The complete design of the alignment mechanism is detailed and elaborated using 3D models. Its components & subassemblies are expanded and presented in the following chapters.

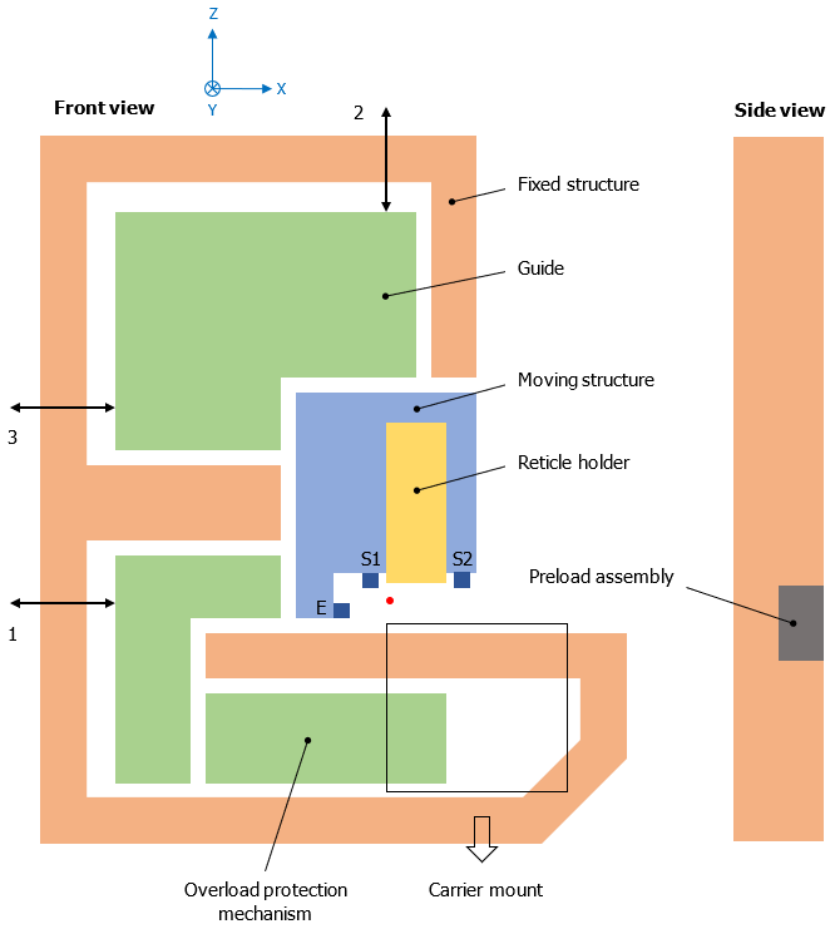

Figure 1.10: Schematic of proposed alignment mechanism (upright orientation)

'1', '2' and '3' are actuators; 'E' is for sideways alignment; 'S1' and 'S2' are support features

1.5.2. Alignment Approach

The alignment between the reticle and carrier follows a particular approach as explained in this section. Two orientations of the alignment mechanism are utilized during the entire process: seated (used during alignment – XZ-plane lies on a flat surface, see figure 1.10) and upright (for all other purposes – XZ-plane is perpendicular to a flat surface). To begin with, it is important to know that the carrier is stiffly mounted on the fixed structure. In case of the reticle, its three alignment DOFs (Tx, Tz and Ry) are left adjustable, while the three remaining DOFs (Rx, Rz and Ty) are constrained by a force from the preload assembly on the back surface of the reticle.

Furthermore, before starting the adjustment of the reticle w.r.t. carrier, the position of the reticle is defined in the alignment mechanism. The mechanical features of the moving structure ('E', 'S1' and 'S2', see figure 1.10), together with the carrier are utilized for this purpose. 'E' is used to define the X-position of the reticle for the sideways alignment. This is done by sliding the reticle (placed on the resting surface of the carrier) towards it until it finds a hard stop. The support features 'S1' and 'S2' are used in combination with the resting surface of the carrier to define the Z-position and the Ry of the reticle. This is carried out by translating the moving structure in the -Z direction until both the support features touch the reticle. If needed, the actuator '3' can be used to correct the Ry rotation. At this point, the holder is turned ON to grip the reticle via its additional components.

Any extra stroke by the moving structure in the -Z direction is transmitted to the overload protection mechanism. The mechanism gets actuated to prevent damage to the reticle when it gets clamped between the support features and the resting surface of the carrier.

1.6. Report Outline

Six main chapters form the main body of the report.
Chapter 2 shows the design requirements of the project. The full list is divided into two categories of "must-haves" and "nice-to-haves". Each requirement is explained and justified. The chapter is summarized with a tabular overview of each category.
Chapter 3 elaborates the concepts for different functionalities and subassemblies of the alignment mechanism: guide, actuator, reticle holder, carrier mount, manipulator body and preload assembly. Sketches and comparison tables are made to evaluate and assess different concepts. Finally, the proposed concepts are brought together in the last section of the chapter.
Chapter 4 details the proposed concept designs in 3D models. The working principle is explained for each of them that are supported by necessary calculations. In addition, the structural analysis of the manipulator body and the magnetic flux analysis of the reticle holder are carried out to simulate their working.
Chapter 5 gives an overview of the complete alignment mechanism. Besides, the chapter covers the assembly and alignment procedures of the mechanism in detail. Thereafter, a plan is described to verify if the matured design meets the set requirements.
Chapter 6 summarizes the main conclusions and discusses the recommendations for future work.

2

Design Requirements

This chapter covers the requirements for designing the alignment mechanism, which are divided into two main categories. First category comprises a set of "must-haves" that are essential to the design and are necessary to build the mechanism. These requirements are to be adhered to or satisfied to achieve the desired objective. Second category comprises a set of "nice-to-haves" that are of less priority. The desired objective does not depend on them, however, including them in the design can be beneficial. Each requirement is shown by a unique code. 'M' stands for must-have and 'N' for nice-to-have, followed by a number '#'.

2.1. Must-haves

(M0): Alignment DOFs: The reticle and carrier must be aligned in three DOFs (adjustable DOFs) w.r.t. each other: translations along the X- and Z-axis (Tx and Tz, respectively), and rotation about the Y-axis (Ry). The coordinate system, along with the three DOFs can be seen in figure 2.1.

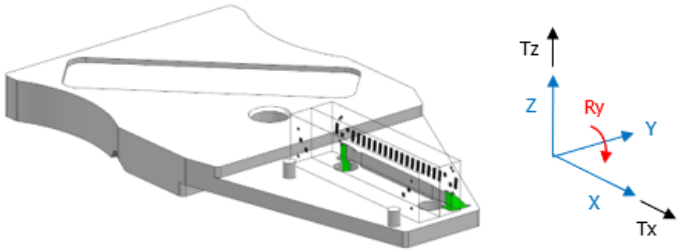

Figure 2.1: ReCa assembly with three alignment DOFs

(M1): Minimum Incremental Motion (MIM): The alignment mechanism must allow for a minimum incremental motion of ≤ 0.1 mrad for the Ry and ≤ 5 µm for the Tx DOFs. Considering the distance between the two desired points of each component (= 16.5 mm, refer tables 1.1 and 1.2) and using the small-angle approximation, the MIM for Tz DOF is calculated as follows:

$$Angle = \frac{Arc}{Radius} \implies 0.1\,\text{mrad} = \frac{Tz}{16.5\,\text{mm}} \implies Tz \leq 1.65\ \mu\text{m} \tag{2.1}$$

For simplicity, the value is rounded off to the multiple of 0.5 µm and represented as Tz ≤ 1.5 µm.

(M2): Stroke: The adjustment strokes needed for angular or linear adjustments are ± 10 mrad or ± 0.5 mm, respectively. If required, these values can be slightly increased.

Note that for linear adjustments (Tx and Tz), the stroke of 0.5 mm is considered based on the tolerances of optical patterns and some additional deviations that can be introduced due to the machining of the mechanism itself.

(**M3**): **Remaining DOFs limits**: The remaining three DOFs (Ty, Rx and Rz) must satisfy the limits of ± 15 mrad for angular deviation or ≤ 50 µm for linear deviation. These values are the combined upper limits of the remaining three DOFs that are defined within the FOV (18.5 mm × 3.5 mm) of CAS.

(**M4**): **Intact reticle**: The reticle shall not undergo any damage during the entire process - especially at its front and back surfaces due to the optical patterns present on them, and around its edges.

(**M5**): **Adhesive bonding**: Once the alignment is performed, the reticle and carrier need to be bonded in-place to fix the aligned assembly. Therefore, the mechanism needs to be designed in a way that the adhesive bond application regions (see figure 1.9) are accessible to the operator.

(**M6**): **Use frequency**: Depending on the need, the mechanism will go through five alignments per year.

(**M7**): **Total time**: The total time to perform the alignment and bond the two sets of the reticle and carrier must be < 30 min. This includes the time taken to prepare the setup.

(**M8**): **Operating temperature range**: The mechanism must be able to work in the temperature range of 15 °C − 25 °C. There are no additional storage requirements.

(**M9**): **Vibration level on site**: A Vibration Criterion (VC) curve is the form in which the allowable vibration level is presented. The site in which the alignment mechanism must operate falls under the 'residential day (ISO)' criterion curve (barely noticeable vibration). This lies between the 'office (ISO)' (noticeable vibration) and 'operation theatre (ISO)' (vibration not noticeable) criterion curves. The use of the criterion is deemed appropriate for computer equipment, probe test equipment and microscopes with less than 40× magnification [51].

The mechanism is considered to lie in the same category as the above-mentioned equipment.

(**M10**): **Shock level during operation**: The alignment mechanism comprises a fragile glass component like the reticle. Therefore, it must be able to endure a certain shock level due to the movement required for performing the alignment and adhesive bonding.

The mechanism must be able to tolerate a shock level of 25g during operation, as the operating process can involve moving the alignment mechanism around. Handling it with care would bring down the required tolerable shock level. Note that the shock level of an instrument during transport without any packaging can reach more than 25g. With packaging, it can be reduced to 15g. The value of ~3g is suited for manual handling of optical instruments [51].

(**M11**): **Alignment Stability**: The alignment performed by the mechanism must be stable for a short-term. This means that the reticle and carrier need to stay in-place without much deviation till the adhesive bonding is carried out.

(**M12**): **Available volume**: The alignment mechanism must fit and work within the available volume. This volume is determined by the microscope setup as shown in figure 2.2. This setup is available at the company and has been used to get visual feedback during the alignment process.

The approximate dimensions measured for the microscope and its surrounding regions are shown in table 2.1. The values shown are suitable for an operator with a height of around 1.72 m.

The working distance of the microscope is represented by the label 'a'. Note that the focal plane of the microscope is considered to be on the table, with its approximate focus area shown by the blue circle (see figure 2.2). For the alignment mechanism, the focal plane will lie at a certain distance above the table. By adjusting the microscope setup, correct focus can be achieved. Taking sufficient clearances with the microscope into account, the available volume to design the mechanism comes out as 300 mm × 210 mm × 170 mm for length, width and height, respectively.

(**M13**): **Budget**: The overall cost of the mechanism must be kept within the budget of € 3000. This includes the purchasing, machining and assembly costs.

Table 2.1: Microscope setup approximate dimensions

Label	Values (in mm)
a	255
b	220
c	185
d	110
e	180
f	160

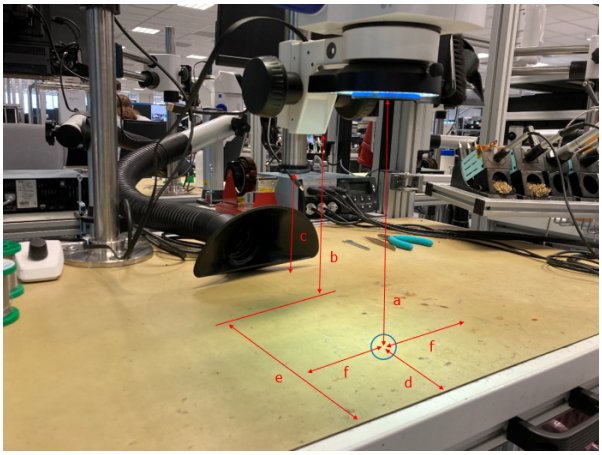

Figure 2.2: Microscope setup

2.2. Nice-to-haves

(**N0**): **Compact & portable**: The design of the alignment mechanism should be such that its entire weight and dimensions can be handled by a single operator. Hence, a compact and portable mechanism is preferred.

(**N1**): **Design for Manufacturing & Assembly (DFM/DFA)**: The mechanism's design should have the potential of being manufactured efficiently (DFM) and assembled with ease (DFA).

(**N2**): **Cost-effective**: The overall cost of the alignment mechanism, including bought-out items and other supporting components, should be low. The two methodologies (DFM/DFA) mentioned in the previous requirement have a direct impact on this.

(**N3**): **Compatibly designed**: The reticle and carrier should not undergo any design changes unless it is absolutely essential. A design of the alignment mechanism compatible with the current revisions of both the components is preferred. If required, additional components can be incorporated without changing the functionality of the main components.

(**N4**): **Integrated adhesive bonding**: Bonding the reticle and carrier so far has been done manually by hand due to a limited number of alignments needed every year. Integrating this process as part of the mechanism would increase the ease and speed with which the ReCa assembly can be formed.

2.3. Requirements Overview

Table 2.2: Must-haves

Code	Characteristic	Requirement	Remark
M0	Alignment DOFs	Tx, Tz & Ry	
M1	MIM	≤ 0.1 mrad, ≤ 5 µm & ≤ 1.5 µm	Ry, Tx & Tz, resp.
M2	Stroke	± 10 mrad, ± 0.5 mm & ± 0.5 mm	Ry, Tx & Tz, resp.
M3	Remaining DOFs limits	± 15 mrad or ≤ 50 µm	combined limits within FOV
M4	Intact reticle		patterned surfaces & edges
M5	Adhesive bonding		accessible bond regions
M6	Use frequency	5 alignments per year	
M7	Total time	< 30 min	two sets (reticle & carrier)
M8	Operating temperature range	15 °C − 25 °C	
M9	Vibration level on site	'residential day (ISO)' VC curve	barely noticeable vibration
M10	Shock level during operation	25g	
M11	Alignment Stability		short-term stable
M12	Available volume	300 mm × 210 mm × 170 mm	X × Y × Z
M13	Budget	€ 3000	purchasing, machining & assembly costs

Table 2.3: Nice-to-haves

Code	Nice-to-have	Remark
N0	Compact & portable	
N1	DFM/DFA	
N2	Cost-effective	
N3	Compatibly designed	reticle & carrier
N4	Integrated adhesive bonding	

3

Concept Design and Selection

This chapter covers concept designs of different functionalities and subassemblies of the alignment mechanism. Concept evaluation is carried out and the proposed design is presented for each of them.

3.1. Guide and Actuator

The guide and actuator are two of the important parts of an alignment mechanism. There are various options available for each of them. However, not all options are equally suitable for different use cases. The two parts, along with their preferred options to design the alignment mechanism, are explained in the coming subsections.

3.1.1. Guide Choice

A guide is a connecting medium between the fixed structure and the moving structure. There are several factors that determine the guide choice for a use case. These factors are precision, stroke, adjustment frequency, load capacity, stiffness, cost, complexity and volume of the alignment mechanism [50]. Some commonly used guide options, along with their pros and cons are covered in detail in Appendix A.1.

Flexures were considered as the preferred guide choice to adjust the 3 DOFs (refer M0 requirement). They offer the merits of high stiffness and frictionless motion with no play or wear. Flexures are especially useful in precision applications that require limited stroke. Furthermore, they can create opportunities to adjust one or more DOFs in parallel, serial and hybrid fashion. Moreover, the advantages to realize a monolithic design using flexures are noteworthy. The design avoids major sources of error due to the assembly & tolerances of parts in an alignment mechanism and produces predictable deformations due to material uniformity [44][7].

3.1.2. Actuator Choice

An actuator is needed to adjust the moving structure relative to a fixed structure. Like the guide, there are several factors that affect the selection of an actuator. These factors are resolution, sensitivity, stroke, velocity, adjustment frequency, load capacity, cost and volume of the alignment mechanism [50]. Some commonly used actuator options, along with their pros and cons are covered in detail in Appendix A.2.

Fine or differential screws were selected as the preferred actuator choice to manipulate the moving structure. These are an economical choice for the applications that require less frequent adjustments and do not require position readout. Additionally, the screws are good for high sensitivity and small stroke applications. They can be actuated by hand, where their MIM depends on the sensitivity of the chosen screw and the operator.

3.2. Reticle Holder

Before adjusting the reticle, an important step is to look at how it is held in the alignment mechanism. A holder is considered for this purpose. The holder can either be part of the mechanism or become integrated as a separate subassembly. As seen in figure 1.4, the reticle has optical patterns on its front and back surfaces.

The component should be handled gently to avoid scrapping off the patterns. To prevent damage anyway, it is preferred to use one or more of the remaining surfaces for holding. Figure 3.1 shows that in the aligned position, the space available between the bottom surface of the reticle and the resting face of the carrier is limited (= 0.3 mm, as per nominal dimensions). Hence, the bottom surface of the reticle should also be avoided for holding. In conclusion, three feasible surfaces (left, right and top) remain available for individual or combined use to hold the reticle (see figure 3.2).

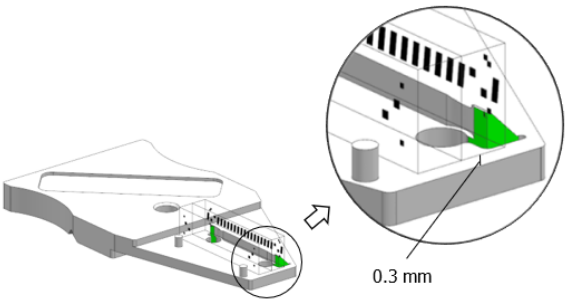

Figure 3.1: Final aligned assembly of reticle and carrier

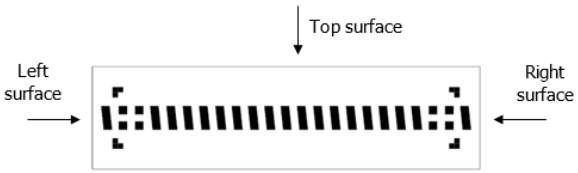

Figure 3.2: Feasible reticle holding surfaces

3.2.1. Holding Options Overview

There are two important conditions to note when checking the holding options for the reticle. Firstly, the holder must be able to release the assembly of the main components post-curing, i.e., after the reticle and carrier are aligned and bonded together. This release of the assembly should not introduce any jerks or disturbance forces that might ruin the alignment or lead to cracks in the cured bond. Secondly, the grip/hold provided by the holder must be stiff without any slip. If needed, some mechanical features can be integrated with the moving structure and utilized in combination with the holder to ensure this condition is satisfied. This condition is necessary for precise adjustments of the components to avoid any undesired effects during the alignment process.

Four main categories are considered to classify the holding options based on their holding methods: vacuum, magnetic, clamping and adhesion. These are covered in detail in Appendix B. A comparative analysis of some promising holding options under each of the four categories can be found in table 3.1. The options are compared against different parameters that are explained below:

- **Working principle**: Briefly explains how the holder works.
- **Compressed air/electric power supply**: If the holder depends on an extra requirement of either a compressed air supply or an electric power supply for its working.
- **Changes to reticle before hold**: If the reticle undergoes any change before holding.
- **Safe release**: If the release of the cured ReCa assembly is safe.
  Ranges from '++' (very safe) to '– –' (extremely risky).
- **Stiff hold/grip**: The stiffness of the grip/hold provided by the holder.
  Ranges from '++' (most stiff) to '– –' (least stiff).
- **Compact**: The compactness of the holder in terms of the volume claimed by it.
  Ranges from '++' (most compact) to '– –' (least compact).
- **Low cost**: For an off-the-shelf design, it is the overall cost of purchasing the holder and its supporting components (if any). In case the design is custom-made, the amount relates to purchasing, machining and assembly costs.
  Ranges from '++' (inexpensive) to '– –' (high-priced).

Table 3.1: Comparative analysis of holding options

Parameter	Vacuum	Magnetic		Clamping	Adhesion
	Plastic suction cup	Electromagnet	Permanent magnet with a knob	Pneumatic parallel gripper	Bond tape
Working principle	Creates a vacuum using an ejector	Generates a magnetic field in the presence of electricity	Alters a magnetic field using a knob	Clamps using a force closure grasp	Uses direct adhesion force
Compressed air/electric power supply	Air supply	Electric supply		Air supply	
Changes to reticle before hold		Metal plate bonded to the top surface	Metal plate bonded to the top surface		
Safe release	+	+	+	+	−−
Stiff hold/grip	+	−	−	+	−
Compact	+	+	+	−	++
Low cost	+	+	+	−−	++

A plastic suction cup uses a vacuum force to hold the reticle to its top surface. Because of the plastic material, the grip provided by the holder remains stiff. However, the option relies on a compressed air supply and a vacuum generator (like a vacuum ejector) for its working [17], together with other vacuum components (refer Appendix B.1 for details). An alternative can be to use a vacuum pump for vacuum generation. Hence, the use of a plastic suction cup adds supporting components for its functioning that increases cost and complexity.

To utilize the magnetic holding category, a ferromagnetic interface shall be added to the glass reticle as it is non-magnetic in nature. A thin flat metal plate can act as that interface. Bonding it to the top surface of the reticle provides the opportunity to hold the reticle via the newly created surface. Furthermore, a bond tape is considered for bonding the metal plate to the reticle. It forms a more or less permanent bond with the holding surface. This means that for the use case, debonding of the metal plate becomes difficult and is therefore not recommended. It is preferred to leave the plate in the bonded position after use. This does not affect the functionality of the reticle or change its existing design revision.

An electromagnet operates like a magnet in the presence of an electric power supply to generate a magnetic field. On the contrary, a permanent magnet produces a persistent magnetic field and does not depend on an electric power supply. Because of this continuous magnetic field, the releasing of a substrate becomes tricky as it can introduce jerks or disturbance forces. Hence, to smoothly release the ReCa assembly post-curing, a knob can be used to turn the holding forces ON and OFF (refer Appendix B.2 for an example). In addition, an air gap can be introduced in the magnetic circuit by using mechanical support features (see figure 1.10) that are integrated with the moving structure. The gap offers the advantage of dealing with tolerances in multiples DOFs. As a result, the metal plate (bonded to the reticle) gets defined by the support features and the tolerances of the holder do not interfere in the holding of the reticle.

A pneumatic parallel gripper uses the clamping force to hold the reticle on its two side surfaces by creating a force closure grasp. Similar to a suction cup, this holding option relies on a compressed air supply for its functioning (refer Appendix B.3 for details). The pneumatic parallel gripper is also relatively expensive and not as compact as other holding options.

Bond tape uses the adhesive force to hold the reticle to its top surface. It is very cheap and easy to use compared to other holding options. The main demerit of the bond tape is the difficulty to release the ReCa assembly post-curing as it forms a more or less permanent bond with the holding surface. In addition, the tape bonds are generally flexible, making them a less stiff option (refer Appendix B.4 for explanation). However, as they are available in different thicknesses, this flexibility can be minimized by using a thin tape.

3.2.2. Concepts for Reticle Holder

Permanent magnet with a knob option within the magnetic category was selected as the preferred option to design the reticle holder. This is because of its ability to function in the absence of a compressed air supply and an electric power supply. Besides, the knob ensures that the held component is smoothly released by controlling the magnetic flux to turn the holding forces ON and OFF. This keeps the cured bond intact and preserves the alignment in the ReCa assembly.

As discussed in the earlier subsection, an air gap is introduced in the magnetic circuit to deal with tolerances in multiple DOFs. The length of this air gap can be maintained by the support features (see figure 1.10) that map to the accessible top surface of the reticle. Hence, the metal plate is not directly attracted by the yoke and is only used to complete the magnetic circuit for adhesion. This is further elaborated in section 4.3.

Three concepts were designed for the reticle holder and are shown in figure 3.3 as section views. The magnets are represented in the form of gradients, with their north poles assumed to be on the darker ends. The black lines indicate the magnetic field lines and the arrows show their flow direction. In all three concepts, the yoke(s) and metal plate are considered to be made of ferritic or martensitic stainless steel as they possess good soft magnetic properties. These properties include high permeability, low coercive force, low residual magnetic flux density and high magnetic saturation flux density. Furthermore, the materials are easy to machine, commonly available, relatively cost-effective and have been used in several magnetic applications [24].

The concepts are presented in the form of two modes - OFF and ON modes that represent the OFF and ON holding forces on the metal plate, respectively.

(I) The first concept is similar to the example shown in figure B.3. The magnetic circuit consists of two

magnets, one yoke, two air gaps and a metal plate. Two diametrically magnetized disc magnets are placed in a cylindrical yoke, with the lower magnet fixed to the yoke. The top magnet can turn over 180° (using a knob) to enable the two modes. The metal plate experiences the adhesion force when the poles of the magnets are aligned one of top of the other (ON mode). The adhesion force is turned off by turning the knob 180°, thus cancelling the force on the plate (OFF mode) [29].

(II) In the second concept, a ferromagnetic screw is used. The magnetic circuit comprises a magnet, two yokes, one screw, two air gaps and a metal plate. A bar magnet is placed between the two rectangular yokes. The yoke on the left possess a mating thread to mount the screw, whereas the one on the right has a clearance hole. When the screw is partially engaged, the magnetic circuit gets completed via the metal plate, thus turning on the adhesion force on the plate (ON mode). On the contrary, in case of a fully engaged screw, the circuit gets completed via the screw, which cancels the force on the plate (OFF mode).

(III) The third concept uses a disc magnet. The magnetic circuit consists of a magnet, two yokes, two air gaps and a metal plate. A diametrically magnetized disc magnet is placed in diametrical cutouts of the two yokes. The magnet can turn over 90° (using a knob) to enable the two modes. The metal plate experiences the adhesion force when the poles are aligned parallel to the plate (ON mode). Turning the magnet 90° cancels the adhesion force as the magnetic field lines pass through the yokes [46].

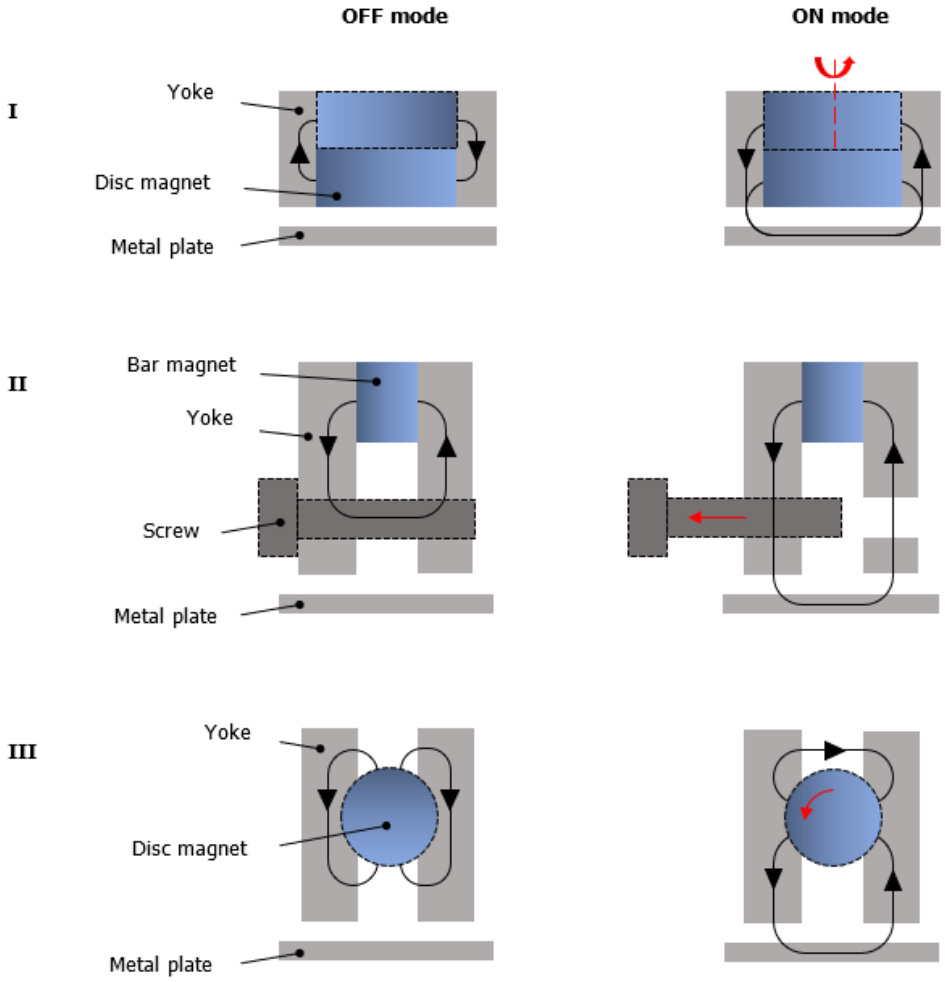

Figure 3.3: Concept designs for reticle holder

3.2.3. Proposed Holder Design

Concept III was selected as the proposed concept to design the reticle holder. This is because it does not have a removable component like the screw of concept II. Besides, there is no indication to the operator on

when to stop slackening the screw in concept II. With too much slackening, the screw will be removed completely. At the same time, limited slackening can partially direct the magnetic field lines via the screw that will reduce the adhesion force on the plate. Moreover, when compared with concept I, there is no need to fix a magnet on the yoke. Concept III offers more convenience by placing the disc magnet in the diametrical cutouts and simply turning it (using a knob) to control the adhesion forces on the metal plate. For the indication of the two modes, a stopping feature for the knob can be integrated in the mechanism.

3.3. Carrier Mount

Like the holder for the reticle, a mount is required for the carrier. The mount must be able to release the assembly of components post-curing and it must provide a stiff grip without any slip (refer subsection 3.2.1). Broadly speaking, there are several ways to mount a component. For the carrier, its existing features were considered for designing the mount. As seen in figure 1.7, the carrier has three V-grooves on its bottom surface. The intersection of these V-grooves coincides with the axis of the M4 thread. Taking these features into account, **a Maxwell kinematic constraint option was chosen to mount the carrier.** The advantages of kinematic constraints are already explained in section 1.2.2. The V-grooves shall come in contact with three bearing balls or hemispherical tips in the presence of a preload to form the constraint. Therefore, a stiff connection without any backlash is formed due to the setting. Lastly, a screw can be used to comfortably unmount the carrier without introducing any jerks or disturbance forces.

3.4. Manipulator Body

A manipulator body is needed to perform the adjustments between the reticle and carrier. Additionally, the purpose of the body is to house the supporting components or subassemblies that are important for its functioning (like actuators, reticle holder etc.). There are several ways in which the adjustment can be performed. One way can be to design the manipulator body such that it allows for adjustments in all 6 DOFs. This removes the need to have an additional setup to constrain the remaining 3 DOFs (refer M3 requirement). Nevertheless, leaving all 6 DOFs adjustable generally adds complexity for the operator.

An alternative can be to design the manipulator body such that it only permits adjustments in the desired 3 DOFs (refer M0 requirement). And utilize a preload assembly (as discussed in section 3.5) to form an in-plane contact between the components, thus constraining the remaining 3 DOFs. The latter way is preferred and the concepts for the manipulator body are designed and described in subsection 3.4.1. Note that there are other alternatives as well like leaving more than the desired 3 DOFs adjustable, but they are also not preferred because of complexity.

3.4.1. Concepts for Manipulator Body

There are a number of factors that contribute to the design of the manipulator body. First is how the alignment DOFs are assigned to the reticle and carrier. One way could be to keep the reticle fixed and manipulate the carrier in Tx, Tz and Ry. Another way could be to assign the Tz adjustment to the reticle and the Tx & Ry manipulations to the carrier. In total, there are 8 possibilities. Second is the type of flexural element or their combinations used to build the concept. Some commonly used elements are: struts, leaf springs, folded leaf springs, circular hinge, cartwheel hinge (or Haberland hinge), cross-axis pivot and LITF pivot [49].

For the manipulator body, top-to-bottom approach is followed to devise concepts. This means that the assignment of the alignment DOFs and the selection of flexural elements (as explained in the earlier paragraph) are not done first. Instead, the basic idea for the manipulations is laid out. This is integrated with the above-mentioned supporting factors based on practicality and functionality.

Eight concepts were designed for the manipulator body and are shown in the form of simple layouts in figure 3.4. All designs are represented in the XZ-plane as per the coordinate system. The orange bodies denote the fixed structure, while the blue bodies are adjustable. The black line is a leaf spring and the red dot is the point of rotation. The actuators are shown in the form of bidirectional arrows and have been given reference numbers. They are placed at approximate locations in the layouts to better understand adjustments. Moreover, the pretension springs necessary to ensure contact between the actuators and adjustable bodies are not shown. Furthermore, the reticle holder and the carrier mount are not part of the concept layouts. As the design of the alignment mechanism progresses, these two will be integrated at the right locations during the detailing phase.

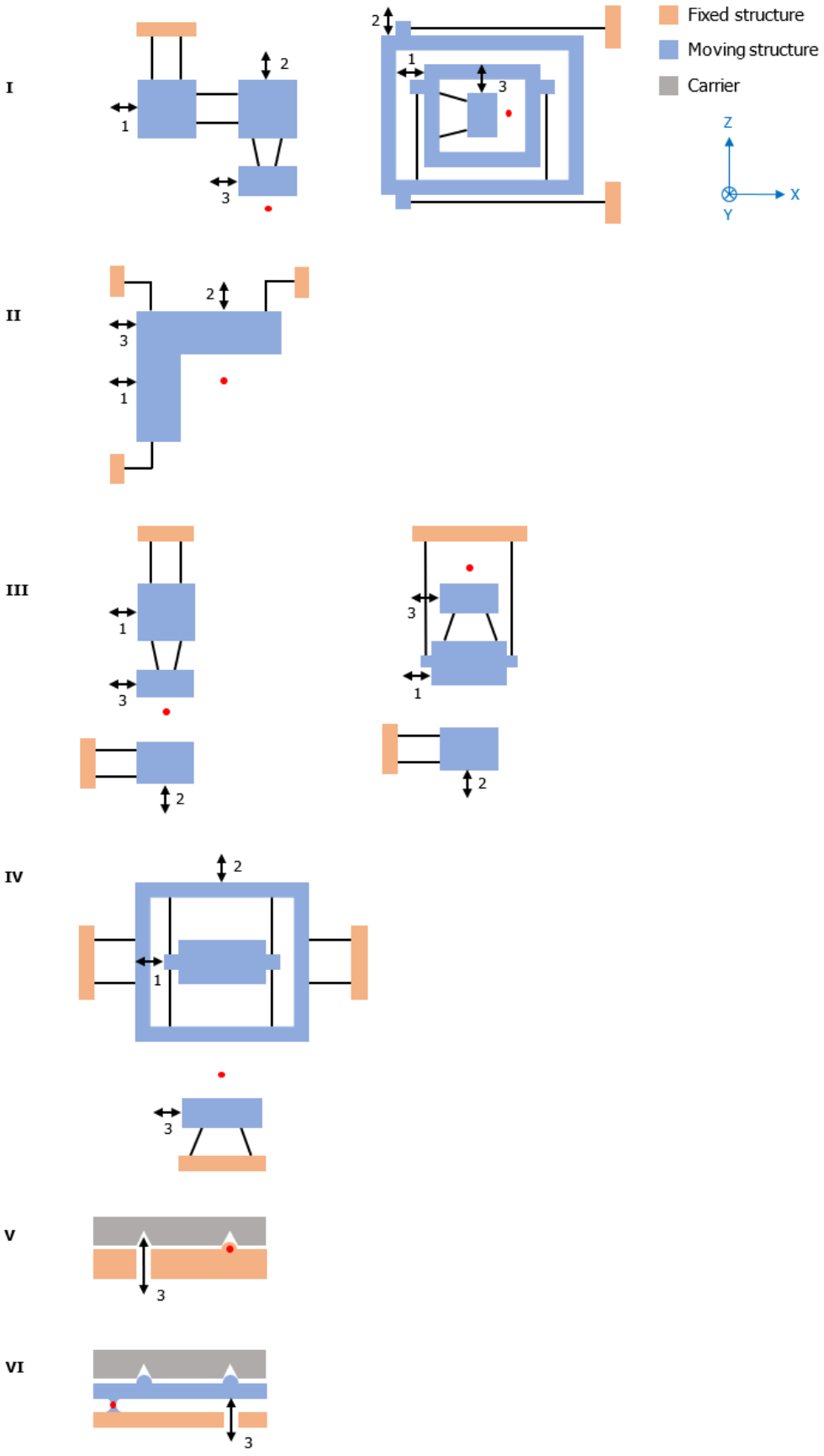
I
II
III
IV
V
VI
Fixed structure
Moving structure
Carrier
Z
X
Y

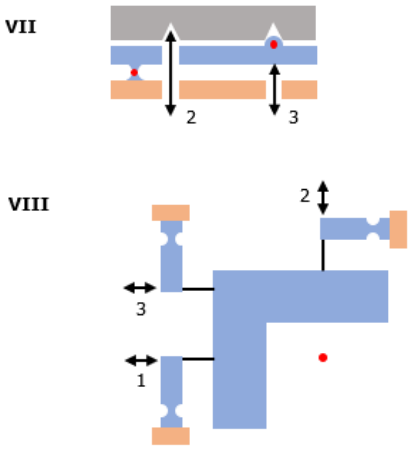

Figure 3.4: Concept layouts for manipulator body

3.4.2. Concept Evaluation

The evaluation of the concepts is done by looking at the pros & cons and the working principle of each of them. As the reticle and carrier have to be aligned via the desired points of each other (refer red highlighted points in figure 3.5), it is preferred to keep the point of rotation for the Ry adjustment at one of these desired points. This is especially useful for concepts where the point of rotation does not undergo any parasitic motion during the Ry adjustment in principle.

Figure 3.5: Preferred Ry rotation points

For the subsequent content of this subsection, please see figure 3.4.

(I) The first concept consists of two parallelogram guides (2×2 leaf springs), together with one LITF pivot (1×2 leaf springs) that has a virtual rotation point. It uses three actuators for the three desired adjustments. Actuator '1' is for the Tx adjustment, '2' is for the Tz adjustment and '3' provides the Ry adjustment. The concept shown in the left has the three DOFs stacked on top of each other, whereas the one on the right has the stacking inside of each other [31]. These layouts are used to adjust only one component in the three in-plane DOFs, while keeping the other one fixed.

Pros: When the pivot is stacked last w.r.t. the fixed structure, the Tx and Tz adjustments are aligned to the X- and Z-axis of the reference coordinate system, respectively.

Cons: Firstly, the concept possess three overconstraints. These can be tackled by using notched leaf springs to free up one DOF each. Secondly, there is parasitic motion along the X- and Z-axis due to the presence of parallelogram guides. For instance, the Tx adjustment moves the connecting blue body along the Z-axis (for the shown layout). The parasitic motion can either be tackled by performing iterations or using a serial flexure setup (increases complexity, see figure A.3 and its explanation in Appendix A.1). Besides, there is also a center-shift of the LITF pivot due to the Ry adjustment. Thirdly, the stacking makes it difficult to follow the manipulations. Also, the stacked arrangement can claim large volume. Finally, there is slip and friction between the actuator tip and the adjustable body due to parasitic motion. For instance, the Tz adjustment will move the connecting blue body leftwards (due to parasitic motion) causing slip at the tip of actuator '2' (for the shown setup). Moreover, the friction near the contact surface can restrict the connecting body to follow during further adjustments.

(II) In the second concept, three folded leaf springs are used to constrain the remaining 3 DOFs (refer M3 requirement). It also uses three actuators for manipulations. The rotation point is virtual, which lies at

the intersection of actuators '1' and '2'. The other rotation point due to the actuators '3' and '2' is not shown. Actuators '3' and '1' together are used for the Tx adjustment, '2' is for the Tz adjustment and '3' provides the Ry adjustment. Since the layout involves the adjustments of the three in-plane DOFs, only one component can be adjusted and the other one has to remain fixed.

Pros: Firstly, the concept is an exact constraint design. Secondly, the rotation point can be controlled to be close to one of the preferred rotation points of the component. Thirdly, there is no parasitic motion between the two translational axes (X- and Z-axis). Fourthly, the layout can be useful for small volume claim. Lastly, the Tx and Tz adjustments can be aligned to the X- and Z-axis of the reference coordinate system, respectively.

Cons: Firstly, there is slip and friction between the actuator tips and the blue body due to adjustments. For instance, the manipulation of the adjustable body in Tz via the actuator '2' will result in slip at the tips of the left two actuators. Besides, the friction near the contact surface of the actuator '2' can restrict the body to follow the Tx adjustment afterwards. Secondly, for the Tx adjustment, a synchronized actuation of the actuators '1' and '3' is required. A sequential adjustment can be carried out as well (with some iterations) to meet the desired end-result.

(III) The third concept uses the same flexural elements and the same number of actuators as Concept I, which provide the same functionality. Although instead of fixing one component and adjusting only the other in the desired three DOFs, these DOFs are spread out between the two components. An example of one such concept layout is shown in figure 3.4. The Tx and Ry adjustments are assigned to one component (top part with actuators '1' and '3'), while the Tz adjustment is given to the other component (bottom part with actuator '1').

Pros: When the pivot is stacked last w.r.t. the fixed structure, its preceding translational adjustment is aligned to the coordinate axis (explained in concept I).

Cons: Firstly, the layout has two overconstraints on the stacked side and one overconstraint on the non-stacked side. These can be tackled by using notched leaf springs to free up one DOF each. Secondly, the parasitic motion due to the parallelogram guides continues with this concept, along with the center-shift of the LITF pivot (explained in concept I). Thirdly, the stacked arrangement can lead to large volume claim. Finally, the issues of slip and friction are also present in this concept (explained in concept I).

(IV) In the fourth concept, two symmetric parallelogram guides (2×4 leaf springs) are used in a nested arrangement, along with one LITF pivot (1×2 leaf springs). The alignment DOFs are spread out between the two components such that the Ry adjustment is assigned to one component. Actuator '1' is for the Tx adjustment, '2' is for the Tz adjustment and '3' provides the Ry adjustment.

Pros: Because of the symmetric arrangement of the leaf springs, there is no parasitic motion observed along the X- and Z-axis.

Cons: Firstly, the layout has the biggest disadvantage of having too many overconstraints. It has 14 overconstraints on the nested side and 1 on the pivot side. Secondly, because of the symmetry in each parallelogram guide, more stresses are observed for the same range of motion in comparison to a parallelogram guide. Lastly, the issues of slip and friction persist in this concept. For instance, actuation along the Z-axis would result in slip at the tip of actuator '1' and friction near the contact surface of actuator '2'.

The concepts V–VII use the V-grooves of the carrier to achieve one or more adjustments in the desired DOFs. The grey body represents the carrier with its V-grooves. For simplicity, these V-grooves are represented in the XZ-plane, instead of their actual orientation of 120° between two groove axes (see figure 1.7).

(V) The fifth concept uses actuator '3' to perform the Ry adjustment. The hemispherical tip of the actuator touches the V-groove located below the resting surface of the carrier (see figure 1.7). The other two V-grooves form contact with two bearing balls (or two hemispherical ball tips). In this layout, the point of rotation is located at the intersection of the contact normals of the V-groove and the bearing ball surfaces. This layout assigns the Ry adjustment to one component and the translational adjustments to the other. For the Tx and Tz adjustments, any of the suited concepts from III (stacked parallelogram guides) or IV (nested symmetric parallelogram guides) can be considered.

Pros: As the existing features of the carrier are utilized, no new layout is needed for the Ry adjustment.

Cons: Firstly, the rotation point cannot be mapped to one of the preferred rotation points as it is located below the resting surface of the carrier. Secondly, because of the rotation of the carrier via its V-groove, slip will occur in the region with bearing balls which is not desirable.

(VI) In the sixth concept, a circular hinge is used instead to get the required Ry adjustment. The Ry rotation point is located at the center of the hinge. Note that the circular hinge provides a small rotation angle because of the stress concentration around its center pivot point [15]. Three bearing balls are used to fix the carrier via V-grooves using the principle of kinematic constraint. This layout also assigns the Ry adjustment to one component and the translational adjustments to the other. For the Tx and Tz adjustments, any of the suited concepts from III (stacked parallelogram guides) or IV (nested symmetric parallelogram guides) can be considered.

Pros: No slip is observed near the V-grooves as the carrier remains fixed to the adjustable body.

Cons: With the current layout, the rotation point cannot mapped to one of the preferred rotation points.

(VII) The seventh concept is a combination of the previous two concepts (V and VI). It uses two actuators to manipulate the carrier in Ry and Tz. Actuators '2' & '3' are for the Tz adjustment and actuator '2' is for the Ry adjustment. While both the actuators can be used for rotational adjustments, actuator '2' is preferred over actuator '3' to have better control over the adjustment. The adjustment from actuator '2' would rotate the carrier about the right highlighted dot, while the adjustment from actuator '3' would result in a combined effect of the rotation about the left highlighted dot and the ball tip of actuator '2'. This concept layout also needs the adjustments of both the components. For the Tx adjustment, any of the suited concepts from III (a parallelogram guide) or IV (a symmetric parallelogram guide) can be considered.

Pros: Firstly, using the existing features of the carrier, two of the desired DOFs are adjusted. Secondly, the layout can be useful for small volume claim.

Cons: Firstly, both the rotation points are below the resting surface of the carrier. Therefore, they cannot be mapped to one of the preferred rotation points. Secondly, slip persists in this concept which is not desirable (explained in concept V). Thirdly, there is crosstalk between the axes that is also not desirable as it increases the number of adjustment steps.

(VIII) In the eighth concept, each folded leaf spring of concept II is replaced with a stacked combination of a leaf spring and an elastic hinge. Moreover, the actuators are placed in line with the leaf springs with their ball tips in contact with the hinged bodies. The rotation point is virtual, which lies at the intersection of actuators '1' and '2'. The other rotation point due to the actuators '3' and '2' is not shown. Actuators '1' and '3' together are for the Tx adjustment, '2' is for the Tz adjustment and '3' provides the Ry adjustment. Furthermore, the layout only permits the adjustments of one component, while keeping the other one fixed.

Pros: Firstly, the slip at the tips of the actuators is greatly reduced. It is only caused in a limited amount due to the rotation of the circular hinge when the corresponding actuator is adjusted. Secondly, the rotation point can be controlled to be close to one of the preferred rotation points of the component. Thirdly, the layout can be useful for small volume claim. Lastly, the Tx and Tz adjustments can be aligned to the X- and Z-axis of the reference coordinate system, respectively.

Cons: Firstly, the layout has three overconstraints because of the presence of hinges. For instance, the hinge in touch with the actuator '2' has a rotational overconstraint about the X-axis. This can be tackled by symmetrically removing the material in the hinged body about the XZ-plane placed at the center along the Y-axis. Doing so creates a rotational axis due to the T cross-section, which relieves the overconstraint. The same operation can be carried out in the other two hinges. Secondly, there is crosstalk between the X- and Z-axis. For instance, the Tz adjustment will move the center adjustable body along the X-axis (for the shown layout). This can be tackled by performing iterations.

3.4.3. Manipulator Body Concepts Overview

A summarized overview of all concept layouts is shown in table 3.2. The concepts are compared against different parameters that are explained below:

- **Compactness**: If the concept claims less volume.
  Either '+' (compact or claims small volume) or '–' (claims large volume).
- **Parasitic motion/crosstalk**: If there is parasitic motion or crosstalk in any part of the concept.
  Either '+' (no or limited parasitic motion or crosstalk in principle) or '–' (parasitic motion or crosstalk present). Besides, '0' can either be '+' or '–' depending on the layout of the translational DOFs for the concept.
- **Slip & friction**: If the issues of slip and friction exist in the concept.
  Either '+' (limited slip and friction) or '–' (ample slip and friction).
- **Overconstraints**: If the concept design in principle has any overconstraints.
  Either '+' (no overconstraint) or '–' (overconstraint present).

Table 3.2: Comparative analysis of manipulator body concepts

Concept	Parameter			
	Compactness	Parasitic motion/crosstalk	Slip & friction	Overconstraints
I	–	–	–	–
II	+	+	–	+
III	–	–	–	–
IV	–	–	–	–
V	–	0	–	–
VI	–	0	–	–
VII	+	–	–	–
VIII	+	–	+	–

3.4.4. Proposed Manipulator Body Layout

Out of all designs for the manipulator body, **concepts II and VIII were shortlisted for further analysis based on their pros & cons (refer subsection 3.4.2) and the comparative analysis (refer subsection 3.4.3).** Concept II has the merit of being an exact constraint design with no parasitic motion or crosstalk in the two translational axes. There is also an opportunity to control the Ry rotation point and map it to one of the preferred rotation points (see figure 3.5). Additionally, due to the layout, the design can be made compact. Nevertheless, the concept has disadvantages of slip and friction between the actuator tips and the moving body.

Concept VIII, on the other hand, has the advantages of limited slip and friction over concept II. Because of the layout, the design can also claim less volume. Similar to concept II, the Ry rotation point can be controlled and mapped to one of the preferred rotation points. Although the issue of overconstraints exist in the design, these can be tackled by symmetrically removing the material in the hinged bodies. This creates a rotational axis in each hinged body due to the T cross-section. However, the concept has a disadvantage of parasitic motion in the two translation axes.

Finally, **concept VIII was selected as the proposed concept layout to design the manipulator body**. This is primarily because of the advantages of limited slip and friction it offers when compared to concept II. Although there is parasitic motion in the design, this can be tackled by performing iterations.

3.5. Preload Assembly

The concepts in the previous section allow the 3-DOF alignment (refer M0 requirement) between the reticle and carrier. This leaves the remaining 3 DOFs (Rx, Rz and Ty) that need to be constrained in some way. For this, the components either need to be in contact with each other (in-plane alignment) or within the specified limits as stated in the M3 requirement. So far, this was carried out by using two O-rings on the cylindrical supports of the carrier (see figure 1.8). Their compression provided the required pretension force that held the reticle and carrier together during adjustments. Nevertheless, there are some disadvantages associated with using this preload method (refer section 1.4 for details).

To avoid the use of O-rings for preload, a new concept was designed as shown in figure 3.6a. It uses two compression springs, which are loaded in a compressed state on the axes of the pins. One end of the springs

is placed in contact with the flange, which is a fixed structure. The pins are connected to the cover that can be actuated along the Y-axis. This actuation moves the pins to generate a preload force. When the back surface of the reticle (see figure 1.4) behind the green faces of the carrier (with the knife edges, see figure 1.6) comes in contact with the pins, it experiences this force. By doing so, an in-plane contact is formed between the two main components that constrains the remaining 3 DOFs.

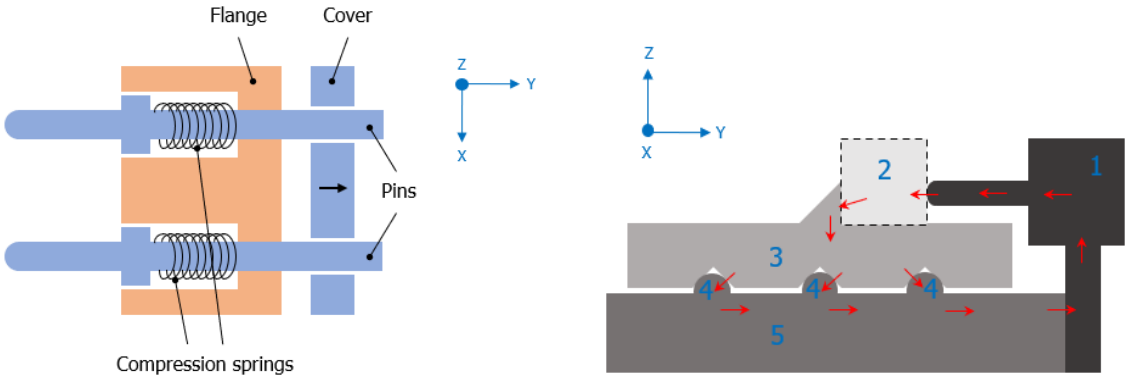

(a) Proposed concept

(b) Force path

Figure 3.6: Preload assembly

Figure 3.6b shows the approximate path (shown by red arrows) the preload force takes due to the preload assembly. For simplicity, the three V-grooves are represented in the YZ-plane, instead of their actual orientation of 120° between two groove axes. The preload is experienced on the back surface of the reticle '2' by two pins. This brings the reticle in contact with the green faces of the carrier '3'. The carrier is mounted '4' using the principle of kinematic constraint via its three V-grooves located below the resting surface. The mount for the carrier is fixed on the manipulator body '5'. In this way, the path gets completed back to the preload assembly '1' that is mounted using the flange.

As the pins are placed in line with the contact surfaces (behind the green faces of the carrier), a better contact is formed between the two components since the preload is experienced in the region of interest. However, the disadvantage of using the limited height of the green faces of the carrier (= 1.6 mm, refer table 1.2) to constrain the Rx DOF continues with this concept. This can be minimized by placing the pins as low as possible (along the -Z direction) while keeping enough clearance from the resting surface of the carrier. As a result, the turning effectiveness of the preload becomes higher to better constrain the Rx DOF. Note that to apply the preload assembly concept, the cylindrical supports of the carrier need to be removed to avoid collision with the pins. This change does not affect the overall dimensions of the carrier or its functionality.

3.6. Conclusions

Flexures are preferred as the guide, together with fine screws/micrometers for manual alignment. The actuators must be selected in such a way that they satisfy the requirement for the MIM (refer M1 requirement).

A magnetic holder for the reticle is proposed that works with a permanent magnet and a knob. The holder provides a stiff grip in combination with mechanical support features to hold the reticle. It can also be used to smoothly release the ReCa assembly post-curing by turning the knob. For the carrier, the kinematic constraint option is chosen to stiffly mount it via its existing V-grooves.

A concept layout for the manipulator body is proposed that uses stacked combinations (3x) of a leaf spring and an elastic hinge to adjust the alignment DOFs (refer M0 requirement). To relieve the underlying issue of three rotational overconstraints in the design, symmetric material removal about the center XZ-plane is suggested. End stops need to be integrated in the design to avoid excess stresses during the adjustments.

A preload assembly that uses two compression springs is proposed to constrain the remaining 3 DOFs (refer M3 requirement) and ensure an in-plane contact between the reticle and carrier.

4

Detailed Design and Analyses

In this chapter, the proposed concept design for each of the functionalities and subassemblies of the alignment mechanism is detailed in a 3D model. Calculations and analyses are performed that contribute to decision making.

4.1. Actuation

As discussed in subsection 3.1.2, fine or differential screws are the preferred actuators to adjust the moving structure. Having looked at various options in the market, a 1/4"–100 screw is selected for actuation [41]. This is because the screw has a pitch (distance travelled in one revolution or 360° turn) of 0.254 mm. The pitch, if translated to the sensitivity for 1° turn, gives a value of 0.71 µm. 1° turn is taken as the minimum achievable movement by an operator with a sensitive touch [47]. Hence, the screw offers the MIM of 0.71 µm for linear adjustments. This value is less than half of the required MIM of the Tz adjustment and around seven times less than the MIM of the Tx adjustment (refer M1 requirement). Besides, the MIM of the Ry adjustment depends on the distance between the axes of actuators '3' and '1' in the manipulator body (see figure 1.10) and the MIM of the actuator '3'. The former is considered while keeping enough clearance between the knobs for ease of operation and the latter is covered in subsection 4.5.4. Note that the actuator screws come with ⌀ 4.8 mm ball tips that are made of SS 440 material. Additionally, each screw can tolerate a maximum load of 6.8 kg (or 66.6 N).

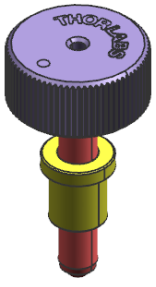

Figure 4.1: Isometric view

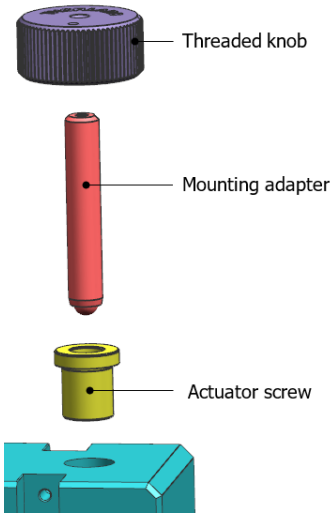

Figure 4.2: Exploded view

Figure 4.3: Actuation

Since the actuators screws are used for adjustments, directly creating the mating threads on the aluminium fixed structure is not preferred. The threads will become worn out with usage. An adapter is utilized instead to mount each screw [42]. The adapter is cylindrical in shape, consisting of a 1/4"–100 internal thread. The supplier recommends bonding the adapter using a clearance fit by applying an adhesive on the external surface of the adapter. The recommended adhesive is a Loctite Anaerobic Adhesive (680 or equivalent) that is used for bonding cylindrical joints [39]. Moreover, since manual adjustment of the screws is needed, a threaded knob is attached to the end of each screw for convenience [40]. The knob of a bigger diameter is preferred for better control over the screw sensitivity. Both the mounting adapter and the actuator knob are also selected from the same supplier for better integration with the actuator screw.

4.2. Carrier Mount

The existing V-grooves of the carrier were chosen to mount it to the fixed structure using the principle of Maxwell kinematic constraint (refer section 3.3). Three bearing balls or hemispherical surfaces of ⌀ 4 mm are needed to form six local contact areas with the carrier. Due to the limited space availability in press fitting the bearing balls and the large load a manual toggle press can generate, the option of press fitting the bearing balls is not chosen. Instead, three adjustment screws with ⌀ 4 mm ball tips are selected [22]. These screws are similar to the ones used for actuation (refer section 4.1) with 1/4"–100 threads on their external surfaces.

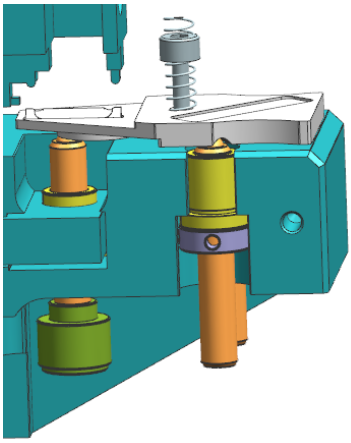

Figure 4.4: Carrier assembled with its mount

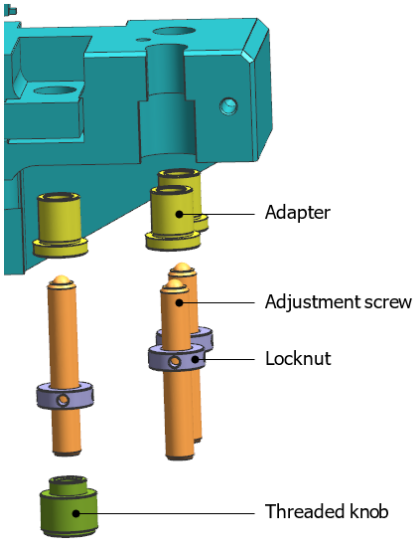

Figure 4.5: Exploded view of carrier mount

Figure 4.5 shows the exploded view of the mount with all its components. Each adjustment screw is mounted to the fixed structure using an adapter (see section 4.1 for explanation). Furthermore, a locknut with a 1/4"–100 internal thread is designed for each adjustment screw to define the height of the ball tip in the carrier mount. The locknuts are bonded at certain distances to the adjustment screws using a threadlocker or via holes using an epoxy adhesive.

Note that the left adjustment screw is used, along with the three actuator screws to unmount the cured ReCa assembly after the alignment. The slackening of these four screws creates space to unmount the ReCa assembly. For that reason and to avoid confusion, a threaded knob is attached to the left adjustment screw (see figure 4.4). The knob is also selected from the same supplier for better integration with the adjustment screw [21]. Concerning the other two adjustment screws, they must not be tampered with once they are assembled on the manipulator body.

4.3. Reticle Holder

Concept III of the reticle holder, which uses a disc magnet, was the proposed design to grip the reticle (refer section 3.2.3). The first subsection describes the design of the magnetic holder (refer subsection 4.3.1). This is followed by the magnetic flux analysis of the holder to simulate its working (refer subsection 4.3.2).

4.3.1. Holder Design

The exploded view of the reticle holder without the holder knob is shown in figure 4.6b. It consists of two yokes, a disc magnet, a bushing and three spacers. A diametrically magnetized disc magnet (⌀ 10 mm × 5 mm) made of NdFeB material is chosen. The material offers strong magnetic force while being lightweight and is well-suited for limited space applications. The magnet also comes with a protective nickel coating to prevent corrosion [33] [32]. Moreover, a cylindrical bushing made of brass is designed to bond the magnet inside it (refer section 5.1), using an epoxy adhesive via the radial holes of the bushing. The reasons for using the bushing are the high strength (for limited wear) and low friction (for relatively smooth movement during turns), along with non-ferromagnetic nature of the brass (to avoid interference with the magnetic circuit).

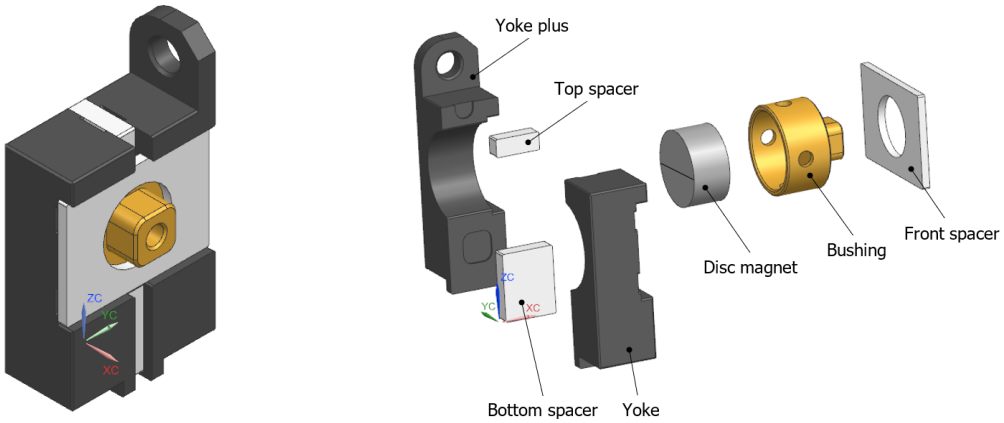

(a) Isometric view (b) Exploded view

Figure 4.6: Reticle holder (without knob)

The bushing, together with the magnet is placed between two yokes in their diametrical cutouts. SS 430 material is considered for the yokes as its a ferritic steel that possesses good soft magnetic properties (refer section 3.2.2 for details), is corrosion resistant, machinable and available at supplier [24] [10]. Besides, the spacing between the yokes is maintained by the top and bottom spacers made of Al 5754, which is a non-ferromagnetic material also available at the supplier. These spacers are bonded to the yokes using an epoxy adhesive applied to the pockets present in the yokes. Lastly, a front spacer of Al 5754 is bonded to the two yokes to restrict the motion of the bushing in that direction. The motion in the other direction is stopped by the manipulator body, when the holder is assembled on the moving structure. To avoid friction between the bushing and the front spacer, a small gap is kept between them in the design. Figure 4.6a displays the assembled design of the reticle holder (without the holder knob).

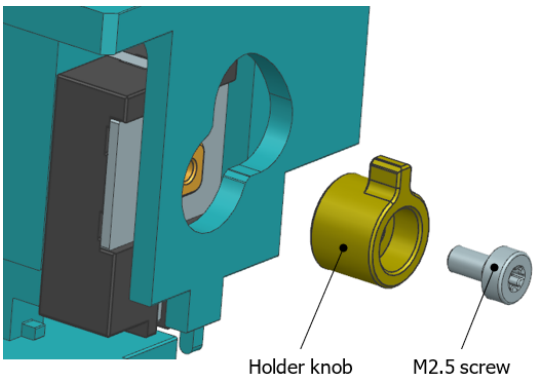

Figure 4.7: Holder knob assembly

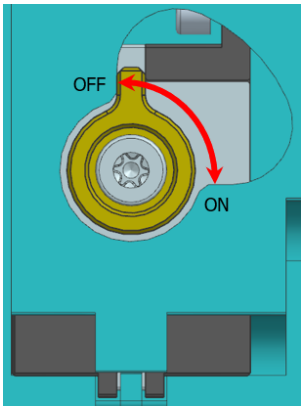

Figure 4.8: Actuation of reticle holder

Once the holder is mounted on the moving structure, a knob is attached to the bushing through a cutout as shown in figure 4.7. The protrusion of the bushing mates with the pocket in the holder knob and the parts are put together using a screw. A threadlocker can be used on the screw thread to prevent loosening of the screw.

Figure 4.8 shows how the knob can be turned 90° to achieve the ON and OFF modes of the holder. Any extra turn of the knob is stopped by the cutout in the moving structure that act as end stops.

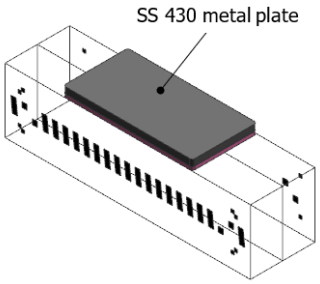

Figure 4.9: Metal plate for reticle

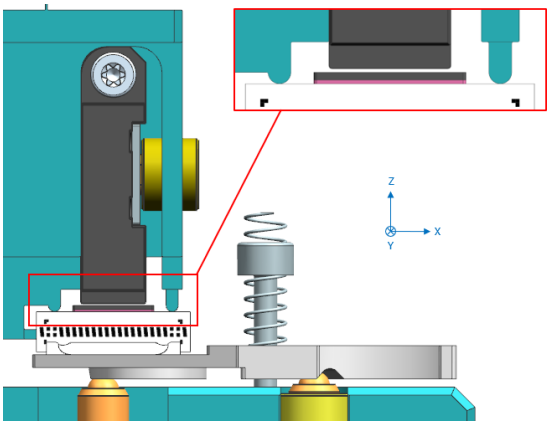

Figure 4.10: Reticle held by magnetic holder

As discussed in subsection 3.2.1, a ferromagnetic interface needs to be added to the reticle to utilize the magnetic holding option. This interface is added in the form of a 0.5 mm thick metal plate made of the same material as the yokes. The plate is bonded to the top surface of the reticle using an adhesive tape, as it is one of the feasible holding surfaces (see figure 3.2). The final assembly of the reticle is shown in figure 4.9.

Figure 4.10 shows the held position of the reticle by the holder (ON mode). The accessible top surface of the reticle maps to the support features (see figure 1.10) to define the Z-position and the Ry of the reticle. Furthermore, the dimensions of the holder are decided in such a way that the yokes never touch the metal plate in the held setting. As a result, an air gap of 0.25 mm in the nominal dimensions is formed in the magnetic circuit to account for the tolerances in multiple DOFs.

4.3.2. Magnetic Flux Analysis

A 2D magnetic flux analysis is performed in FEMM Magnetics to simulate the working of the magnetic holder. The 2D plane selected is the YZ-plane as shown in figure 4.10. Additionally, it is assumed that the part of the magnetic circuit that mainly contributes to the magnetic force is determined by the thickness of the disc magnet. Therefore, a depth of 5 mm is fed into the model to scale up the integral results during post-processing.

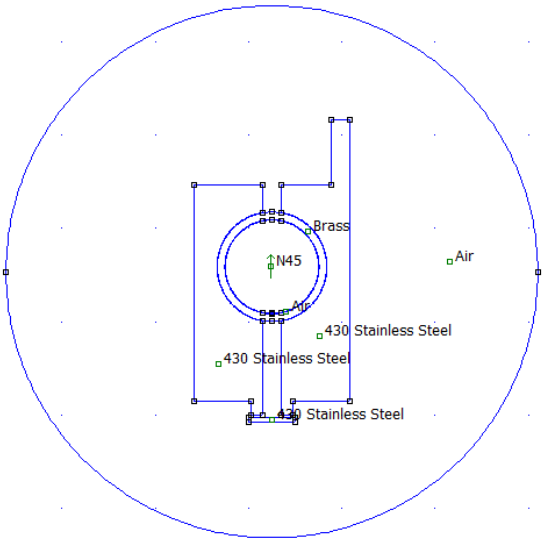

Figure 4.11: FEMM model (OFF mode)

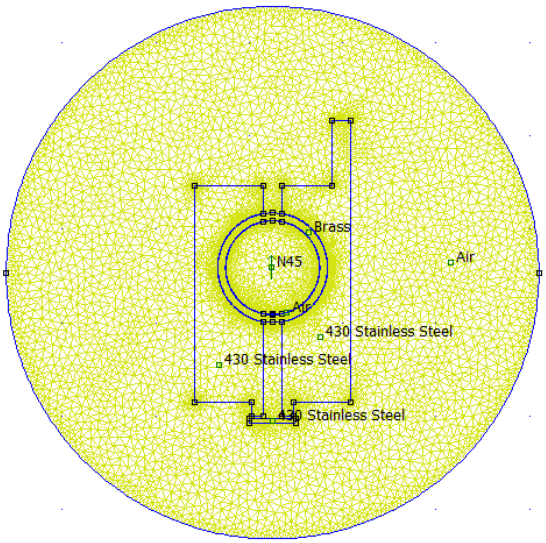

Figure 4.12: Default mesh generated (OFF mode)

Figure 4.13: Simulation model of reticle holder

The FEMM model of the reticle holder in its OFF mode is shown in figure 4.11. It is built up using nodes with the appropriate holder dimensions, where each area formed by the nodes is assigned the respective material. These are NdFeB (N45 magnetization) for the magnet, brass for the bushing, SS 430 for the yokes and the metal plate, and lastly, air for the surrounding and air gaps. Figure 4.12 shows the default mesh generated by the solver.

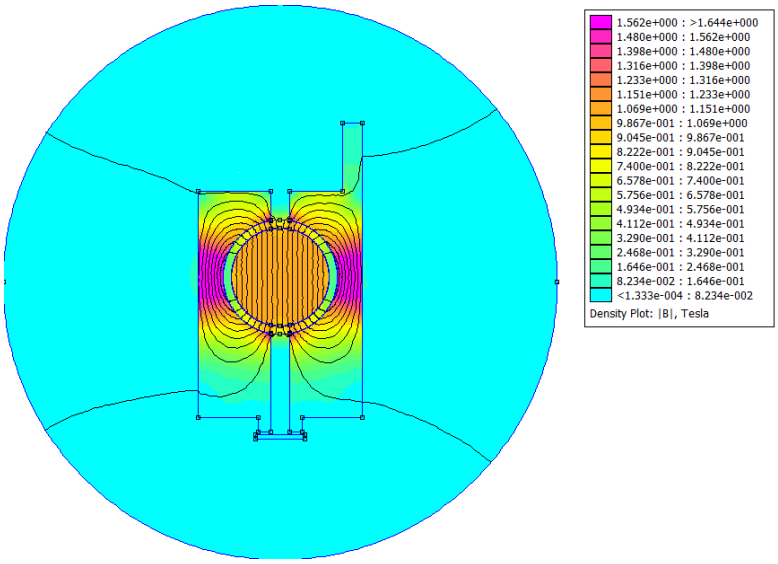

Figure 4.14: Plot of magnetic flux density (OFF mode)

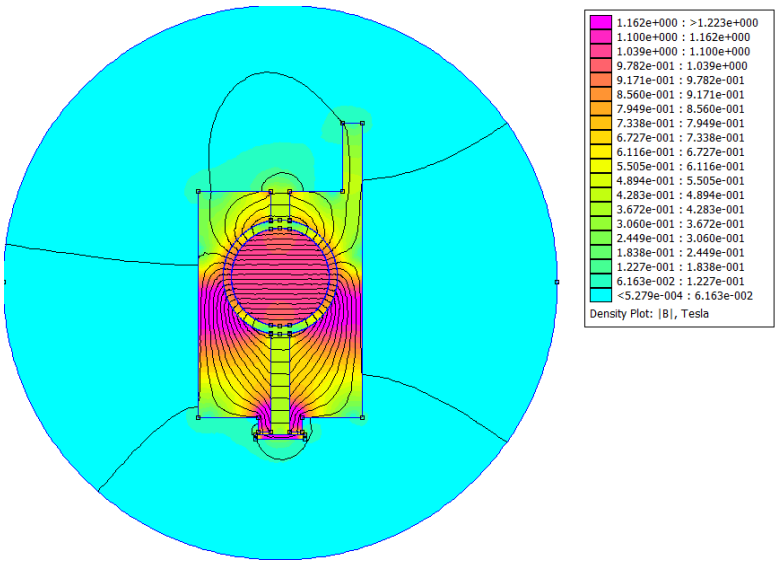

Figure 4.15: Plot of magnetic flux density (ON mode)

Table 4.1: Results of magnetic flux analysis

Parameter	OFF mode	ON mode
$\|B\|$	$< 1.3e^{-4}$ T	> 1.223 T
F_{hor}	$-6.4e^{-5}$ N	-0.001 N
F_{ver}	0.003 N	2.592 N

The solver is run to get the flux density plots for the OFF and ON modes as shown in figures 4.14 and 4.15, respectively. The magnetization direction of the magnet is altered to get the two modes of the holder. Besides,

the results of the study are represented in table 4.1, where $|B|$ is the magnetic flux density (in T), F_{hor} and F_{ver} are the forces experienced by the plate along the horizontal and vertical directions, respectively (in N).

In the OFF mode, it is observed that almost no field lines pass through the metal plate and they get directed to the yokes because of the orientation of the disc magnet. This produces a negligible attraction force on the metal plate in the vertical direction. Furthermore, SS 430 material has the magnetic saturation value of 1.66 T [10]. It is seen that because of the dimensions of the yoke and the strength of the magnet, the saturation takes place in both the yokes (pink region). On the contrary, in the ON mode, the field lines pass through the metal plate in combination with passing through the yokes. Hence, an attraction force of 2.6 N is experienced by the plate in the vertical direction. This value is five times more than the frictional force generated between the reticle and carrier due to the force applied via the preload assembly (refer section 4.4 for details). Thus, the holding action is performed without any issue.

Figure 4.10 (see the zoomed in region) shows how the stiffness loop goes through the support features and the reticle, while the force loop goes through the reticle holder and the metal plate. Considering the friction coefficient of 0.5 (refer section 4.4 for explanation) between the support features & the reticle and the holding force of 2.6 N (refer table 4.1), the lateral force required to move the reticle comes out to be 1.3 N.

Moreover, to take care of the misalignment of the plate along the Y-axis, the width across the yokes near the metal plate (= 4.6 mm) is kept less than the width of the plate (= 5 mm) in their nominal dimensions. This is done to allow most of the field lines to pass through the metal plate that avoids the generation of force in the horizontal direction on the plate. Consequently, it minimizes the disturbance to the in-plane contact of the reticle with the carrier that is important for the alignment. An analysis for this horizontal force was performed. It is observed that for every increase in misalignment in multiples of 0.2 mm (checked till 0.6 mm), there is a corresponding increase in the horizontal force of approximately 0.1 N in the direction opposite to the misalignment. A similar thing is done along the X-axis by keeping the length of the plate more than the width across the two yokes. Lastly, it is observed that the attraction force on the metal plate decreases exponentially with the increase in the air gap distance in the magnetic circuit.

4.4. Preload Assembly

Figure 4.16a shows the isometric view of the preload assembly needed to constrain the remaining 3 DOFs (refer M3 requirement). It comprises a flange, two pins, two compression springs, four circlips, one cover and a screw (see figure 4.16b). Each compression spring is placed on the axis of pins. The spring has an initial length of 4 mm and a stiffness of 0.5 N/mm [37]. In the nominal dimensions, each spring is compressed by 1 mm, resulting in a preload force of 1 N (in total). This value is taken as an approximation to press the reticle against the carrier (in-plane contact) without doing any damage to the former.

Parallelly, the friction is seen between the reticle and carrier as a consequence of the applied preload. With a coefficient of friction of 0.5 (glass-metal contact) [5] and the preload force of 1 N, the frictional force comes out to be 0.5 N. Therefore, 0.5 N of extra force needs to be overcome by the actuators to adjust the reticle w.r.t. the carrier. Note that the friction between the pins and reticle is neglected for simplicity.

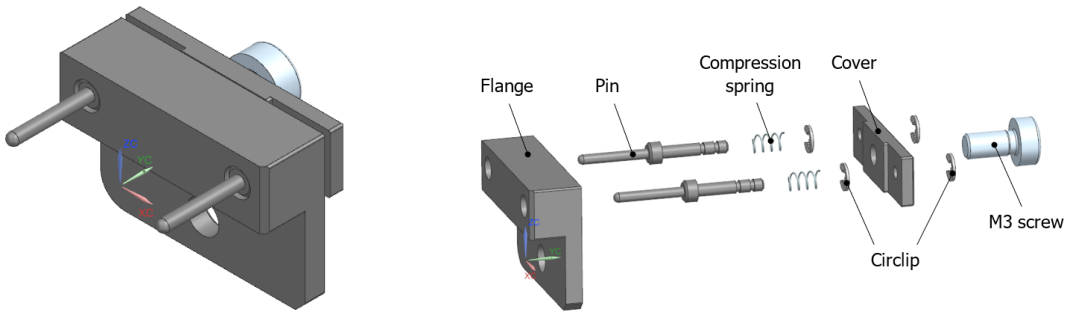

(a) Isometric view

(b) Exploded view

Figure 4.16: Preload assembly

The groove ends of the pins are connected to the cover using four circlips (two for each pin, see figure 4.17). Furthermore, the cover contains a thread that mates with the screw. The base of this screw rests in a pocket

on the flange. Since the preload assembly is mounted on the manipulator body via the flange, the clockwise rotation of the screw retracts the cover that in turn retracts the pins (see the arrow in figure 4.18). In this way, the contact with the reticle gets lost to remove the preload force experienced on the component. The retraction of the pins is done before removing the preload assembly from the alignment mechanism – to unmount the cured ReCa assembly and mount the next batch of the carrier for alignment.

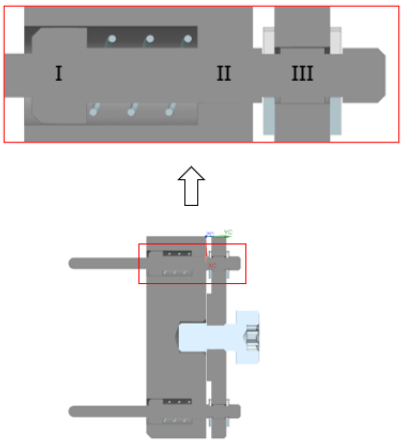

Figure 4.17: Section view of preload assembly

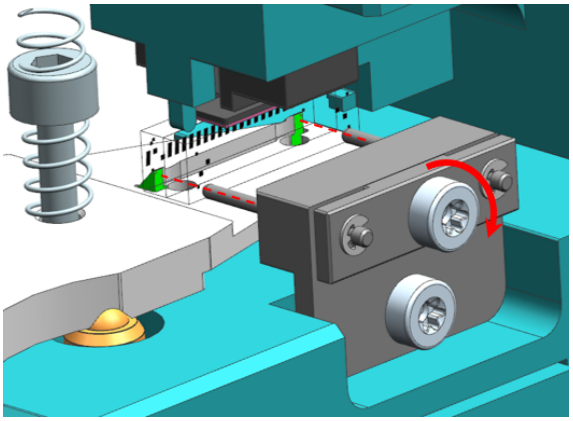

Figure 4.18: Retracting pins in preload assembly

To avoid any overconstraints in the preload assembly, each pin must only permit 2 DOFs, i.e., translation along the Y-axis and rotation about the Y-axis. Therefore, the pin is kept in contact with only a part of the flange – region II. The other regions (I and III) are designed keeping some clearance with the pin diameters (see figure 4.17). Additionally, the mounting position for the preload assembly is designed in such a way that the pins come in line with the contact surfaces (shown by dotted lines in figure 4.18). This is done to ensure that the preload is experienced in the region of interest, i.e., within the green faces of the carrier. As the height of the green faces is only 1.6 mm (refer table 1.2), the design is made in such a way that the pins are brought as close to the resting surface of the carrier as possible. Finally, to utilize the preload assembly, the cylindrical supports of the carrier are removed to avoid collision with the pins (see figure 4.19). This does not change the functionality or overall dimensions of the carrier.

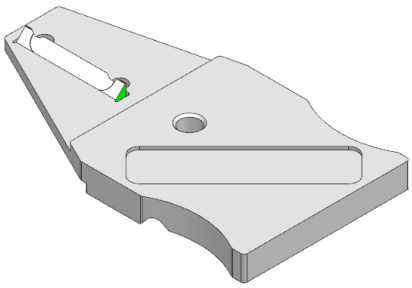

Figure 4.19: Carrier without cylindrical supports

4.5. Manipulator Body

This section is divided based on the main functionalities of the manipulator body: the part of the body that provides the required 3-DOF manipulation (subsections 4.5.1 and 4.5.2) and an overload protection mechanism to prevent reticle damage during adjustments (subsection 4.5.3). Besides, the subsections 4.5.4 and 4.5.5 cover the structural analysis of the body to simulate its working, along with spring calculations for the pretension forces. The final subsection covers additional components designed for handling, transporting and operating the alignment mechanism.

A monolithic design of the manipulator body (using flexures, refer subsection 3.1.1) is preferred because of the significant advantages it offers in avoiding the errors due to assembly and tolerance of parts in an

alignment mechanism and producing predictable deformations due to material uniformity as the part is machined out of one material. The design is realized by the process of WEDM [7]. Additionally, based on the material availability at suppliers, aluminium 7075 is preferred to design the manipulator body. This is one of the strongest alloys of aluminium that offers the advantages of high strength, wear resistance and low density. Although it has less corrosion resistance than other alloys, its strength more than justifies the drawback [38].

4.5.1. Calculations for 3-DOF Manipulation

Concept VIII of the manipulator body, which uses an elastic hinge stacked on top of a leaf spring (3x), was the proposed concept layout to adjust the moving structure in the 3 DOFs (refer section 3.4.4).

The moving structure is connected to three leaf springs, each in line with the actuators. The parameters of a leaf spring are: length (L), thickness (t_{leaf}) and width (b_{leaf}) (see figure 4.20). The calculation of one leaf spring is performed using the following relations [12]:

$$C_x = \frac{E b_{leaf} t_{leaf}^3}{L^3} \tag{4.1}$$

$$I = \frac{b_{leaf} t_{leaf}^3}{12} \tag{4.2}$$

$$F_{buck} = \frac{4\pi^2 EI}{L^2} \text{ (when } u_{xleaf} = 0 \text{ mm)} \tag{4.3}$$

$$u_{xleaf} = \frac{F_x}{C_x} \tag{4.4}$$

$$u_{zleaf} = \frac{3u_{xleaf}^2}{5L} \tag{4.5}$$

where C_x is the stiffness of the leaf spring along the X-axis (in N/m), E is the modulus of elasticity of Al 7075 (refer Appendix C), I is the area moment of inertia of the leaf spring (in m^4), F_{buck} is the buckling force of the leaf spring along the Z-axis (in N), u_{xleaf} is the stroke of the leaf spring along the X-axis (in m), F_x is the force applied along the X-axis (in N) and u_{zleaf} is the parasitic displacement along the Z-axis (in m) [12].

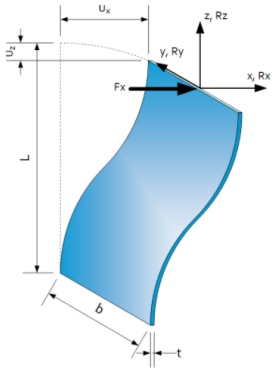

Figure 4.20: Leaf spring [12]

where $t_{leaf} = t$, $b_{leaf} = b$, $u_{xleaf} = u_x$ and $u_{zleaf} = u_z$

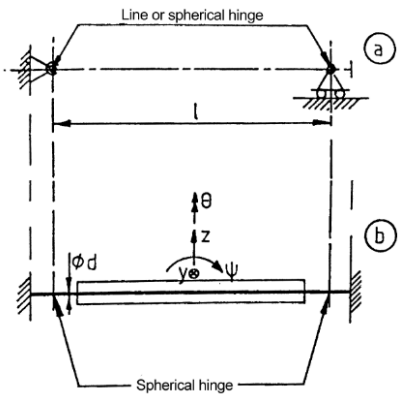

Figure 4.21: Conversion to reinforced leaf spring [25]

Based on the initial parameters considered for a leaf spring and the total force needed via the actuator for the adjustments, the leaf spring provides sufficient resistance against buckling. As a nice-to-have feature, the leaf springs are converted to reinforced leaf springs to increase its buckling limit by a factor of nine (see figure 4.21). This is carried out by choosing the length of the reinforced part as $L_{RF} = \frac{5}{6}L$ and the thin parts as $\frac{1}{6}L$ each [25]. Thus, the length of the full reinforced leaf spring becomes $L_{leaf} = \frac{7}{6}L$. The thickness of the reinforced part is considered as $t_{RF} = 5t_{leaf}$ [13], while the thin sections continue to remain at t_{leaf} each.

Furthermore, three circular hinges are connected to each of the reinforced leaf springs. The parameters of a circular hinge are: length (L_{hin}), diameter (D_{hin}), thickness of the thin section (h_{hin}) and width (t_{hin}) (see

figure 4.22). The calculation of one circular hinge is performed using the following relations [14]:

$$\beta = \frac{h_{hin}}{D_{hin}} \tag{4.6}$$

$$D_{hin} = \frac{2d_1 d_2}{d_1 + d_2} \tag{4.7}$$

$$C_{Az} = \frac{0.56 E t_{hin} \sqrt{\beta}}{1.2 + \frac{1}{\beta}} \tag{4.8}$$

$$K_{Ay} = 0.093 E t_{hin} h_{hin}^2 \sqrt{\beta} \tag{4.9}$$

$$C_{Bz} = \frac{C_{Az} K_{Ay}}{K_{Ay} + C_{Az} L_{hin}^2} \tag{4.10}$$

$$u_{zhin} = \frac{F_z}{C_{Bz}} \tag{4.11}$$

$$R_{hin} = \frac{F_z L_{hin}}{K_{Ay}} \tag{4.12}$$

where β is the circular hinge parameter (the recommended range is $0.01 < \beta < 0.5$), d_1 and d_2 are the two hinge diameters (assumed to be equal for simplicity; in m), C_{Az} is the stiffness of point A along the Z-axis (in N/m), K_{Ay} is the rotational stiffness of point A along the Y-axis (in Nm/rad), C_{Bz} is the stiffness of point B along the Z-axis (in N/m), u_{zhin} is the stroke of hinge along the Z-axis (in m), F_z force applied on point B along the Z-axis (in N) and R_{hin} is the rotation angle formed (in rad) [14].

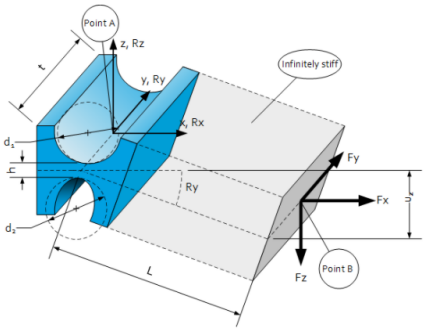

Figure 4.22: Circular flexure hinge [14]

where $L_{hin} = L$, $D_{hin} = D$, $h_{hin} = h$ and $t_{hin} = t$

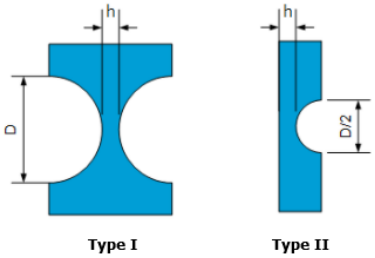

Figure 4.23: Two hinge versions [14]

where $D_{hin} = D$ and $h_{hin} = h$

Figure 4.23 shows two versions of the circular hinge with equal h_{hin}, C_x and K_y [14]. Type II is preferred in the alignment mechanism over Type I as it claims less volume.

(a) Initial orientation of hinge

(b) Proposed orientation of hinge

Figure 4.25: Schematic of flexural elements

A simple schematic of the flexural elements (reinforced leaf spring and Type II circular hinge) in the stacked format is shown in figure 4.25a. In this orientation, the thin section of the hinge (h_{hin}) is perpendicular to the actuation direction. This is not desirable as with the application of force, the part of the hinge that is right of this thin section would move along the Z-axis. To minimize this effect, a new orientation of the hinge is proposed in figure 4.25b. It is rotated 90° while keeping its rotation point on the same contact plane to avoid an offset. Note that the proposed orientation also has undesirable effects due to the friction between the tip of the actuator and the contact surface, and the reaction because of the elastic deformation of the reinforced leaf spring. However, these effects are less than what is experienced by the thin section in the initial orientation.

The parameter values considered to design the flexural elements are mentioned in table 4.2. These values solved the purpose of adjusting the moving structure in the 3 DOFs, while providing the required stroke (refer M2 requirement) and keeping the elemental stress (von Mises) levels below the fatigue and yield strengths of Al 7075 (refer Appendix C). This is further elaborated using a simulation study in subsection 4.5.4.

Table 4.2: Parameters of flexural elements for 3-DOF manipulation

(a) Reinforced leaf spring

Parameter	Value ($\times 10^{-3}$ m)
L_{leaf}	46.67
L_{RF}	33.34
t_{leaf}	0.27
t_{RF}	1.35
b_{leaf}	41

(b) Type II circular hinge

Parameter	Value ($\times 10^{-3}$ m)
L_{hin}	48
D_{hin}	5
h_{hin}	0.27
t_{hin}	41

4.5.2. End Stops, Overconstraints and Interface Strips

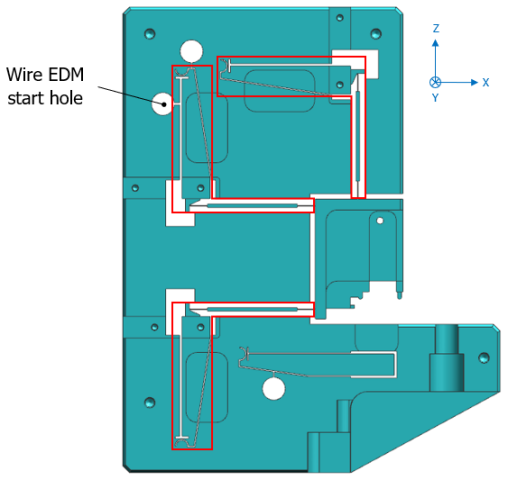

Figure 4.26: Flexural elements in manipulator body for 3-DOF manipulation

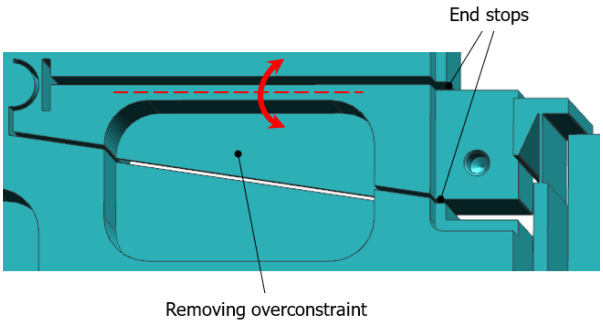

Figure 4.27: End stops; removing overconstraints

Figure 4.26 shows the location of the flexural elements in the manipulator body for 3-DOF manipulation (upright orientation). In addition, a zoomed in version of the top hinge is shown in figure 4.27. To ensure the hinge stops after a certain stroke and its stress levels lie within the acceptable limits (below the fatigue and yield strengths of Al 7075), the end stops are integrated in the manipulator body for the +Z and -Z strokes. For the hinge length of 48 mm, the required stroke is 0.5 mm. The end stops run until a distance of 38.4 mm from the rotation point of the hinge, with a gap of 0.4 mm for the required stroke along the Z-axis ($\frac{48}{38.4} = \frac{0.5}{0.4}$). Note that the gap of the end stop in the +Z direction is kept at 0.8 mm (= 2×0.4 mm) to allow the hinge for an extra stroke of 0.5 mm (in total 1 mm) in the +Z direction ($\frac{48}{38.4} = \frac{1}{0.8}$). The extra stroke helps in creating enough space to unmount the cured ReCa assembly after the alignment.

As seen in section 3.4.4, Concept VIII has an underlying issue of overconstraints in the design. The overconstraint, for instance, is observed in the form of rotation about the X-axis for the top hinge (see figure 4.27).

This is because the same DOF (Rx) is also restricted by the presence of a reinforced leaf spring that is stiff in rotation about the X-axis. To remove this overconstraint, milling can be performed to create a pocket. An identical pocket is mirrored about the center XZ-plane to create a rotational axis (refer dotted line) due to the T cross-section. The features for the end stops and the removal of overconstraints are also implemented for the other two hinges (see figure 4.26).

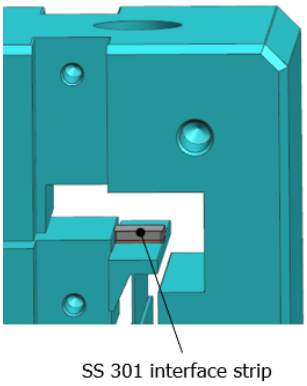

Figure 4.28: Interface strip for actuation

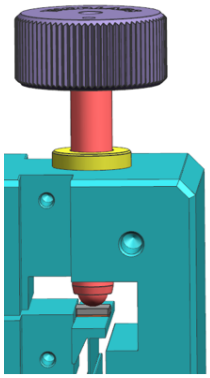

Figure 4.29: Actuation in manipulator body

Since aluminium is a relatively softer material, a hard contact of the actuator tip (made of SS 440 material) directly to the manipulator body is undesirable as it leads to high stresses on the latter. To avoid this, a high strength interface is added in the form of 1 mm thick SS 301 metal strips between the actuator tips and the manipulator body (see figure 4.28). The strips are bonded to the manipulator body near the contact surfaces using an epoxy adhesive. Figure 4.29 displays how the actuator tip interacts with the interface strip. Note that the pretension springs needed to avoid backlash between the actuator tips and their respective contact surfaces are covered in subsection 4.5.5.

4.5.3. Overload Protection Mechanism

As discussed in subsection 1.5.2, the support features ('S1' and 'S2') are used to define the Z-position and the Ry of the reticle. This is done by translating the moving structure in the -Z direction until these features touch the reticle. At this point, the knob of the magnetic holder is turned to grip the reticle. However, stopping the adjustment of the moving structure exactly at the right moment is difficult. At the same time, any extra stroke in the -Z direction clamps the reticle between the support features and the resting surface of the carrier. This is not desirable as it can damage the glass component due to load build up.

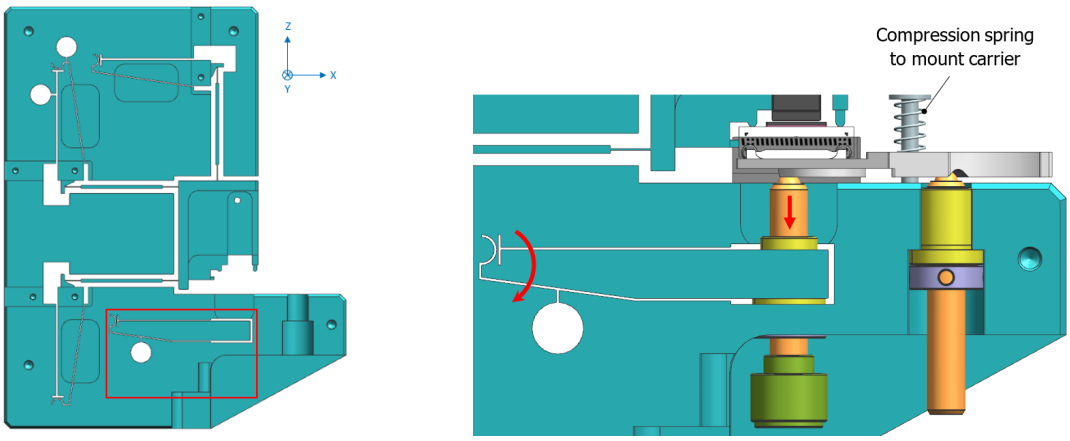

(a) Location in manipulator body

(b) Basic working principle

Figure 4.30: Overload protection mechanism

To tackle this issue, an overload protection mechanism is integrated in the manipulator body as shown in figure 4.30a. It consists of a hinge that possesses the same parameters as the other three hinges (refer table

4.2b for details). Its end stop features are designed in such a way that the hinge allows for a stroke of ± 0.5 mm (or 1 mm along the -Z direction after pretension). Hence, the value is taken as a safe value considering the maximum stroke possible of the reticle in the mechanism (leaves 0.8 mm extra stroke in the -Z direction in nominal dimensions). Note that the default position of the hinge is when it touches its end stop in the +Z direction. This is because of the presence of a pretension spring for the preload, which is covered in subsection 4.5.5.

Figure 4.30b shows the basic working principle of the mechanism. The hinge has a cylindrical cutout to mount the left adjustment screw using an adapter. In the default position of the hinge, the tip of the screw makes contact with the V-groove of the carrier. Besides, a compression spring is used to mount the carrier using kinematic constraint. The spring has an initial length of 16.4 mm and a stiffness of 0.38 N/mm [34]. In the nominal dimensions, the spring is compressed by approximately 8 mm, resulting in a preload force of approximately 3 N. As the adjustment screws are placed at different distances from the point of application of the preload force, they receive different forces on the ball tips (see figure 4.31).

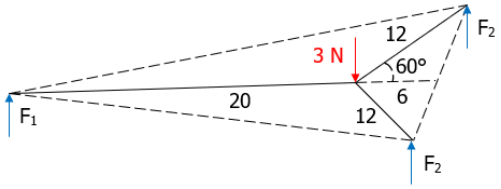

Figure 4.31: Forces on adjustment screws due to compression spring of carrier

$$\sum F = 0 \implies F_1 + 2F_2 = 3 \tag{4.13}$$

$$\sum T = 0 \implies -3\,(6) + F_1\,(26) = 0 \tag{4.14}$$

Equations mentioned above explain how the forces on the adjustment screws are calculated. The first equation is for the force equilibrium along the Z-axis, whereas the second equation performs torque balance about the rotational axis (formed by the right adjustment screws). F_1 is the force received on the left adjustment screw and F_2 is the force received on each of the two right adjustment screws (assumed the same due to equal distance). On calculation, it is found that the left adjustment screw receives a force of approximately 0.7 N (= F_1).

The overload protection mechanism is designed in such a way that the hinge can take in this force on the ball tip and still remains in the default position to fulfil its purpose of mounting the carrier. In addition, any extra load (keeping a small force difference) in the -Z direction rotates the carrier about the tips of the two right adjustment screws. This motion is further transmitted to the left adjustment screw and the hinge gets actuated to prevent reticle damage (refer arrows in figure 4.30b).

4.5.4. Structural Analysis

A structural analysis of the manipulator body (upright orientation) is performed in Simcenter Nastran to simulate its working. The parts of the manipulator body for 3-DOF manipulation and overload protection mechanism are verified in the study. The maximum elemental stresses (von Mises) generated in the body are checked and shown for a stroke of 0.5 mm in one direction, along with checking them for a stroke of 1 mm in the other direction (during mounting and unmounting). In addition, the MIM of the Ry adjustment is calculated. Note that for the analysis, the interface strip for each actuator is assumed to be integrated with the manipulator body for simplicity.

Using the material properties of Al 7075, a CTETRA10 mesh type is generated with the element size of 2 mm. This value is less than the default value suggested by the software that gives a nice balance between the computing time and accuracy. The mesh is followed by the application of loads and constraints (see figures 4.32a and 4.32b for the Tz and Tx adjustments, respectively). The outer surfaces are considered fixed. Red arrows on the contact surface(s) indicate the force(s) applied, while the blue arrows show the restricted translation(s) due to the presence of actuator(s).

Figures 4.33, 4.34 and 4.35 show the results of the structural analysis for the Tz adjustment, the Tx adjustment and the overload protection mechanism, respectively (for a visual scale of 10%). The values for the stroke of 0.5 mm are represented in table 4.3.

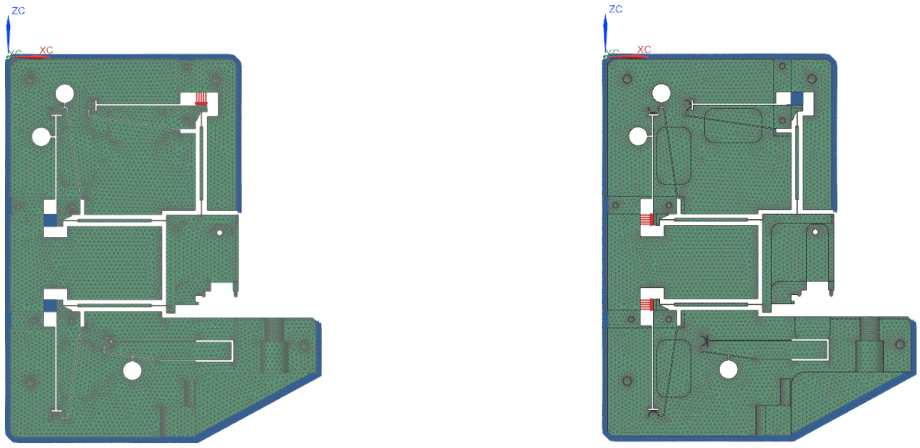

(a) Load and constraints for Tz adjustment

(b) Loads and constraints for Tx adjustment

Figure 4.32: Simulation model of manipulator body for 3-DOF manipulation

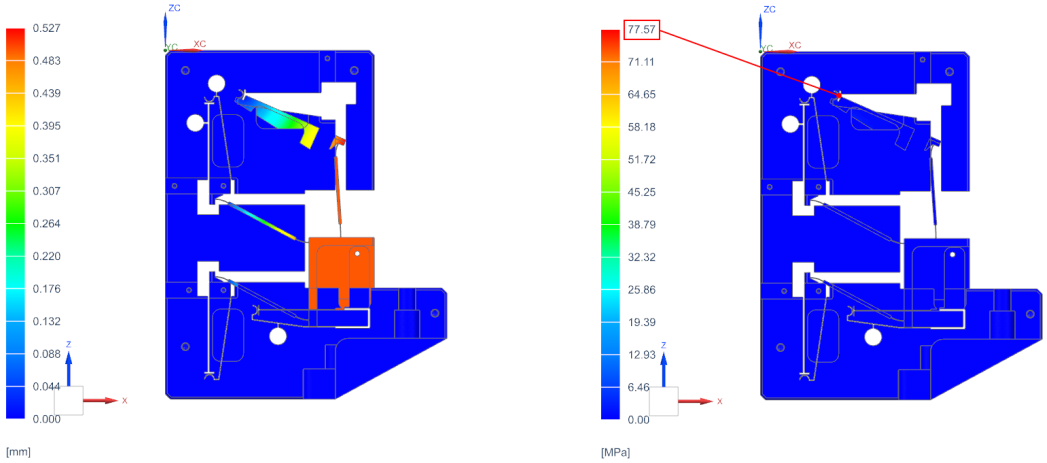

(a) Stroke

(b) Elemental stress (von Mises)

Figure 4.33: Analysis for Tz adjustment

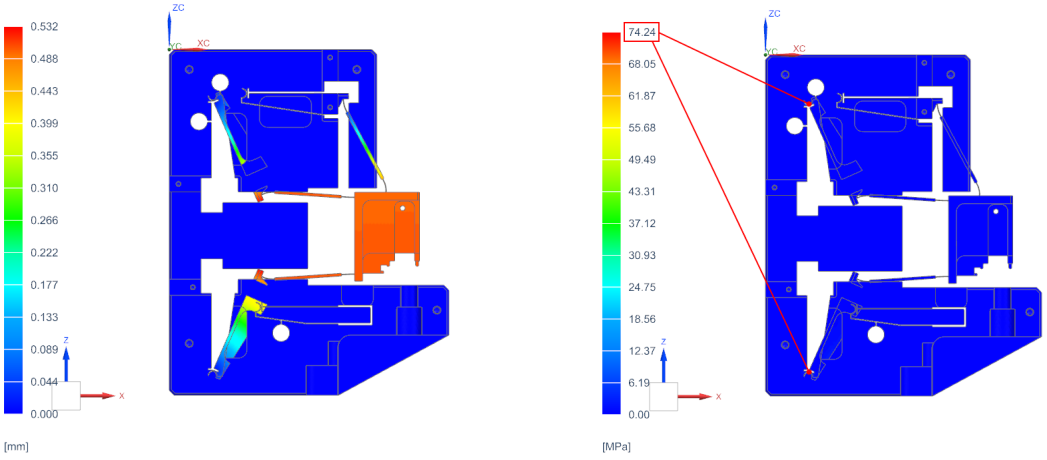

(a) Stroke

(b) Elemental stress (von Mises)

Figure 4.34: Analysis for Tx adjustment

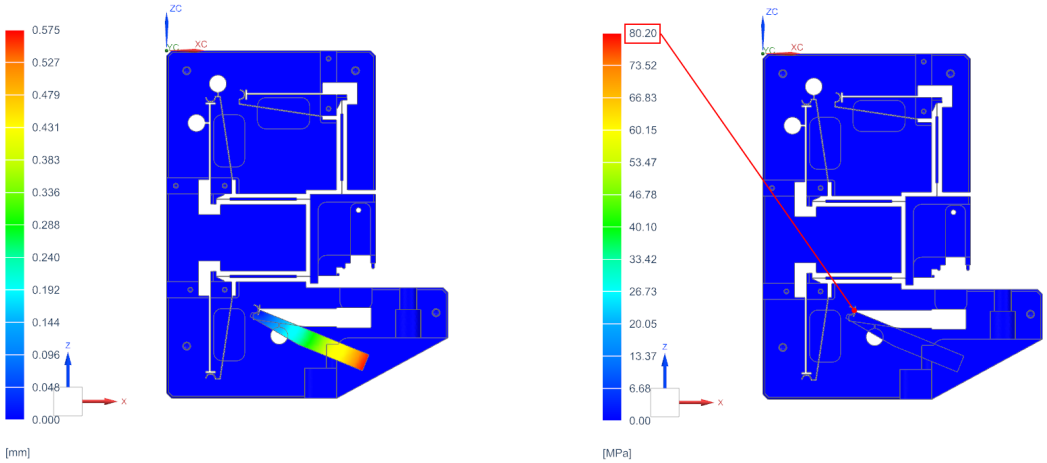

(a) Stroke

(b) Elemental stress (von Mises)

Figure 4.35: Analysis for overload protection mechanism

Table 4.3: Results of structural analysis for 0.5 mm stroke

Parameter	3-DOF manipulation		Overload protection mechanism
	Tz adjustment	Tx adjustment	
Force	2.66 N (actuator '2')	2.55 N (actuator '3') 1.13 N (actuator '1')	1.34 N
Max. elemental stress	77.57 MPa	74.24 MPa	80.2 MPa

It is observed that for a stroke of 0.5 mm in all cases, the stress values are over six times less than the yield strength and around two times less than the fatigue strength of Al 7075 (refer Appendix C for values). A similar analysis was performed to verify the stress levels for a stroke of 1 mm in the other direction, for the Tx and Tz adjustments. Consequently, the stress values come out to be over three times less than the yield strength and around the same as the fatigue strength of Al 7075. Hence, the results are within the acceptable limits. Moreover, to get a translation along the X-direction (without the Ry rotation), the actuator '3' has to be applied with more force than the actuator '1'. This means that the upper half of the moving structure is more stiff when compared to its lower half. It can further be understood by looking at the geometry, where the connection of an extra reinforced leaf spring (the vertical one, parallel to the Z-axis) to the moving structure makes the upper half relatively stiff.

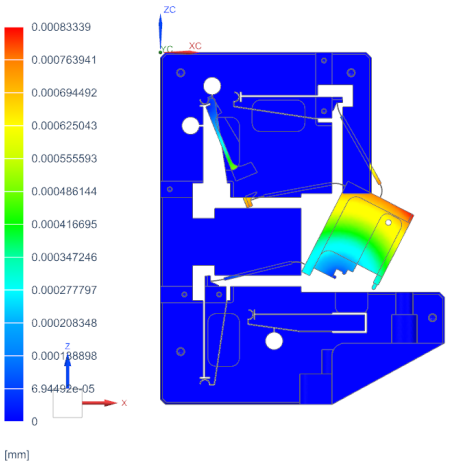

Figure 4.36: Analysis for MIM of Ry adjustment

On top of that, the MIM of the Ry adjustment is simulated in figure 4.36 (for a visual scale of 10%). It is seen that for the least possible stroke of 0.71 µm (sensitivity) via the actuator '3' in the +X direction, the moving structure rotates by an angle of 13 µrad between the two left leaf springs. Therefore, the MIM of the Ry adjustment is satisfied (refer M1 requirement).

4.5.5. Pretension Springs and Contact Stresses

Figure 4.37 shows the location of the pretension springs on the manipulator body for the 3-DOF manipulation. The pretension force required for each actuator is divided equally between two springs that are placed symmetrically using screws on the back and front sides of the body. Because of the space availability, an extension spring (6x in total) is considered for this purpose that provides a pull force on getting extended.

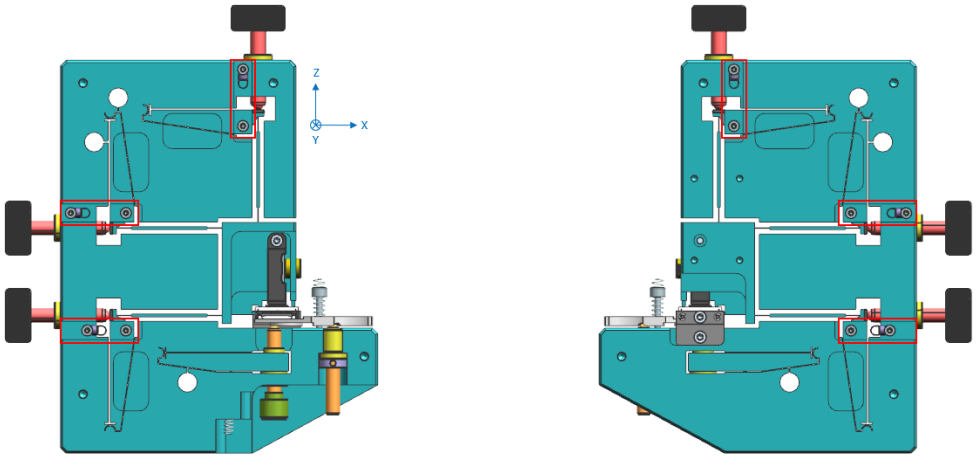

(a) Front view (b) Back view

Figure 4.37: Extension springs on manipulator body for 3-DOF manipulation

As seen in table 4.3, it is clear that despite having the same dimensions of the flexural elements, the forces needed to provide the required stroke in the X- and Z-axis are different for all actuators. The extension spring selected has an initial length of 10.9 mm (L_o), a stiffness of 0.35 N/mm (C_{spring}) and an initial force of 0.51 N (F_o) [36]. A safety factor of approximately 1.6 is considered to calculate the pretension forces of the springs. One such example of pretension springs (on the front and back sides) for the top actuator (actuator '2') is explained hereupon. A force of 5.32 N (= 2×2.66 N, refer table 4.3) is needed to overcome the stiffnesses of the flexural elements and get a stroke of 1 mm in the +Z direction. Therefore, a preload force of approximately 8.8 N is needed in line with the actuator. However, as the extension springs are placed at an offset from the actuator force, the use of the transmission ratio is taken into account for calculating the correct pretension forces. A simple sketch of the arrangement is shown in figure 4.38, along with the calculation of the transmission ratio in equation 4.15.

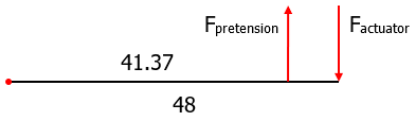

Figure 4.38: Use of transmission ratio in pretension force calculation for extension springs

$$F_{pretension} \times 41.37 = F_{actuator} \times 48 \implies F_{pretension} = \frac{F_{actuator}}{0.86} \tag{4.15}$$

$$\frac{F_{pretension}}{2} = F_o + C_{spring} s \implies s = \frac{\frac{F_{pretension}}{2} - F_o}{C_{spring}} \tag{4.16}$$

The pretension force $F_{pretension}$ (= 10.2 N) is divided between two springs. In each spring, this force has to overcome the initial force of the extension spring, along with the stiffness for the desired stroke (refer equation

4.16). Considering s as the spring extension, the length of the extension spring for the least extension (when the hinge rests in the +Z direction) is calculated as $(L_o + s)$ mm. Additionally, using the transmission ratio, the value of 0.86 mm (for the actuator stroke of 1 mm) is added to get the spring extension in the neutral position of the hinge (as visible in CAD). Hence, the screw mounting points are placed at a distance of $(L_o + s + 0.86)$ mm. Similarly, the pretension forces for the remaining extension springs are calculated and the screw mounting points are added for the 3-DOF manipulation.

Figure 4.39a shows the section view of the overload protection mechanism. Based on the space availability, a compression spring is used to provide the necessary pretension force to the hinge. The spring has an initial length of 31 mm and a stiffness of 0.46 N/mm [35]. It is also placed at an offset from the force experienced by the adjustment screw. A simple sketch of the arrangement is represented in figure 4.39b, along with the calculation of the transmission ratio in equation 4.17.

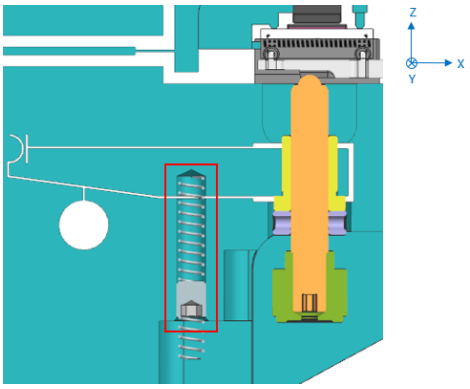

(a) Compression spring for overload protection mechanism (section view)

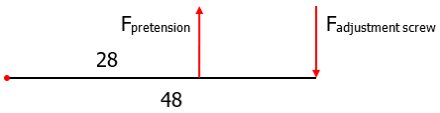

(b) Use of transmission ratio in pretension force calculation

Figure 4.39: Compression spring on manipulator body for overload protection mechanism

$$F_{pretension} \times 28 = F_{adjustment\ screw} \times 48 \implies F_{pretension} = \frac{F_{adjustment\ screw}}{0.58} \tag{4.17}$$

The pretension force (= 6.1 N) for the compression spring is calculated considering that the force of 3.54 N is needed in line with the left adjustment screw. This force of 3.54 N is the sum of four values: 1.34 N required to rest the hinge to its default position in the +Z direction (refer table 4.3), 0.7 N to counteract the force acting on the left adjustment screw via the compression spring of the carrier (refer subsection 4.5.3), 0.5 N of frictional force between the reticle & carrier and 1 N as a small force for the activation of overload protection mechanism (assumption). Accordingly, the compression spring is compressed by using a set screw (refer section 5.1) to achieve the pretension force in the overload protection mechanism.

With the forces now known in the alignment mechanism, an important parameter to check is the contact stresses developed between the actuator tips and their respective contact surfaces. The force applied via an actuator screw overcomes the following: the force by the stiffnesses of the flexural elements (hinge(s) and leaf spring(s)), the pretension forces by the extension spring for maximum extension and the frictional force between the reticle and carrier. As the actuator '3' utilizes the most force (refer table 4.3) to overcome the stiffnesses of the flexural elements, it is considered for the study. The total force applied by the actuator '3' equals the sum of 2.66 N, 9.2 N and 0.5 N, respectively (= 12.4 N), as stated in the above paragraph. HertzWin is used to calculate the Hertzian contact stress as shown in figure 4.40. Body 1 is the ⌀ 4.8 mm actuator tip made of SS 440 material and Body 2 is the flat interface strip made of SS 301 material.

It is observed that the von Mises stresses of 1028 MPa are generated in the two bodies, with a Hertzian contact stress of 1646 MPa. Nevertheless, as the yield strengths (or maximum stress, see figure 4.40) of both materials are more than the von Mises stresses with some difference, there is no issue. Besides, the results also justify the use of SS 301 for the interface strip as a suitable material. Note that some localized deformations are possible in the interface strip as the Hertzian contact stress is more than the yield strength of SS 301 material. However, as the contact area formed is minimal, these deformations are neglected.

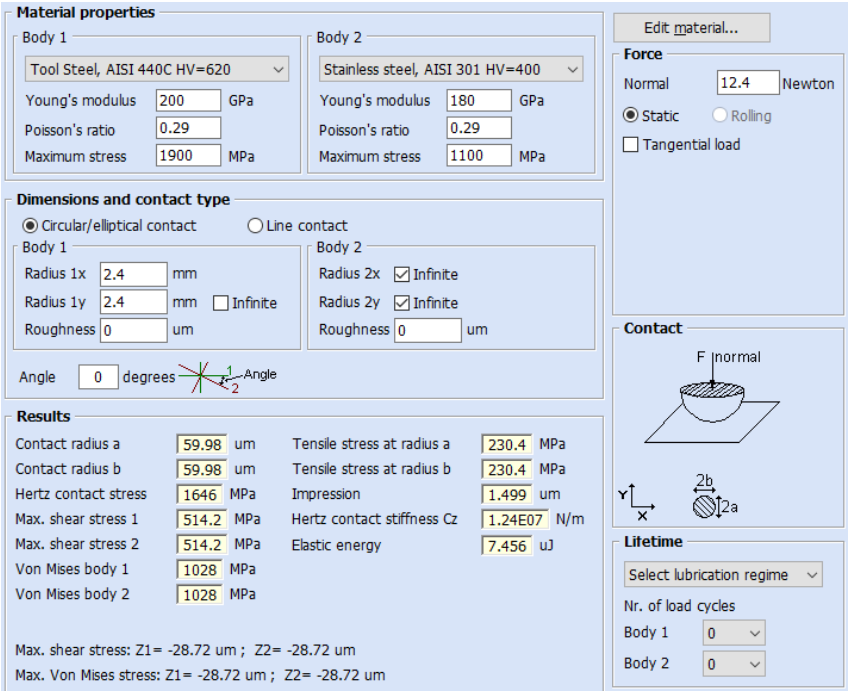

Figure 4.40: Contact stress calculation using HertzWin [45]

4.5.6. Transport Lock, Protective Covers and Rubber Feet

As seen in figure 4.26, the moving structure is supported by flexural elements in the manipulator body and is free to move in the 3 DOFs (refer M0 requirement). This is not ideal during handling and transport as the structure will collide with the fixed structure. To prevent this, a transport lock is designed in the form of a 1 mm thick sheet metal plate. The plate is assembled between the moving structure and the fixed structure using two screws on each side (with spacers) to prevent motion in the desired three DOFs (encircled in figure 4.41). The same transport lock can also be utilized during the anodizing process when the manipulator body is immersed into an electrolyte.

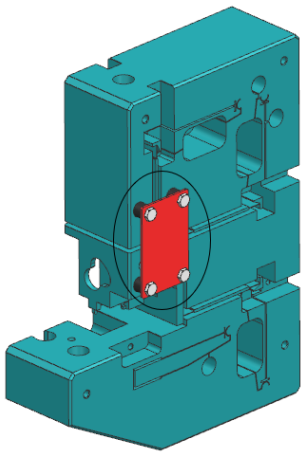

Figure 4.41: Transport lock (encircled)

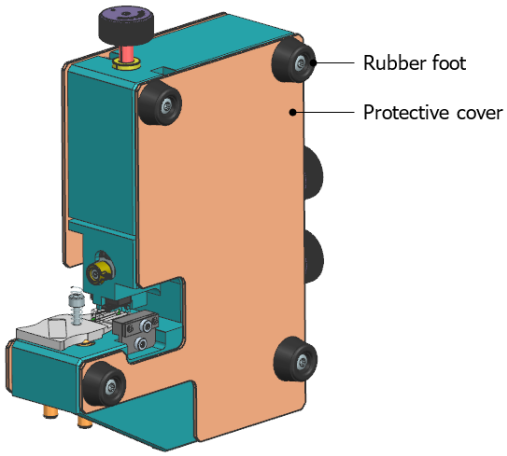

Figure 4.42: Protective covers and rubber feet

Furthermore, a protective cover is designed in the form of a 1.5 mm thick sheet metal plate. It is assembled on the alignment mechanism on the front and back sides using shims for clearance (see figure 4.42). The purpose of the cover is to protect the weak regions of the alignment mechanism during handling and operation. Additionally, four rubber feet are attached to the mechanism to place it in the seated orientation during the adjustments. They minimize slip of the alignment mechanism against the contact plane, thus ensuring convenience for use.

5

System Overview and Procedures

This chapter gives an overview of the complete alignment mechanism with all its components. Assembly procedures are described for the mechanism and its subassemblies. Alignment steps are elaborated for operating the alignment mechanism and forming the ReCa assembly. Verification plan is described to check if the matured design meets the set requirements.

5.1. Assembly Procedure

Figure 5.1a shows an isometric view of the complete alignment mechanism with all its components. In the upright orientation, the system fits within a volume of 165 mm × 60 mm × 198 mm for the X-, Y- and Z-axis, respectively. Figure 5.1 shows the same mechanism without the protective covers and rubber feet assembled.

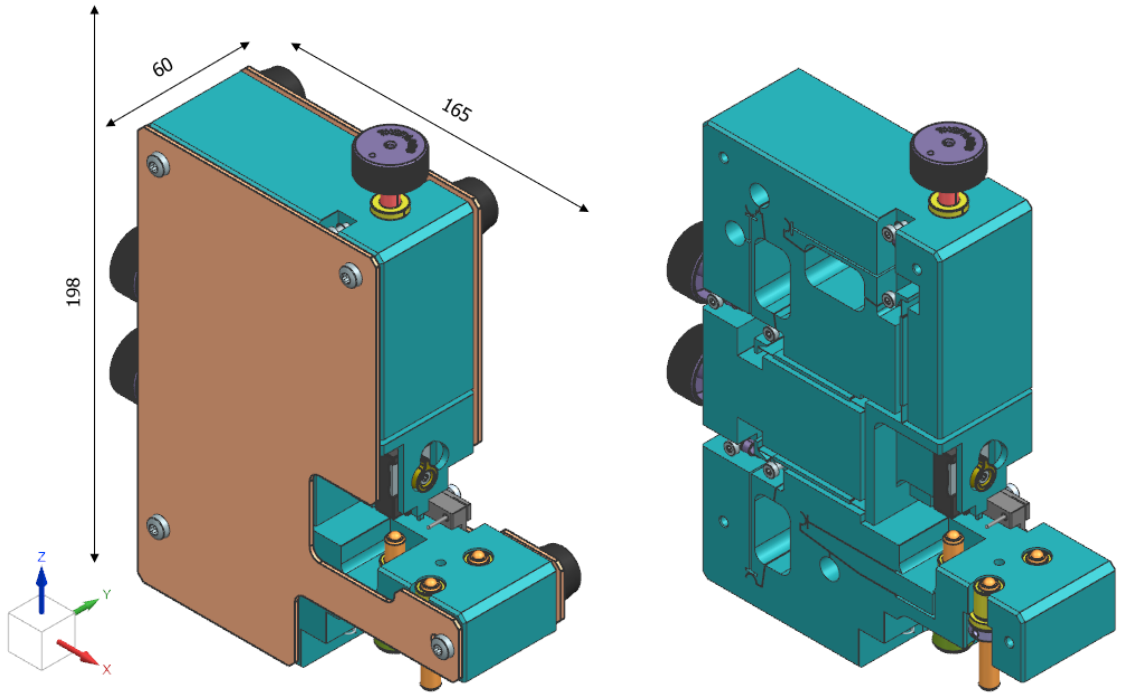

(a) With all components

(b) Without protective covers and rubber feet

Figure 5.1: System overview of alignment mechanism

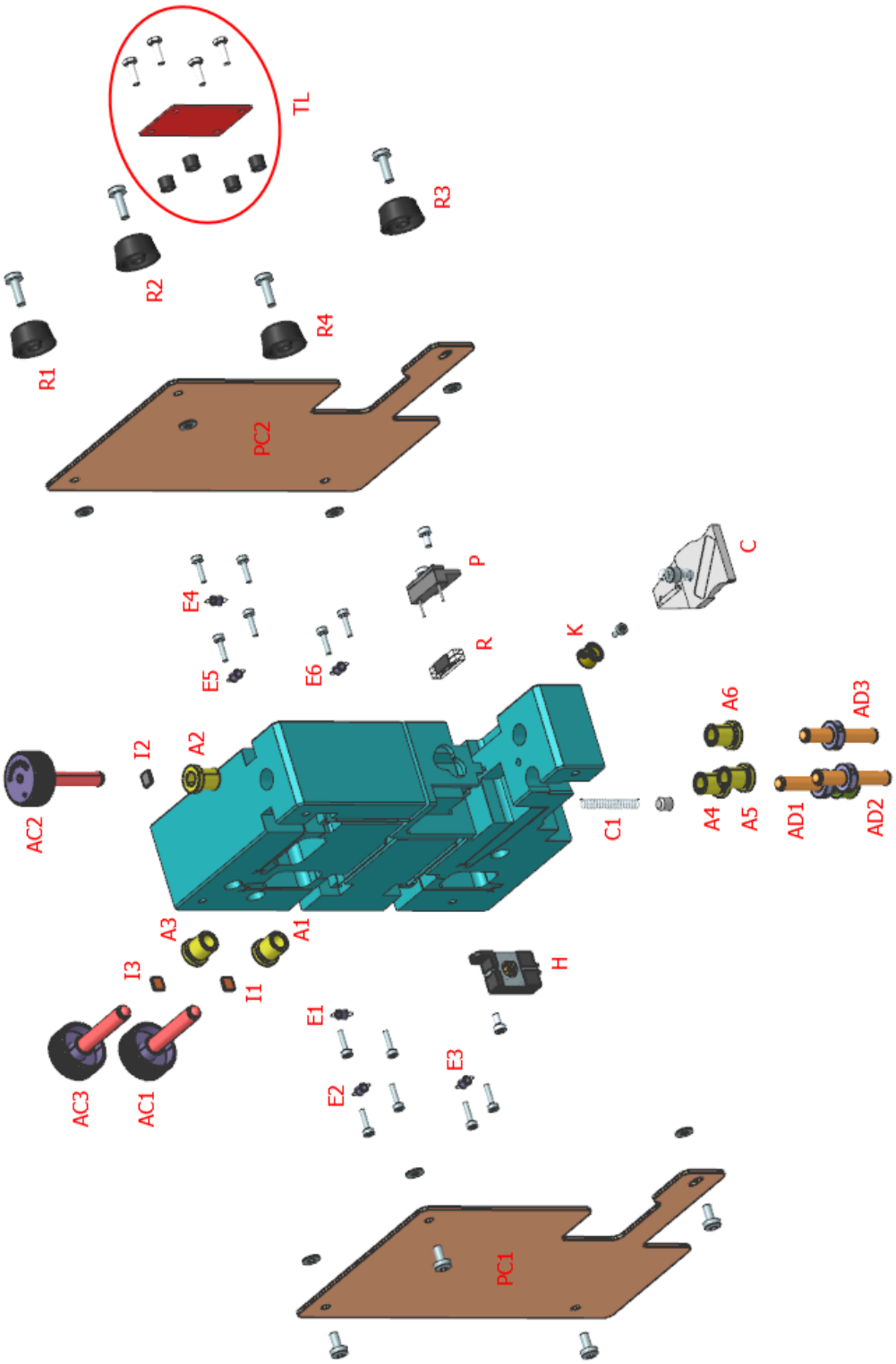

Figure 5.2: Exploded view of alignment mechanism (with reticle and carrier)

The procedure to assemble the alignment mechanism is enumerated below:

1. The manipulator body is received with transport lock TL assembled. Place the body in the upright orientation.

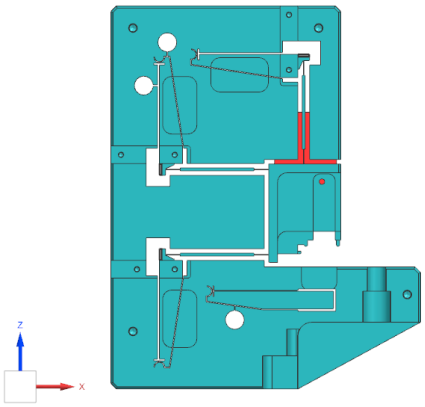

2. Bond I1–I3: Hold interface strip I2 using a tweezer, put an epoxy adhesive on its surface and bond it near the contact area by peeking through the adapter hole (approximately in the center along the Y-axis). The X-position of the strip is defined by bringing it in contact with the blue surface. Repeat this step for the other two strips.

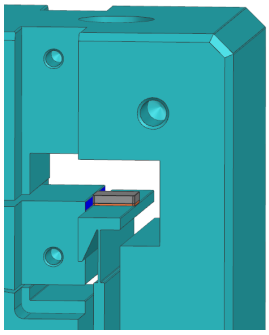

3. Cure I1–I3 and remove TL: Cure interface strips I1–I3 depending on the adhesive used. Next, remove transport lock TL (see in figure).

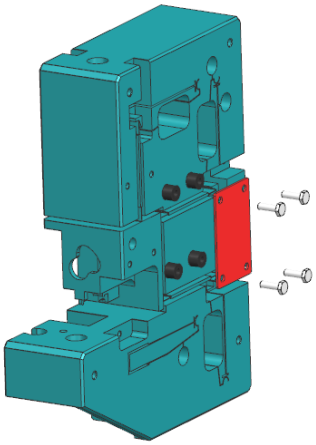

4. Mount E1–E6: Mount extension spring E1 using two M2.5x10 screws (with a medium strength threadlocker) until the screw heads lie within the front surface of the manipulator body. Repeat this step for the other five extension springs.

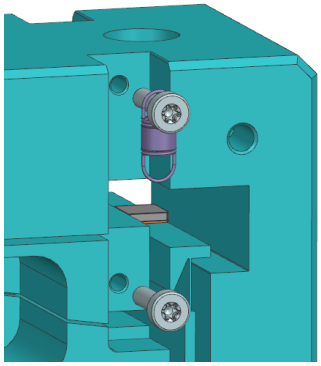

5. Mount C1: Mount compression spring C1 and compress it using a M6x6 set screw (with a medium strength threadlocker) until the red surface of the screw head is flushed inside the blue surface (by approximately 0.7 mm).

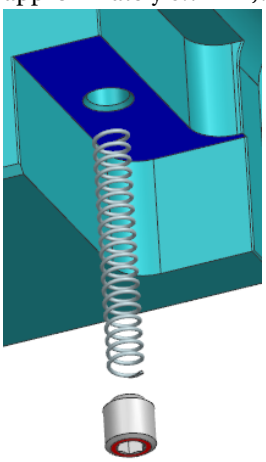

6. Bond A1–A6: Bond adapter A2 by placing an adhesive for cylindrical joints on its external surface. Repeat this step for the other five adapters.

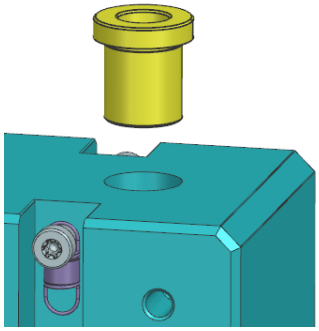

7. Mount AC1–AC3: Attach the fine screw & the knob together (with a medium strength threadlocker) to form AC2 and mount the assembly to adapter A2. Rotate the knob until the ball tip of the screw touches the interface strip. Repeat this step for the other two actuators.

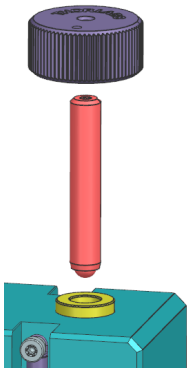

8. Form AD1–AD3: Attach the locknuts to the adjustment screws at the shown distances (measure using a Vernier caliper). Fix them in place with a medium strength threadlocker or bond them via holes using an epoxy adhesive. Next, attach the knob on AD1 with a medium strength threadlocker.

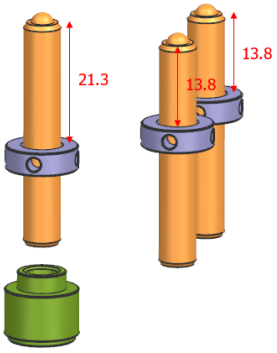

9. Mount AD1–AD3: Mount AD1–AD3 on adapters A4–A6 (using an Allen key) until the locknuts touch their corresponding adapters.

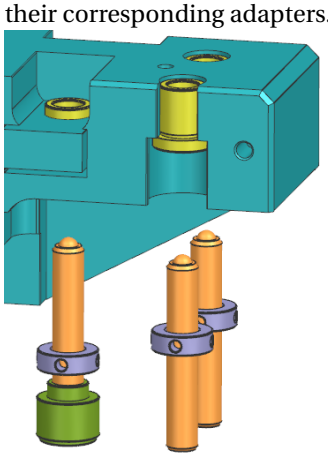

10. Mount H and K: Bring reticle holder H in contact with the two red surfaces and mount it using a M3x6 screw (with a medium strength threadlocker). Knob K is mounted using a M2.5x5 screw (with a medium threadlocker) in its vertical orientation that represents the OFF mode of the holder.

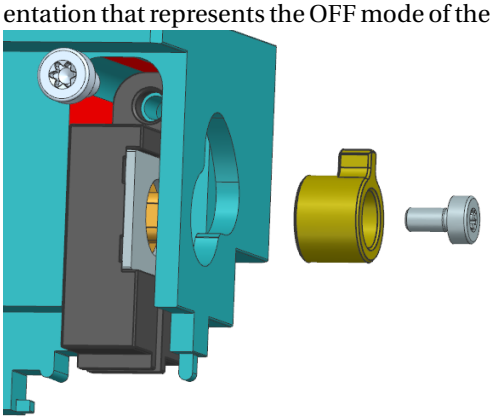

11. Check that all screws for extension springs E1–E6 are flushed inside the manipulator body.

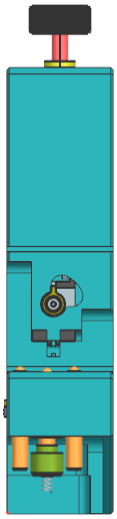

12. Mount PC2 and R1–R4: Place four 2×0.5 mm shims, a protective cover PC2 (= PC1) and four rubber feet R1–R4 together on the back surface of the manipulator body. Fix them using four M4x10 screws.

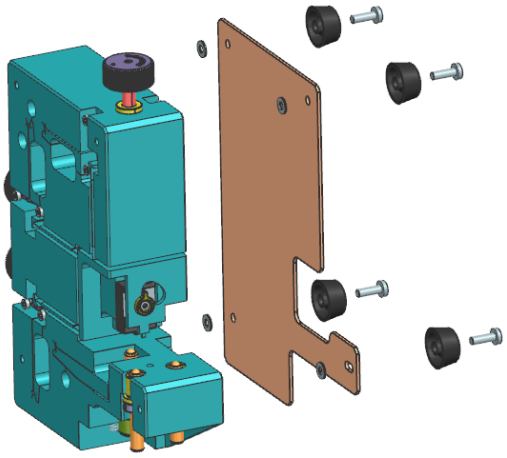

13. Mount PC1: Place the assembly of the previous step in the seated orientation. Place four 2×0.5 mm shims on the front surface of the manipulator body and mount protective cover PC1 using four M4x8 screws.

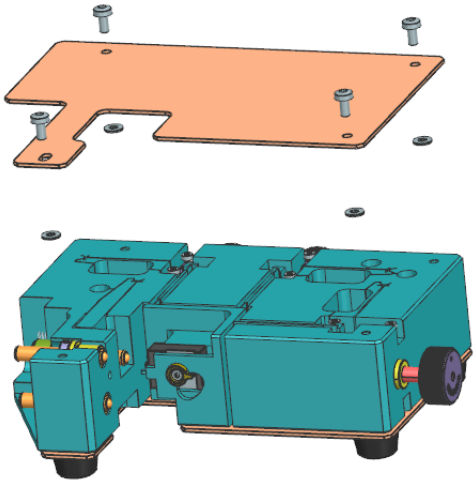

14. Assembled alignment mechanism (without preload assembly P):

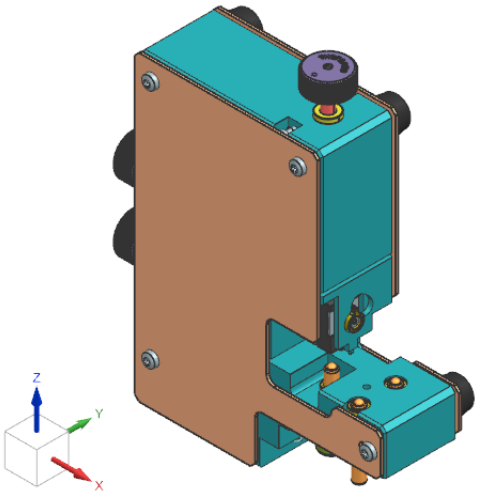

The procedure to assemble the reticle holder H is enumerated below:

1. To estimate and mark the neutral line on the diametrically magnetized disc magnet, three magnets can be put together as shown in the figure. The neutral line (black line) is the one perpendicular to the line formed by the intersection points of the magnets.

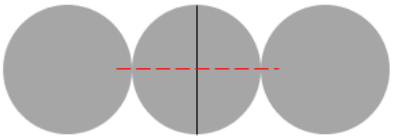

2. Insert the magnet inside the bushing with the magnet's neutral line parallel to the red surface. Mark the red surface on the bushing to keep track of the magnet's neutral line.

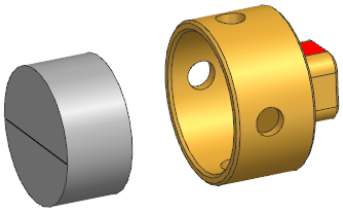

3. As a second check or alignment, bring a secondary magnet (see figure) in contact with the bushing to align the poles of the inside magnet properly. Once done, bond the bushing and the inside magnet together via holes using an epoxy adhesive. Note that the adhesive must lie within the outer diametrical surface of the bushing.

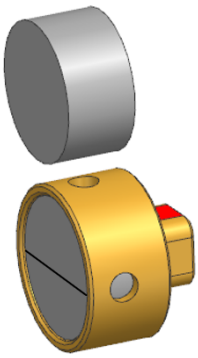

4. Keep the bigger yoke on a flat surface (YZ-plane, see figure). Bond two spacers to it using an epoxy adhesive in the two pockets of the yoke. Note that the bigger spacer must not cross the red dotted line along the -Z direction. Moreover, both the spacers must not enter the diametrical cutout.

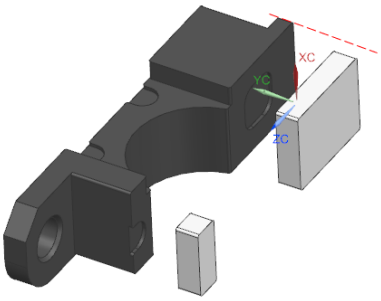

5. Once cured, keep the assemblies of steps 4 and 3 on a flat surface (YZ-plane, see figure). Slide the bushing in the diametrical cutout of the bigger yoke and bond the smaller yoke to the two spacers by using an epoxy adhesive in the two pockets of the yoke.

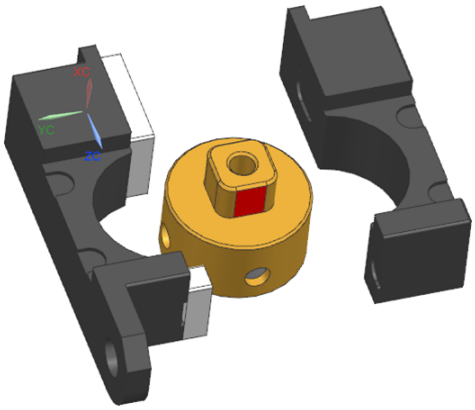

The blue surfaces in the assembly formed are parallel to each other.

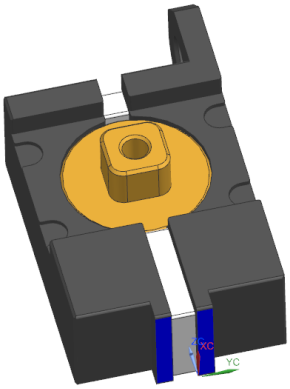

6. Keeping the cured assembly of step 5 on the flat surface, bond the top spacer to the two yokes in a similar fashion. The green surface of the spacer must not cross the blue surface of the bigger yoke in the +Y direction.

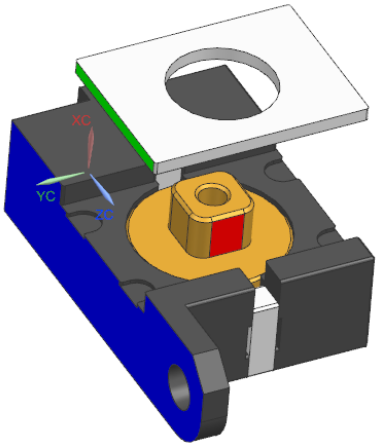

7. Assembled reticle holder (without knob) is shown below. The orientation of the red surface in the holder must be kept as shown in the figure.

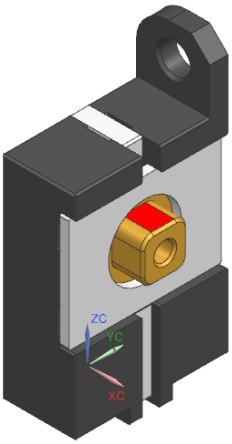

The procedure to assemble the preload assembly P is enumerated below:

1. Place the compression springs on the axes of the pins (from the groove ends).

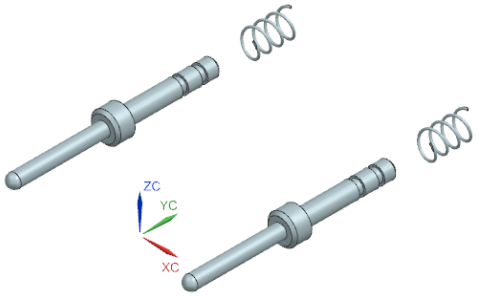

2. Insert the assembly of step 1 in the flange such that the groove ends of the pins protrude out of the flange.

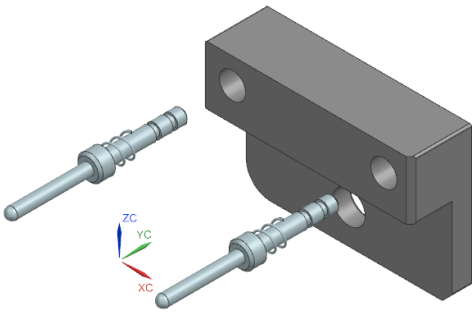

3. Mount two circlips on the inner grooves (along the -Y axis) of the pins using a tweezer.

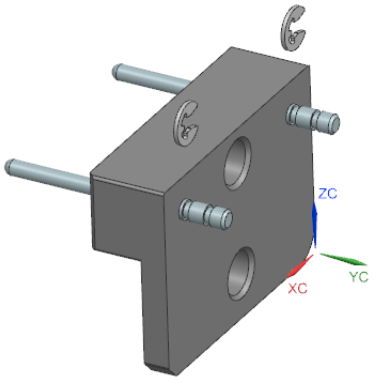

4. Insert the cover via the groove ends of the pins and mount two circlips on the outer grooves (along the +Y axis) using a tweezer.

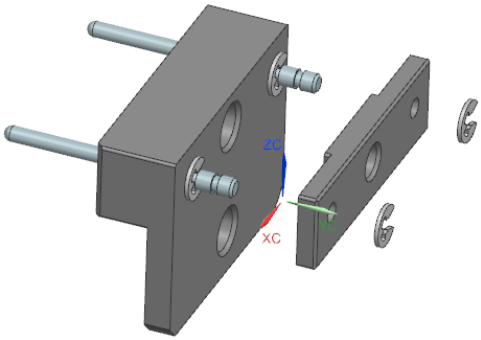

5. Mount a M3x6 screw with the mating thread on the cover and rotate clockwise until it touches the pocket in the flange.

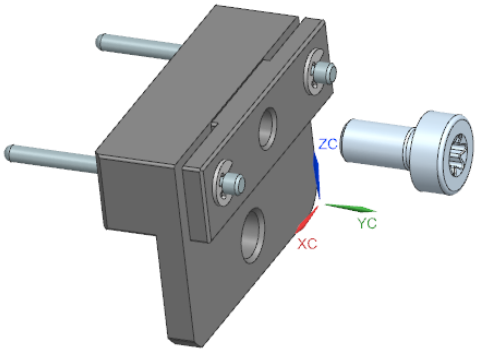

6. Assembled preload assembly:

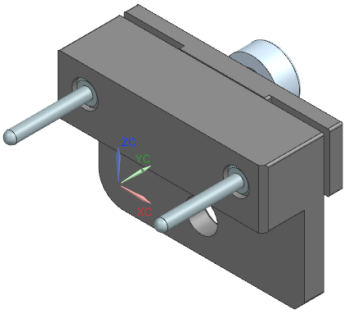

The fully retracted position of the pins is shown in the figure, where the cover is in touch with the screw surface.

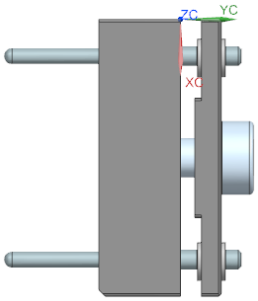

The procedure to assemble the metal plate on the reticle (together represented as R) is enumerated below:

1. Stick a 0.25 mm thick adhesive tape on the metal plate. Cut and remove any extra tape that lies outside the dimensions of the plate.

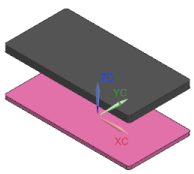

2. Clean the top surface of the reticle using IPA. Once it is dry, peel the other end of the tape and stick the assembly of step 1 on the top surface of the reticle (approximately in the center along the X-axis). The Y-position of the metal plate is defined by flushing its red surface with the front surface of the reticle.

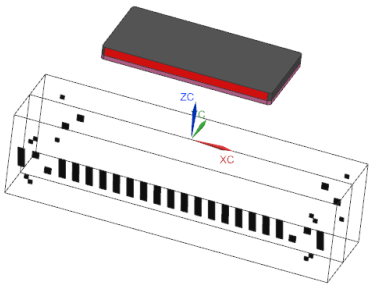

4. Assembled metal plate on top of the reticle:

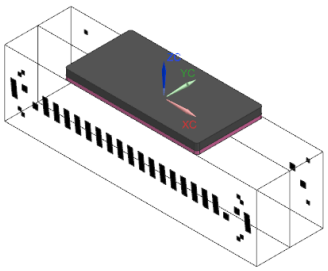

5.2. Alignment Procedure

The alignment procedure between the reticle and carrier to form the ReCa assembly is enumerated below:

1. Place the assembled alignment mechanism in the upright orientation (XY-plane on the table). Slacken the actuator screws, together with the left adjustment screw to create space for mounting the carrier.

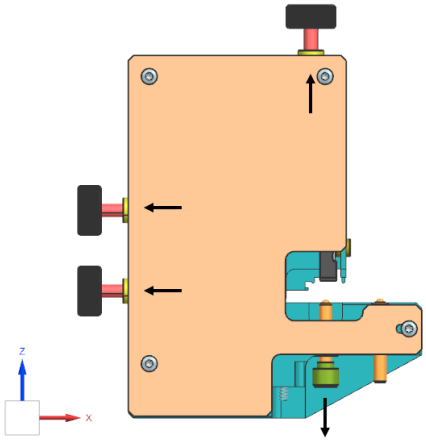

2. Mount the assembly of the carrier C on the balls tips of the adjustment screws.

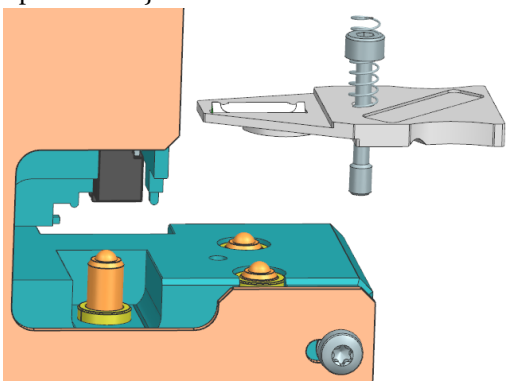

3. Slide the assembly of the reticle R from the back side.

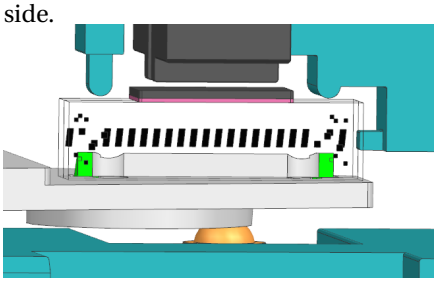

4. Bring the preload assembly P (in its fully retracted position, refer its assembly procedure) in contact with the two red surfaces of the manipulator body and mount it using a M3x6 screw.

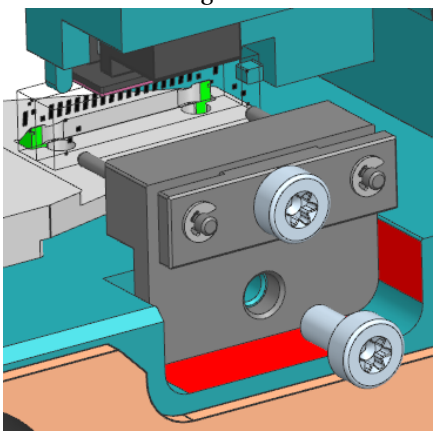

5. Apply the preload by turning the screw in the anticlockwise direction until the pins touch the back surface of the reticle. Thereafter, use a tweezer to move the reticle towards the hard stop (shown by the yellow surface).

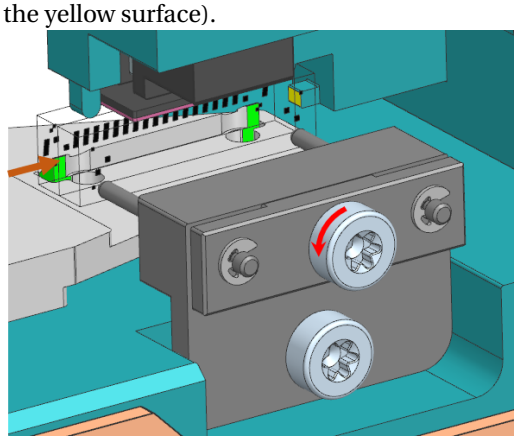

6. Tighten actuator screw '2' to translate the moving structure along the -Z direction until the support features touch the reticle. Actuator '3' can be used (if needed) to correct for the Ry rotation to ensure both the support features touch the reticle.

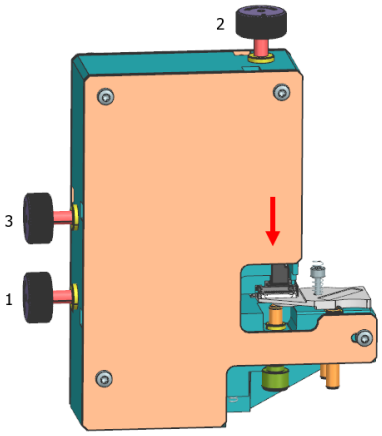

7. Rotate the holder knob K in the clockwise direction (ON mode of the holder) to grip the metal plate, and so the reticle.

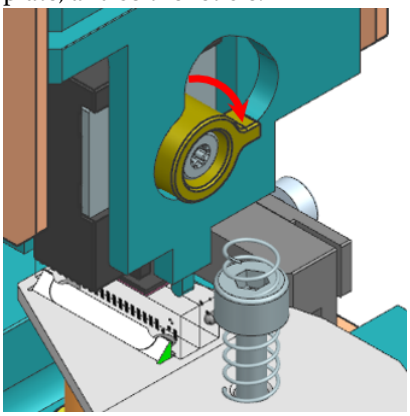

8. Tilt the alignment mechanism and rest it on the rubber feet (seated orientation) under the microscope. Perform the alignment using the three actuator screws.

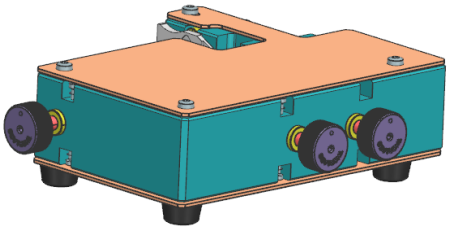

9. Once aligned, apply UV adhesive in the four regions (shown by the arrows) and cure for 30 s using a handheld UV light.

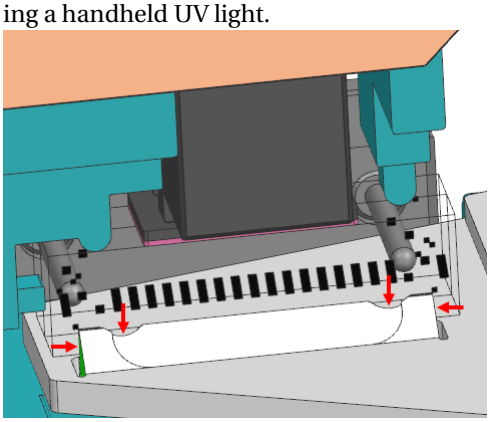

10. Place the mechanism again in the upright orientation.

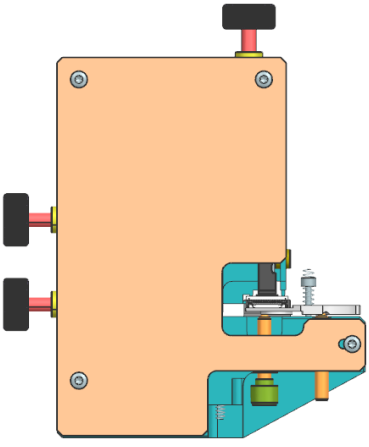

11. Rotate the holder knob back to its default position to ungrip the metal plate.

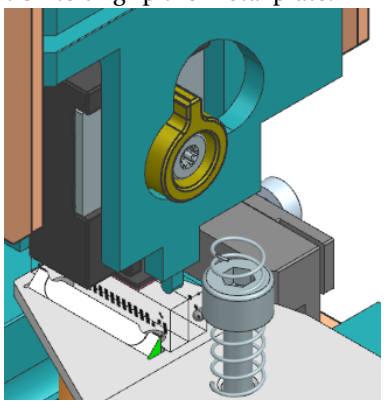

12. Retract and unmount the preload assembly.

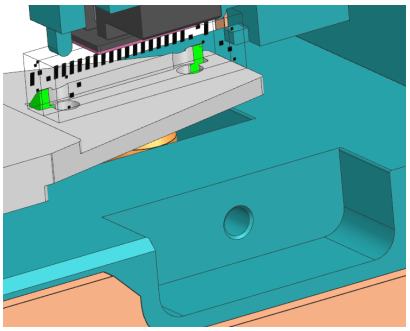

13. Slacken the actuator screws and the left adjustment screw to create space for unmounting the ReCa assembly.

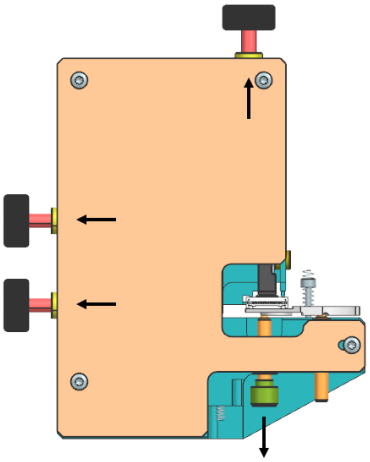

14. Unmount the ReCa assembly.

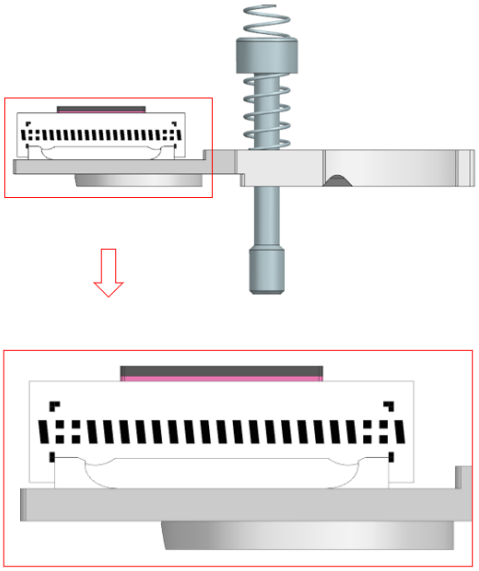

5.3. Verification Procedure

Once the alignment mechanism is built, it is important to check if the design meets the set requirements. For this, two sets of the reticle and carrier can be used to examine the working of the alignment mechanism. The process of performing the alignment and bonding the main components together is carried out to form the ReCa assemblies. However, this does not verify the functionalities that constitute the overall performance of the system, especially the ones that involve operator intervention. For the 3-DOF manipulation, a verification of the MIM in the 3 DOFs (refer M1 requirement) if useful. It is important to check if the desired actuation stroke results in the expected motion of the moving structure. Additionally, for the reticle holder, its performance can be verified. The vertical holding force on the metal plate by the holder and the tolerable horizontal force on the reticle before it moves laterally. Two of these verification plans are covered in this section.

Vertical holding force on the metal plate by the reticle holder:
The magnetic circuit in the design has an air gap of 0.25 mm between the yoke and the metal plate (see figure 4.10). In the ON mode, the holder produces a force of 2.6 N in the vertical direction to grip the metal plate (refer table 4.1). To verify if this simulated holding force value is achievable in a real-life setting, a verification setup is devised for the reticle holder as discussed below:

1. An aluminium body is milled to mount the reticle holder and perform the verification.

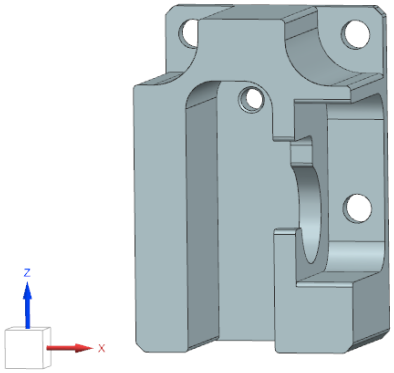

2. The holder H is mounted using a M3x6 screw.

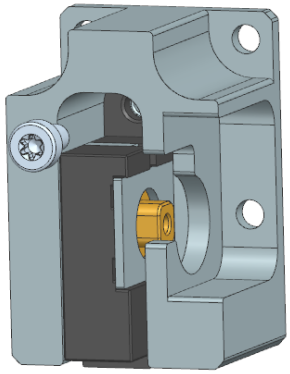

3. Two M2.5x5 set screws are used as support features to map to the accessible top surface of the reticle. Besides, these set screws can be adjusted to vary the air gap distance between the yoke and the metal plate. A Vernier caliper can be used to measure the protrusion of the screws.

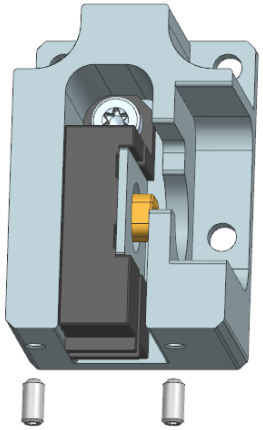

4. The aluminium body is mounted using two M3 screws (see figure) on a fixed structure that possesses the corresponding mating threads.

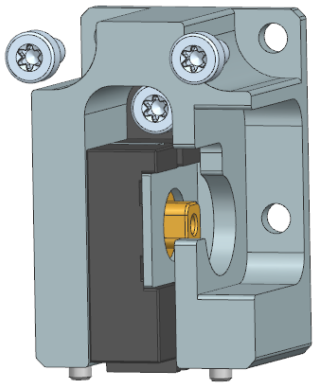

5. The knob K is assembled using a M2.5x5 screw in its OFF mode (along the +Z direction).

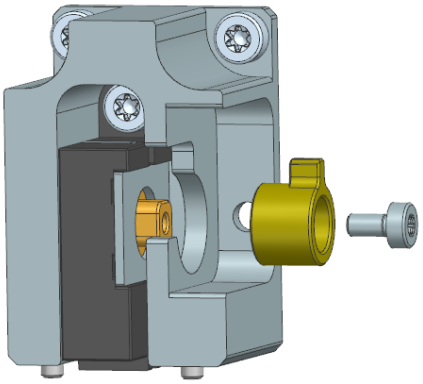

6. The setup is now ready to use for verifying the holding force on the metal plate in the vertical direction (along the Z-axis).

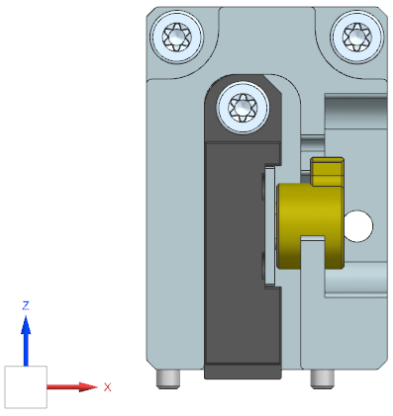

7. An assembly of a dummy glass piece and the metal plate is taken. An adhesive ceiling hook is attached on the bottom surface of the glass piece.

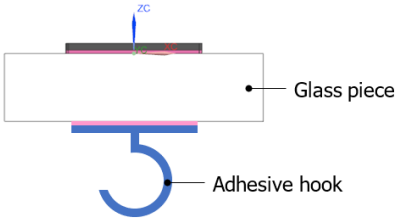

8. The assembly of step 7 is attached to the setup of step 6 by turning the knob 90° (ON mode). The set screws are adjusted in such a way that an air gap of 0.25 mm is maintained in the magnetic circuit.

To estimate the value of the holding force, an equivalent force exerted by the gravity is calculated. This can be done by gently hanging a hook weight (see figure 5.3 for an example) on the adhesive hook without introducing any jerk or disturbance. If required, a series of hook weights of different sizes can be used. The sum of masses of the glass piece, the adhesive hook and the hook weight(s) are considered to calculate the equivalent force. The moment at which the force of gravity by these masses just exceeds the holding force by the holder, the assembly of the glass piece will detach and fall down. This is further explained in the equations below:

$$2.6 = \left(m_{glass\ piece} + m_{adhesive\ hook} + m_{hook\ weight(s)}\right) \times g \tag{5.1}$$

$$0.26 = m_{glass\ piece} + m_{adhesive\ hook} + m_{hook\ weight(s)} \tag{5.2}$$

As seen in equation 5.2, the combined mass of the glass piece, the adhesive hook and the hook weight(s) should lie around 0.26 kg to balance with the vertical holding force of 2.6 N by the holder. An alternative to using hook weight(s) is a force gauge (see figure 5.4 for an example). The equipment can be used manually for the pull action by pulling the assembly of step 8 via the adhesive hook. In this way, the peak force can be estimated when the assembly of the glass piece detaches and falls down.

Figure 5.3: Hook weight [6]

Figure 5.4: Force gauge [9]

Furthermore, the air gap distance in the magnetic circuit can be varied (by adjusting the set screws) to check its effect on the vertical holding force. This can be done by repeating the aforementioned verification plan for different air gap distances. Looking at the tolerances of the yoke and metal plate (with adhesive tape), the air gap values of 0.15 mm – 0.35 mm can be considered. A vertical holding force of at least 2 N (safe value) is acceptable to grip the metal plate. This value is four times the frictional force between the reticle and the carrier. Also, the value of 2 N produces a 1 N tolerable lateral force on the reticle (refer section 4.3.2), which is two times the friction between the main components. Note that even though the set screws are made of stainless steel and not aluminium, the friction coefficient is still taken as 0.5 for a glass-metal contact [5].

Tolerable horizontal force on the reticle before it moves laterally:
Considering the friction coefficient of 0.5 between the support features & the reticle [5] and a vertical holding force of 2.6 N (refer table 4.1), the lateral force of 1.3 N can be tolerated by the reticle before it starts moving. To verify if this calculated lateral force is true in a real-life setting, a similar verification plan can be followed as described hereon. Steps 1–3 remain the same as before.

4. The aluminium body is mounted using two M3 screws (see figure) on a fixed structure that possesses the corresponding mating threads. Note that the body is tilted 90° anticlockwise about the Y-axis from the earlier setting.

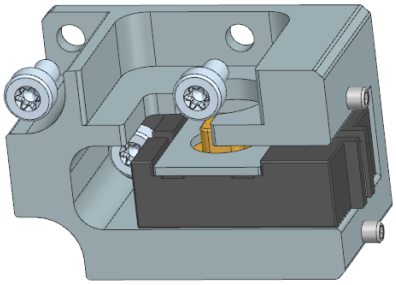

5. The knob K is assembled using a M2.5x5 screw in its OFF mode (along the -X direction).

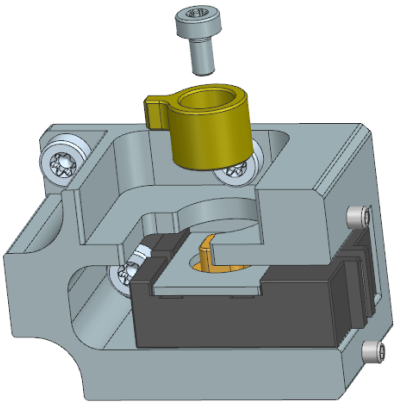

6. The setup is now ready to use for verifying the lateral force the reticle can tolerate before it starts moving.

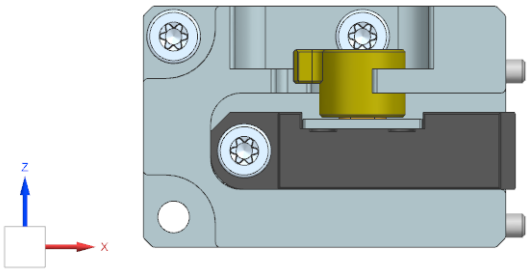

7. An assembly of a dummy glass piece and the metal plate is taken. An adhesive ceiling hook is attached to the left surface of the glass piece.

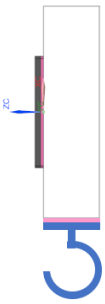

8. The assembly of step 7 is attached to the setup of step 6 by turning the knob 90° (ON mode). The set screws are adjusted in such a way that an air gap of 0.25 mm is maintained in the magnetic circuit.

The combined masses remain the same as before. Subsequently, the hook weight(s) (see figure 5.3 for an example) of different sizes are gently hung in a similar fashion without introducing any jerk or disturbance. The tolerable lateral force is estimated by using the equations below:

$$1.3 = \left(m_{glass\ piece} + m_{adhesive\ hook} + m_{hook\ weight(s)}\right) \times g \tag{5.3}$$

$$0.13 = m_{glass\ piece} + m_{adhesive\ hook} + m_{hook\ weight(s)} \tag{5.4}$$

Thus, the combined mass of the glass piece, the adhesive hook and the hook weight(s) should lie around 0.13 kg or less to prevent the reticle from moving laterally. As covered earlier, a force gauge (see figure 5.4 for an example) can be used as an alternative to estimate the peak force at which the assembly of the glass piece starts moving.

6

Conclusions and Recommendations

This chapter sums up the main conclusions and discusses the recommendations for future work.

6.1. Conclusions

A flexure-based alignment mechanism is designed to perform the 3-DOF in-plane alignment of a glass reticle and a stainless steel carrier w.r.t. each other. Various design principles are applied to construct a stiff and compact mechanism that uses a limited number of adjustment steps for the alignment. The process is supported by calculations and analyses that contribute to decision making. Furthermore, the proposed design is detailed in a complete 3D model and the PMI documentation is made.

The alignment mechanism fits within a volume of 165 mm × 198 mm × 60 mm for the X-, Y- and Z-axis, respectively. A monolithic manipulator body made of aluminium forms the core of the mechanism. Three stacked combinations of a reinforced leaf spring and a circular hinge are incorporated to adjust the moving structure in the desired 3 DOFs (Tx, Tz and Ry). Material is symmetrically removed in the hinged bodies to form T cross-sections and free up the overconstraints in the design. Besides, three fine screw actuators are used with knobs for manual actuation. In addition, stainless steel interface strips are bonded to the manipulator body to avoid high stresses due to actuation at the contact areas.

Three ball tip adjustment screws are used to mount the carrier with high precision and repeatability via its V-grooves using the principle of kinematic constraint. A locknut is bonded to each of these screws to define the position of the carrier. In addition, a metal plate is bonded to the top surface of the reticle and held by a magnetic holder. The holder offers the advantage to function as a standalone unit by turning a knob to turn the holding forces ON and OFF. Additionally, the mechanical features of the moving structure, together with the carrier are used to define the position of the reticle in the mechanism. To simulate the working of the reticle holder, a 2D magnetic flux analysis is performed. The holding force on the metal plate in the holding direction is around 5 times more than the frictional force between the main components, and around 2.5 times more in the lateral direction (perpendicular to the holding direction).

Furthermore, a preload assembly is used to constrain the remaining 3 DOFs (Rx, Rz and Ty). Two compression springs are used to provide a small force via pins on the back surface of the reticle that ensures an in-plane contact between the main components. A screw can be turned to retract the pins and remove the preload. Moreover, an overload protection mechanism is integrated in the manipulator body to prevent reticle damage during the adjustments. This mechanism becomes actuated when the reticle get clamped between the mechanical support features and the resting surface of the carrier. Various springs are installed on the manipulator body to provide the necessary pretension forces that avoid backlash in the mechanism. The effects of the transmission ratio are taken into account to calculate these forces, keeping a safety factor of approximately 1.5. To simulate the working of the manipulator body, a structural analysis is performed. The elemental stresses are found to be over 6 times less than the yield strength and around 2 times less than the fatigue strength of Al 7075, for the stroke of 0.5 mm. For the 1 mm stroke (extra stroke for mounting and unmounting the ReCa assembly), the elemental stresses are over 3 times less than the yield strength and around the same as the fatigue strength of Al 7075.

The process to form the ReCa assembly follows a particular approach that utilizes two orientations of the alignment mechanism: seated (during alignment) and upright (for all other purposes). The microscope setup is used to get visual feedback of the alignment. Once aligned, the components are bonded in place using UV adhesive and cured using a handheld UV light. Subsequently, the cured ReCa assembly is unmounted by slackening the actuators, along with one of the carrier mount screws to create space.

To ensure the design of the alignment mechanism meets the formulated requirements, a verification is done as seen in tables 6.1 and 6.2. Only the requirements that can be verified by the matured design are considered.

Table 6.1: Verification: Must-haves

Code	Requirement	Satisfied	Remarks
M0	Alignment DOFs	Yes	The mechanism enables the 3-DOF in-plane alignment.
M1	MIM	Yes*	0.71 µm for the linear adjustments and 13 µrad for the angular adjustment.
M2	Stroke	Yes	End stops are integrated to restrict the stroke to 0.5 mm in one direction and 1 mm on the other (extra stroke for mounting and unmounting the ReCa assembly).
M3	Remaining DOFs limits	Yes*	An in-plane contact is formed between the main components (due to the preload assembly) to constrain the remaining three DOFs.
M4	Intact reticle	Yes	Care has been taken to design a mechanism that minimizes the risk of reticle damage.
M5	Adhesive bonding	Yes	Care has been taken to design a mechanism that leaves the adhesive bond regions accessible to the operator.
M12	Available volume	Yes	The design fits within the available volume determined by the microscope setup.

Table 6.2: Verification: Nice-to-haves

Code	Nice-to-have	Satisfied	Remark
N0	Compact & portable	Yes	The mechanism is closely-packed and easy to be carried around by one person.
N1	DFM/DFA	Yes	Care has been taken to design a mechanism that can be manufactured efficiently and assembled with ease.
N3	Compatibly designed	Reticle – Yes Carrier – No	The same reticle is bonded to a metal plate. Besides, The cylindrical supports of the carrier are removed. This does not change its functionality or overall dimensions.
N4	Integrated adhesive bonding	No	The adhesive bonding process remains the same as before.

** means the requirement should also be verified in a real-life setting (refer section 6.2).*

6.2. Recommendations

Although the alignment mechanism is detailed into a complete 3D model as per the requirements, some additional work can give more confidence into its working and improve the overall functionality of the system.

A start is made with a plan to verify the performance of the reticle holder in section 5.3. However, a verification plan for the working of different aspects of the manipulator body is not devised. The plan must include the MIM of the three DOFs (refer M1 requirement). These can be checked to see if the desired stroke by an actuator results in the expected adjustment in the region of interest. The same microscope setup, which is

used for visual feedback during the alignment, can be connected to a digital output. To get the stroke for 1° turn of the fine screw, a motorized actuator can be mounted instead in the same adapter. In this way, the outputs for different actuator strokes can be recorded and compared to digitally measure the travelled distances in the region of interest. A reference point on the fixed structure near the region of interest can be considered for taking measurements.

Once the mechanism is realized, two sets of the reticle and carrier can be used to check the overall functioning of the mechanism. Consequently, two ReCa assemblies are formed by the operator. Nevertheless, there is no indication of how accurately the main components are aligned w.r.t. each other in each assembly or how does one assembly differ from the other. This is true for any other set of the reticle and carrier. Hence, it can be beneficial to perform an absolute measurement of the alignment in the ReCa assembly and give an estimate of how this measurement differs in each assembly. Further studies can be conducted to discover the appropriate measurement method and tools needed to realize the measurement.

The preload assembly uses pins that are placed in line with the contact surfaces (behind the green faces of the carrier). Thus, the preload is experienced in those areas. However, the assembly continues to utilize the limited height of the green faces of the carrier (= 1.6 mm, refer table 1.2) to constrain the Rx DOF during the alignment. It is therefore worthwhile to investigate if the requirement for that DOF is satisfied, along with the other two DOFs (Rz and Ty). Besides, an alternative can be to look into the possibility of design change of the target that allows for more freedom to constrain the remaining 3 DOFs (refer M3 requirement).

A

Guide and Actuator Options

A.1. Guide Options

The commonly used guide options are: bearings (ball and roller), air bearing, dovetail slide, plain bearing and flexure. Ball and roller bearings are suitable for long strokes. Ball bearings (see figure A.1) are less expensive, less stiff and have lower load capacity than roller bearings. Air bearings have the advantage of frictionless stroke. They offer high accuracy, load capacity, stiffness and stroke. However, air bearings are quite expensive and complex. They also need a supply of clean and dry air that brings in additional components pertaining to air supply. A dovetail slide (see figure A.2) is less expensive and offers high stiffness and load capacity. The main disadvantage of a dovetail slide is high friction due to large contact surface area (depending on force), when compared to ball or roller bearings [50].

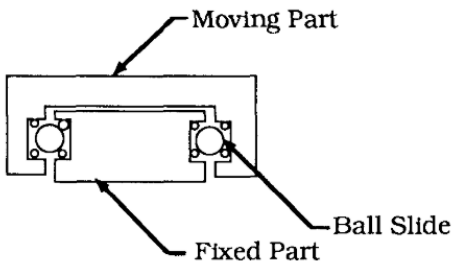

Figure A.1: Ball bearing [50]

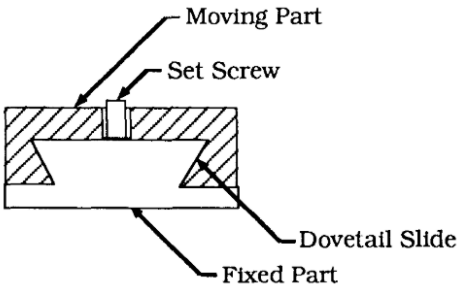

Figure A.2: Dovetail slide [50]

Plain bearings allow sliding motion by making use of a lubricant (unless self-lubricated). The lubricant film is critical to avoid the shaft and bearing surfaces from making a contact. This is necessary to prevent premature failure [20]. Flexures are elastic deformable elements that are especially suited for short stroke. They have the merits of high stiffness and frictionless motion with no play or wear. Therefore, flexures are very good for precision applications. For a monolithic design, they are commonly realized by the process of wire EDM [44].

Depending on the use, a flexure can carry a disadvantage of parasitic motion (or undesired motion). Figure A.3A shows a parallelogram flexure system that uses two leaf springs. The system does not allow for a perfect horizontal translation of the rigid stage as it tends to follow an arc-like path over its stroke. This leads to a parasitic motion along the vertical axis, which results in crosstalk between the two axes. This parasitic motion can be tackled by using a serial flexure system (see figure A.3B) that consists of two parallelogram flexure systems nested (or stacked) together. Because of the arrangement, the undesired motion of the two systems gets cancelled out and the lower rigid stage translates without parasitic errors. The combination of both parallel and serial flexure systems is called as a hybrid flexure system (see figure A.3C) [11].

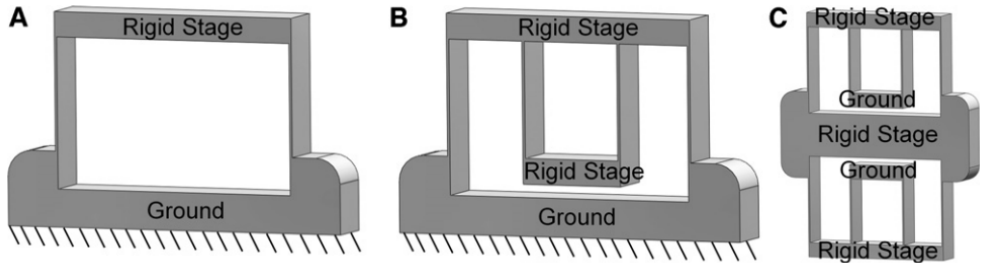

Figure A.3: Parallel, serial and hybrid flexure systems [11]

A.2. Actuator Options

The commonly used actuator options are: screws (coarse, fine and differential type), micrometers and motorized actuators (DC, linear and stepper motors, along with piezoelectric actuators). Screws and micrometers are used for less frequent adjustments. Screws are usually preferred if the position readout is not required. These are less expensive and bulky than micrometers. Screws can further be divided into coarse, fine and differential types based on sensitivity requirements. The differential screws and micrometers are used for small stroke. These are usually bigger in size and more expensive than coarse or fine screws [50].

For frequent and real time adjustments, motorized actuators are used. DC, linear and stepper motors, along with piezoelectric actuators are all part of motorized actuators. Their main merits are long stroke, high resolution and velocity. These actuators are often costlier and bulkier than screws. Piezoelectric actuators offer additional demerits of creep, hysteresis and travel non-linearity vs the applied voltage [50].

B

Reticle Holding Options

The holding options for the reticle are classified into four main categories based on their holding methods: vacuum, magnetic, clamping and adhesion [4]. 'Adhesion' category is added based on the use case. Each of them is described in detail in the coming sections.

B.1. Vacuum

Vacuum holders use the vacuum force to hold the parts. A smooth and clean holding surface is required to ensure the holding is proper. One common example of the vacuum category is the suction cup [4].

Suction cup:
Suction cups (or vacuum cups) work by evacuating air from the space inside the cup, thus creating a pressure below ambient pressure [27]. This pressure difference between the inside and ambient determines the force a suction cup can apply. The force is calculated by the pressure difference times the area covered by the cup on the holding surface. The higher the pressure difference, the higher is the force exerted by the suction cup [48].

Suction cups are commonly used in heavy industries, packaging industries and automobile assembly lines [4]. There are several factors that affect the shape, size and selection of a suction cup. These are discussed in detail below:

- Geometry: Suction cups are available in several geometries like circular type for general-purpose handling and oval type for handling long objects. The cups often have reinforcements in the form of ribs for increased strength [26].
- Shape: Suction cups are commonly available in two shapes: flat type and bellow type (see figure B.1 for both shapes). Flat type is good for handling flat or slightly curved surfaces like glass plates, metals and plastic sheets. This type can handle high shear forces and have good stability. Bellow type, due to its shape, can compensate for varying object heights. Therefore, this type is suited for curved or uneven surfaces. Bellow type suction cups are used in the handling of car body parts and tubes [26].
- Material: Suction cups are made of rubber or other elastomeric materials. Depending on the application, plastic can be used as well [4]. Some examples are: NBR (a cost-effective choice for general-purpose uses), silicone (food-grade applications) and PU (offers good wear resistance and strength) [26].
- Theoretical holding force (F_{th}): For a horizontal suction cup that has a vertical lifting force (see figure B.2), the theoretical holding force is calculated by [27]:

$$F_{th} = m\left(g + \frac{a}{\mu}\right)S \tag{B.1}$$

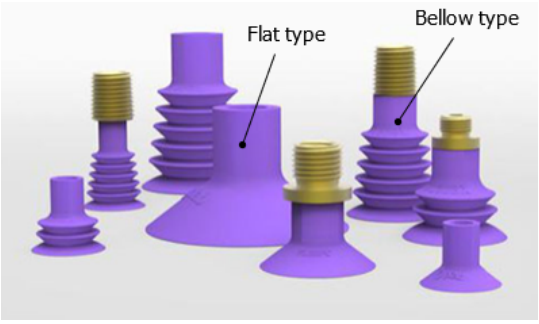

Figure B.1: Suction cups [26]

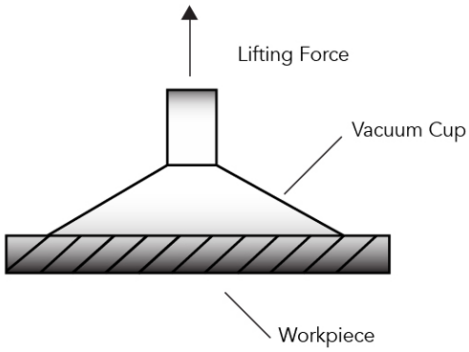

Figure B.2: Horizontal suction cup [27]

where m represents the mass of the held component, g is the acceleration due to gravity ($= 9.81\,\mathrm{m\,s^{-2}}$), a is the acceleration of the system in horizontal direction, μ is the coefficient of friction and S is the safety factor [27].

- Shore-A hardness and stiffness: In general, the value of stiffness can be calculated from Shore-A hardness by using a well-known empirical relation called as the Gent's relation. This is shown below [18]:

$$Y = \frac{0.0981\ (56 + 7.62336\ Sh)}{0.137505\ (254 - 2.54\ Sh)} \tag{B.2}$$

where Sh is the Shore-A hardness in the range of 20 to 80 and Y is the Young's modulus calculated in MPa [18]. The relation can be used to get the approximate stiffness value of the suction cup.

To utilize a suction cup, the vacuum system also comprises other supporting parts. These are a compressor (for a compressed air supply), a vacuum generator like an ejector (to create vacuum), intake filter (for removing impurities), valves (to control the air and vacuum), hose pipes (for air flow), tank (to reserve vacuum for system safety) etc [17]. A vacuum pump can also be used to create vacuum in the absence of a compressed air supply. The use of these parts depends on the application.

B.2. Magnetic

The magnetic-based category uses magnetic force for holding soft magnetic materials [4]. This category is classified into two options: electromagnet and permanent magnet with a knob. The basic working principle of both options remains same. The primary difference between them is that the former behaves like a magnet by the flow of current that generates a magnetic field, and the latter does not need any current source as its magnetic field is persistent [2]. The two options are explained in further detail below:

Electromagnet:
Electromagnets are easy to control and very practical when the component has to be released after use. The use of an electromagnet depends on a power supply that creates an electric current. A controller unit can be used to minimize the residual magnetism on the part. This is done by bringing down the polarity level prior before turning off the supply to release the component [4].

Permanent Magnet (PM) with a knob:
Permanent magnets offer the advantage of a continuous magnetic field in the absence of a power supply. They are simple to use, require less maintenance and provide less risk for accidental release of the component due to power failures [4].

Releasing of the component after use becomes tricky in the permanent magnet option. To tackle this, the magnetic flux can be cleverly controlled to turn on and off adhesion forces. An example of this is the Magnetic Switchable Device (MSD) as shown in figure B.3. It consists of two diametrically magnetized disc magnets (rotor and stator) placed on top of each other. The stator is fixed to the iron part and the rotor can rotate over 180°. In the off mode, the poles of the two magnets are aligned opposite to each other. Therefore, the flux goes through both magnets, thus cancelling the adhesion force on the metal plate. In on mode, the rotor is

turned 180° that aligns the poles of the two magnets. Hence, the flux is routed through the metal plate thus producing the adhesion force [29].

The on and off modes can be achieved by using a knob, which is connected to the rotor. The knob can be turned to control the magnetic flux [16].

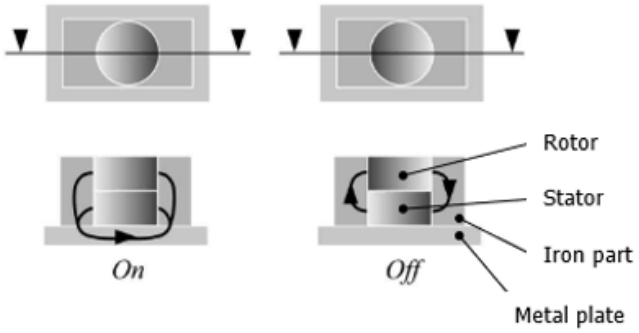

Figure B.3: Magnetic Switchable Device (MSD) with on and off modes [29]

B.3. Clamping

A clamp can either be part of the alignment mechanism (monolithic design) or become integrated as a sub-assembly. Depending on how the motion of an object is constrained, it can be classified into two grasping principles: form closure and force closure grasps [3].

In the case of form closure grasp, the object is fully constrained and remains in equilibrium. It cannot move at all and is not affected by any external force and moment. Form closure grasp relies on frictionless contact constraints and depends on the geometric nature of contacts. On the other hand, force closure grasp uses frictional contact forces to grasp an object. In this grasp, the contacts do not prevent the object from motions in all directions [3][43].

One option within the clamping category is the parallel gripper that is used for pick-and-place applications [4].

Parallel gripper:
The parallel gripper works by closing its jaws around the object to be picked, holding the object for use and releasing it later. These can further be divided into two suboptions based on actuation methods: pneumatic and electric parallel grippers [28].

Pneumatic grippers are connected to a compressed air supply. The gripper jaws close when air is applied on the pistons and open when the pressure is released, or vice versa. The force exerted by the jaws can be controlled by using a valve or managing the air intake. The main drawback of this gripper is there are not many settings that can be controlled. The stroke is fixed for a given gripper and the force depends on the air pressure and internal friction. The right pressure level for a use case can be determined by some trials [[28]]. Electric grippers use motors (stepper, servo etc.) for actuation. The main advantage of this gripper is its ability to control the stroke (in some cases, even speed and force). Electric grippers are a good choice for gripping a wide variety of objects like picking bins, tending machines and many others [28][4]. Some examples of commercial pneumatic and electric parallel grippers are shown in figures B.4 and B.5 [4].

Depending on the use case, the parallel gripper can either be commercially bought or custom-designed based on the grasping principles.

Figure B.4: Commercial pneumatic gripper [4]

Figure B.5: Commercial electric grippers [4]

B.4. Adhesion

Based on the use case, adhesion is added as one of the holding categories. This category is classified into two options: acrylic foam tape [1] and thermal release tape [23][30].

Acrylic foam tape (or bond tape):
3M™ VHB™ Tape, a type of an acrylic foam tape, is a good alternative to mechanical fasteners and liquid adhesives. It is a double-sided tape that has the advantages of high strength and ability to bond to a wide range of substrate materials. Depending on the application, there are several factors that determine the selection of a suitable tape. These are covered below [1]:

- Substrate: The tape interacts and forms the bond with each substrate differently. This depends on the surface energy of the substrate and how the adhesive flows onto its surface [1].
- Surface preparation: A clean surface is preferred for good adhesion. Additionally, pressure needs to be exerted after the application [1].
- Thickness: A large thickness value is preferred for the surfaces with more flatness irregularity [1].
- Flexibility and movement: The tape bonds are generally flexible. They can tolerate movement in the shear plane up to three times their thickness [1].

Thermal release tape:
REVALPHA, a thermal release tape, is a tape that adheres like any other adhesive at room temperature. The tape can be peeled off by heating causing no damage to the substrate. Hence, thermal release tapes see their use in temporary holding of substrates and is generally used in the electronics industry. The tapes come in two forms: single- and double-sided. Both forms use polyester as the core layer. The single-sided tape has a thermal release layer on one side, whereas the double-sided tape utilizes a combination of a thermal release layer and pressure-sensitive adhesive on either side. Depending on the application, thermal release tapes offer different options in terms of thickness, release temperature and adhesion strength [23][30].

C

Al 7075 Material Properties

The material properties of Aluminium 7075 are displayed in the table below:

Table C.1: Al 7075 material properties [19]

Parameter	Value
Density	2810 kg m^{-3}
Modulus of elasticity	71.7 GPa
Poisson's ratio	0.33
Fatigue strength	159 MPa
Shear strength	331 MPa
Yield strength	503 MPa
Tensile strength	572 MPa
Coefficient of thermal expansion	23.6 µm m^{-1} °C

Bibliography

[1] 3M. 3m™ vhb™ tape design guide, 2020. URL https://multimedia.3m.com/mws/media/12041680/3m-vhb-tape-design-guide-high-res-pdf.pdf. Accessed on March 21, 2021.

[2] Adams Magnetic Products Co. Permanent magnets vs electromagnets. URL https://www.adamsmagnetic.com/permanent-magnets-vs-electromagnets. Accessed on March 19, 2021.

[3] A Bicchi. On the closure properties of robotic grasping. *The International Journal of Robotics Research*, 1995.

[4] Wenjie Chen, Su Zhao, Siew Loong Chow, and Mechatronics Group. *Handbook of Manufacturing Engineering and Technology*. 2013. ISBN 9781447149767. doi: 10.1007/978-1-4471-4976-7.

[5] Engineering ToolBox. Friction and friction coefficients. URL https://www.engineeringtoolbox.com/friction-coefficients-d_778.html. Accessed on July 23, 2021.

[6] Flinn Scientific. Replacement hook weight, 50 g. URL https://www.flinnsci.com/replacement-hook-weight-50-g/ob2121/. Accessed on August 2, 2021.

[7] Peter Giesen and Noenke van der Lee. Design of a flexure-based alignment device for adjustable and stable mounting of optical components. *Space Systems Engineering and Optical Alignment Mechanisms*, 5528:272, 2004. ISSN 0277786X. doi: 10.1117/12.560941.

[8] Layton C. Hale and Alexander H. Slocum. Optimal design techniques for kinematic couplings. *Precision Engineering*, 25(2):114–127, 2001. ISSN 01416359. doi: 10.1016/S0141-6359(00)00066-0.

[9] Hans Schmidt. Force gauge fgjn. URL https://www.hans-schmidt.com/en/produkt-details/force-gauge-fgjn/. Accessed on August 10, 2021.

[10] Alvaro E. Hoffer, Juan A. Tapia, Ilya Petrov, and Juha Pyrhönen. Design of a Stainless Core Submersible Permanent Magnet Generator for Tidal Energy. *IECON Proceedings (Industrial Electronics Conference)*, 2019-October(October):1010–1015, 2019. doi: 10.1109/IECON.2019.8927156.

[11] Jonathan B. Hopkins and Martin L. Culpepper. Synthesis of precision serial flexure systems using freedom and constraint topologies (FACT). *Precision Engineering*, 35(4):638–649, 2011. ISSN 01416359. doi: 10.1016/j.precisioneng.2011.04.006. URL http://dx.doi.org/10.1016/j.precisioneng.2011.04.006.

[12] JPE. Flexure engineering fundamental: Leaf spring, . URL https://www.jpe-innovations.com/precision-point/flexure-engineering-fundamental-leaf-spring/. Accessed on July 21, 2021.

[13] JPE. 2 leaf springs in parallel, . URL https://www.jpe-innovations.com/precision-point/2-leaf-springs-parallel/. Accessed on July 21, 2021.

[14] JPE. Flexure hinge or elastic hinge, . URL https://www.jpe-innovations.com/precision-point/flexure-hinge-elastic-hinge/. Accessed on July 21, 2021.

[15] Dongwoo Kang and Daegab Gweon. Analysis and design of a cartwheel-type flexure hinge. *Precision Engineering*, 37(1):33–43, 2013. ISSN 01416359. doi: 10.1016/j.precisioneng.2012.06.005. URL http://dx.doi.org/10.1016/j.precisioneng.2012.06.005.

[16] K&J Magnetics, Inc. Magnets with an off switch. URL https://www.kjmagnetics.com/blog.asp?p=magswitch. Accessed on March 19, 2021.

[17] Guido La Rosa, Michele Messina, Giovanni Muscato, and R. Sinatra. A low-cost lightweight climbing robot for the inspection of vertical surfaces. *Mechatronics*, 12(1):71–96, 2002. ISSN 09574158. doi: 10.1016/S0957-4158(00)00046-5.

[18] Kent Larson. Can You Estimate Modulus From Durometer Hardness for Silicones? *Dow*, pages 1–6, 2019.

[19] MatWeb. Aluminum 7075-t6; 7075-t651. URL http://www.matweb.com/search/DataSheet.aspx?MatGUID=4f19a42be94546b686bbf43f79c51b7d. Accessed on July 24, 2021.

[20] R. K. Mobley. *Maintenance Fundamentals*. 2004. ISBN 9780750677981. doi: 10.1016/B978-075067798-1/50030-3.

[21] Newport. Threaded knob, . URL https://www.newport.com/p/KN-10QG-3. Accessed on July 22, 2021.

[22] Newport. Fine thread adjustment screw, . URL https://www.newport.com/p/SW-10Q5-3. Accessed on July 22, 2021.

[23] Nitto. Thermal release sheet for electronic component processing revalpha. URL https://www.nitto.com/eu/en/products/e_parts/electronic001/. Accessed on April 7, 2021.

[24] Paul Oxley, Jennifer Goodell, and Robert Molt. Magnetic properties of stainless steels at room and cryogenic temperatures. *Journal of Magnetism and Magnetic Materials*, 321(14):2107–2114, 2009. ISSN 03048853. doi: 10.1016/j.jmmm.2009.01.002.

[25] P.C.J.N. Rosielle. Selected Basic Design Principles for precise motion and positioning purposes. *Eindhoven University of Technology*, (October):138, 2018.

[26] Pneumatic Tips. How do you select a vacuum cup?, 2016. URL https://www.pneumatictips.com/how-do-you-select-a-vacuum-cup/. Accessed on March 19, 2021.

[27] Pneumatic Tips. How do you size a vacuum cup?, 2016. URL https://www.pneumatictips.com/size-vacuum-cup/. Accessed on March 18, 2021.

[28] Robotiq. How does a parallel robot gripper work?, 2016. URL https://blog.robotiq.com/how-does-a-parallel-robot-gripper-works. Accessed on March 20, 2021.

[29] Frederic Rochat, Patrick Schoeneich, Michael Bonani, Stephane Magnenat, Francesco Mondada, Hannes Bleuler, and Christoph Hürzeler. Design of magnetic switchable device (MSD) and applications in climbing robot. *Emerging Trends in Mobile Robotics- Proceedings of the 13th International Conference on Climbing and Walking Robots and the Support Technologies for Mobile Machines, CLAWAR 2010*, pages 375–382, 2010. doi: 10.1142/9789814329927_0047.

[30] Semiconductor Equipment Corp. Heat release tape. URL https://www.semicorp.com/product/heat-release-tape/. Accessed on April 7, 2021.

[31] H. Soemers. Design Principles for Precision Mechanisms, 2012.

[32] supermagnete.de. Should i buy a ferrite or neodymium magnet?, . URL https://www.supermagnete.de/eng/faq/Should-I-buy-a-ferrite-or-neodymium-magnet. Accessed on July 22, 2021.

[33] supermagnete.de. Disc magnet Ø 10 mm, height 5 mm, . URL https://www.supermagnete.de/eng/disc-magnets-neodymium/disc-magnet-10mm-5mm_S-10-05-DN. Accessed on July 22, 2021.

[34] Tevema. D11060, . URL https://webshop.tevema.com/gb/d11060. Accessed on July 24, 2021.

[35] Tevema. D21240, . URL https://webshop.tevema.com/gb/d21240. Accessed on July 25, 2021.

[36] Tevema. T40720, . URL https://webshop.tevema.com/gb/t40720. Accessed on July 25, 2021.

[37] Tevema. D20250, . URL https://webshop.tevema.com/gb/d20250. Accessed on July 23, 2021.

[38] Thomas Publishing Company. All about 7075 aluminum (properties, strength and uses). URL https://www.thomasnet.com/articles/metals-metal-products/all-about-7075-aluminum-properties-strength-and-uses/. Accessed on August 16, 2021.

[39] Thorlabs. 1/4"-100 adjusters, . URL https://www.thorlabs.com/newgrouppage9.cfm?objectgroup_id=1208. Accessed on July 21, 2021.

[40] Thorlabs. Ø0.925" 1/4"-100 removable adjuster knob, . URL https://www.thorlabs.com/thorproduct.cfm?partnumber=F25USK2. Accessed on July 21, 2021.

[41] Thorlabs. Fine hex adjuster, 1/4"-100, 1 1/2" long, . URL https://www.thorlabs.com/thorproduct.cfm?partnumber=F25US150. Accessed on July 21, 2021.

[42] Thorlabs. Mounting barrel adapter, 1/4"-100 to Ø3/8", . URL https://www.thorlabs.com/thorproduct.cfm?partnumber=F25USA1. Accessed on July 21, 2021.

[43] Jeffrey C. Trinkle. A Quantitative test for form closure grasps. *IEEE International Conference on Intelligent Robots and Systems*, 3(August 1992):1670–1677, 1992. ISSN 21530866. doi: 10.1109/IROS.1992.594246.

[44] Noenke van der Lee, J. P. Kappelhof, and Roger Hamelinck. Flexure-based alignment mechanisms: design, development, and application. *Optomechanics 2003*, 5176:94, 2003. ISSN 0277786X. doi: 10.1117/12.509135.

[45] Vink System Design & Analysis. Hertz contact stress calculations. URL https://www.vinksda.com/toolkit-mechanical-calculations/hertz-contact-stress-calculations/. Accessed on July 24, 2021.

[46] Wikipedia. Magnetic switchable device, . URL https://en.wikipedia.org/wiki/Magnetic_switchable_device. Accessed on July 11, 2021.

[47] Wikipedia. Fine adjustment screw, . URL https://en.wikipedia.org/wiki/Fine_adjustment_screw. Accessed on August 7, 2021.

[48] Jonas O. Wolff and Stanislav N. Gorb. Suction Cups. pages 87–93, 2016. doi: 10.1007/978-3-319-45713-0_6.

[49] Pei Xu, Yu Jingjun, Zong Guanghua, and Bi Shusheng. The stiffness model of leaf-type isosceles-trapezoidal flexural pivots. *Journal of Mechanical Design, Transactions of the ASME*, 130(8):0823031–0823036, 2008. ISSN 10500472. doi: 10.1115/1.2936902.

[50] P. Yoder. Critical Review Vol. CR43, Optomechanical Design, ed. P.R. Yoder, Jr. (July 1992) Copyright SPIE. *Proceedings of SPIE*, C(July):305–328, 1992. ISSN 0307-6938 (Print).

[51] Paul R Yoder and Daniel Vukobratovich. *Opto-Mechanical Systems Design*. 4th edition, 2015. ISBN 9781482257717.